REVIEW

Check for updates

Molecular Separation by Using Active and Passive Microfluidic chip Designs: A Comprehensive Review

*Aliakbar Ebrahimi, Kutay Icoz, Reza Didarian, Chih-Hsin Shih, E. Alperay Tarim,
Behzad Nasseri, Ali Akpek, Berivan Cecen, Ayca Bal-Ozturk, Kadri Güleç,
Yi-Chen Ethan Li, Steven Shih, Burcu Sirma Tarim, H. Cumhur Tekin, Emine Alarçin,
Mehdi Tayybi-Azar, Hamed Ghorbanpoor, Ceren Özel, Ayla Eker Sarıboyacı, Fatma Dogan
Guzel, Nicole Bassous, Su Ryon Shin, and Huseyin Avci**

Separation and identification of molecules and biomolecules such as nucleic acids, proteins, and polysaccharides from complex fluids are known to be important due to unmet needs in various applications. Generally, many different separation techniques, including chromatography, electrophoresis, and magnetophoresis, have been developed to identify the target molecules precisely. However, these techniques are expensive and time consuming. "Lab-on-a-chip" systems with low cost per device, quick analysis capabilities, and minimal sample consumption seem to be ideal candidates for separating particles, cells, blood samples, and molecules. From this perspective, different microfluidic-based techniques have been extensively developed in the past two decades to separate samples with different origins. In this review, "lab-on-a-chip" methods by passive, active, and hybrid approaches for the separation of biomolecules developed in the past decade are comprehensively discussed. Due to the wide variety in the field, it will be impossible to cover every facet of the subject. Therefore, this review paper covers passive and active methods generally used for biomolecule separation. Then, an investigation of the combined sophisticated methods is highlighted. The spotlight also will be shined on the elegance of separation successes in recent years, and the remainder of the article explores how these permit the development of novel techniques.

1. Introduction

Biomolecule separation, purification, and analyses have a high potential in different fields, including but not limited to diagnosis, genetic research, biopharmaceuticals, fine chemicals manufacturing, and biological characterizations.[1] These biomolecules are commonly present in complicated biological matrices or physiological fluids, and biological activities of the components can only be understood after each one is analyzed separately.[2] In addition, to characterize a biomolecule or cellular component and to understand its biological function exclusively, it must be pure and biologically active.[3] To this end, rapid and effective sample preparation procedures are required to aid in diagnosis in which sample preparation processes frequently need high quantities (>mL) and skilled people to reduce analysis time and costs.

Traditionally, three main methods have been used for the separation,

A. Ebrahimi, H. Ghorbanpoor, C. Özel, A. Eker Sarıboyacı, H. Avci
Cellular Therapy and Stem Cell Production Application and Research
Center (ESTEM)
Eskişehir Osmangazi University
Eskişehir 26040, Turkey
E-mail: havci@ogu.edu.tr
A. Ebrahimi, R. Didarian, H. Avci
Department of Metallurgical and Materials Engineering
Eskisehir Osmangazi University
Eskişehir 26040, Turkey

K. Icoz
Electrical and Electronics Engineering Department
Abdullah Gül University
Kayseri 38080, Turkey
R. Didarian, F. Dogan Guzel
Department of Biomedical Engineering
Ankara Yıldırım Beyazıt University
Ankara 06010, Turkey
C.-H. Shih, Y.-C. E. Li
Department of Chemical Engineering
Feng Chia University
Taichung 40724, Taiwan
E. A. Tarim, H. C. Tekin
Izmir Institute of Technology
Department of Bioengineering
Izmir 35433, Turkey

purification, and analysis of biomolecules: chromatography, electrophoresis, and ultracentrifugation. Each performs the separation and purification process based on the specific physicochemical properties of the target biomolecules. Technologies presently utilized in biomolecules separation, purification, and analyses sometimes require purchasing expensive gear or establishing sophisticated testing laboratories, neither of which is practical in many developing countries or isolated areas. As a result, portable, low-cost, fast, and user-friendly technologies are needed for the advancements in biomolecule analyses, particularly in developing nations or distant locations with inadequate infrastructure.[4]

Due to their suitability for point-of-care testing, microfluidic devices with good features, such as low cost per unit, quick analysis times, and minimal sample needs,[5–12] can potentially change the way of medical testing.[4] Many microfluidic devices that can conduct on-chip sample preparation processes before quantification, such as preconcentration, purification, and labeling, have recently been established.[13–15] Separation techniques for the on-chip study of biomolecules have also rapidly progressed.[16,17] On the other hand, a fully integrated system necessitates incorporating extra properties and substantial complexity into the microchip design. Precise fluidics control in various parts is also necessary while remaining cost-effective for disposability.

Analytical microchips, at the first stages of development, were only used for separations carried out in a capillary and helped as a proof-of-concept for the technological transfer from the capillary platform to the microchip.[5]

In the last two-decade, a considerable increase in chip-based sample separation research has resulted in the development of different passive, active, and hybrid on-chip separation methods.[4,18–41] As a result, incorporation of microdevices with cutting-edge analytical technologies has become possible while revolutionizing the approaches for biomolecule separation and analysis.

This review comprehensively investigates microfluidic approaches described recently for biomolecular separation.[36,42–44] This article breaks down and categorizes the microfluidic techniques for separating molecules. In this regard, various passive methods are first discussed, such as open-channels, pillar-structures, incorporated technics, and liquid-liquid extraction. Then, we discuss active processes, such as magnetic and acoustic separation, followed by combination methods known as hybrid methods, which incorporate both active and passive systems. The most current discoveries, inventions, and breakthroughs are also documented within the scope of each of these sub-sections. To narrow down the subject, the review only focused on on-chip biomolecular separation.

B. Nasseri
Department of Medical Biotechnology
Faculty of Advanced Medical Sciences
Tabriz University of Medical Sciences
Tabriz 5166616471, Iran

A. Akpek
Faculty of Electrical and Electronics, Biomedical Engineering
Yildiz Technical University
Istanbul 34220, Turkey

A. Akpek, A. Bal-Ozturk
Sabanci University Nanotechnology Research & Application Center
Tuzla, Istanbul 34956, Turkey

B. Cecen
Department of Mechanical Engineering
Rowan University
Glassboro, NJ 08028, USA

B. Cecen
Department of Biomedical Engineering
Rowan University
Glassboro, NJ 08028, USA

A. Bal-Ozturk
Department of Stem Cell and Tissue Engineering
Institute of Health Sciences
Istinye University
Istanbul 34010, Turkey

A. Bal-Ozturk
Department of Analytical Chemistry
Faculty of Pharmacy
Istinye University
Istanbul 34010, Turkey

K. Güleç
Department of Analytical Chemistry
Graduate School of Health Sciences
Anadolu University
Eskişehir 26470, Turkey

S. Shih
Department of Nutrition
University of California
Davis, CA 95616, USA

B. Sirma Tarim
Izmir Institute of Technology
Department of Chemical Engineering
Izmir 35430, Turkey

H. C. Tekin
METU MEMS Center
Ankara 06530, Turkey

E. Alarçin
Department of Pharmaceutical Technology
Faculty of Pharmacy
Marmara University
Haydarpasa, Istanbul 34668, Turkey

M. Tayybi-Azar
Department of Biophysics
Yeditepe University School of Medicine
Yeditepe University
Istanbul 34755, Turkey

H. Ghorbanpoor
Department of Biomedical Engineering
Eskişehir Osmangazi University
Eskişehir 26040, Turkey

C. Özel, A. Eker Sarıboyacı
Department of Stem Cell
Institute of Health Sciences
Eskisehir Osmangazi University
Eskisehir 26040, Turkey

N. Bassous, S. R. Shin
Division of Engineering in Medicine
Department of Medicine
Harvard Medical School
Brigham and Women's Hospital
Cambridge, MA 02139, USA

H. Avci
Translational Medicine Research and Clinical Center (TATUM)
Eskişehir Osmangazi University
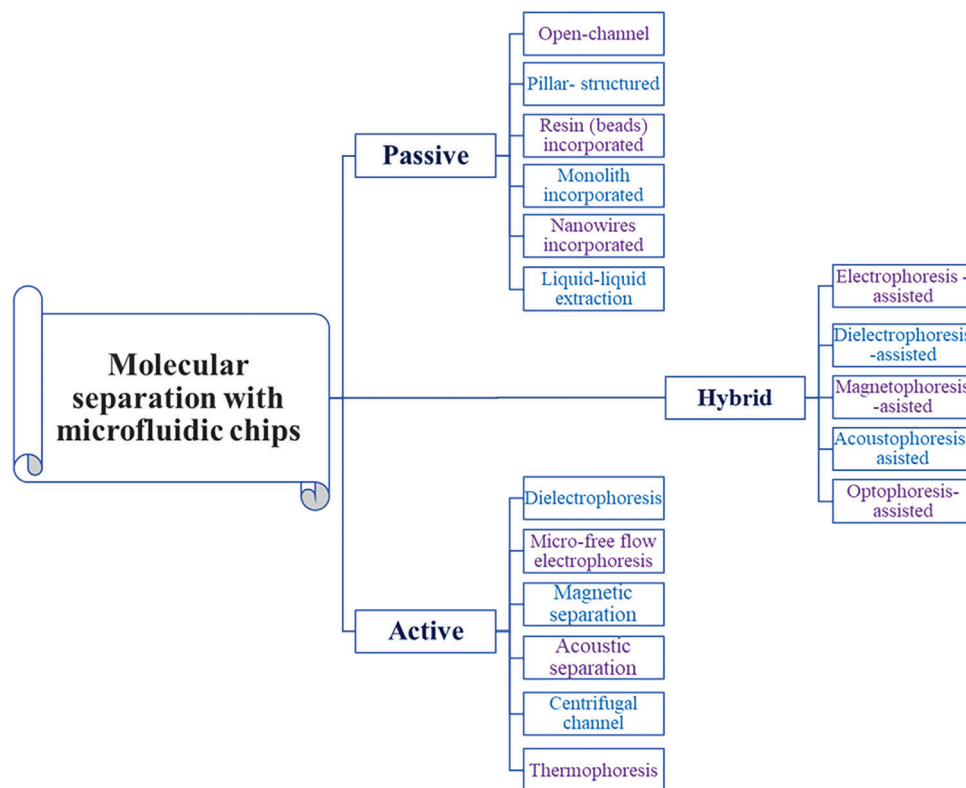Eskişehir 26040, Turkey

Figure 1. Different active, passive, and hybrid techniques of microfluidic-based biomolecule separation.

2. Microfluidic-Based Separation Methods

As mentioned above, this review is about the application of passive and active microfluidic-based methods for separation of biomolecules. **Figure 1** schematizes different techniques for cellular separation by using microfluidic devices. In the following parts, all methods summarized in Figure 1 are discussed in detail by focusing on different examples from the literature.

2.1. Passive separation methods

In passive separation techniques, microfluidic devices use the forces and interactions between molecules, cells and particles, and the flow field in the microchannels to separate the target samples without any external forces.[45] **Table 1** summarizes some critical parameters like channel structure, surface modification, separated molecules, and chip material type used in the chip fabrication.[36,46–73] Here, the primary methods used for passive molecular separation in the last decade are listed and discussed in the order listed in the table.

2.1.1. Open-Channel Microfluidic Chips

Microfluidic technology has demonstrated that miniaturized systems can replace large-scale laboratory instruments. This technology offers various advantages, such as reduced reagent/sample consumption, parallel processing, and a short turn-around time.[74] Basic analytical steps can be integrated to perform complex testing/screening tasks on a microfluidic system.[10] In addition, the rapid mixing of samples and reagents is essential to chemical reactions and biomedical analysis in microfluidic systems.[75]

Open microfluidic system is generally defined as a microfluidic system with at least one boundary wall removed so that the fluidic flow can contact a second fluid phase, such as another liquid or air. Although closed microfluidic chips have been widely used in biological analysis, the high cost of precision devices and the requirement of a rigorous clean environment for fabricating microfluidic chips conflict with the affordability in general laboratories.[76] Moreover, blocking of the microchannels by air bubbles is a major challenge for the users since the clogging of the channels could easily cause sample aggregation, undesired flow patterns, the death of cultured cells, and other complications.[77,78] Open-channel microfluidics has attracted many researchers within the past decade to overcome those limitations in closed microfluidic systems.

Open microfluidic systems are powerful tools with broad applications such as collecting and separating molecules, proteins, and cell cultures. Open microfluidic systems are generally categorized into open-channel/open-space, paper-based, and thread-based systems. In open-channel/open-space microfluidic systems, capillary force is the major driving force for fluid movement. External pumps are not required in these systems for fluid transportation. Additionally, without a physical boundary, it is possible to allow the fluid to flow between two different interfaces, such as air–liquid or liquid–liquid, and this provides

Table 1. List of passive microfluidic-based molecular separation methods.

Method	Channel structure	Surface modification	Separated Molecules	Chip materials	Ref.
Open-channel	Open channel	3-aminopropyltriethoxysilane (APTES), Polyethylene glycol (PEG), Bovine serum albumin (BSA), Amine-poly(ethylene glycol) (PEG–NH$_2$), O-amine-functionalized dextran, and Immobilized antibodies	DNA, RNA, IgG, Aptamer, Protein, Peptide, Catecholamines	Cyclo olefin polymer (COP), Polymethyl methacrylate (PMMA), Poly(dimethylsiloxane) (PDMS)	[36,46–48]
Pillar-structured	Pillar or Microbed	Organosilanes, RNA aptamer coated microbead, Oligonucleotide coated, Surface modified with SiO$_2$	DNA, RNA, Bacterial DNA	PMMA, PDMS	[36,49–51]
Resin (beads) incorporated	Agarose gel, Silica resin particles, Chitosan-coated silica particles, Chitosan-coated microchannels	Chitosan grafted, IgE-functionalized microbeads,	DNA, RNA	Borofloat glass, PDMS, PDMS-printed circuit boards (PCB), PDMS-glass, Glass	[36,52,53]
Monolith incorporated	Silica, C18 Silica, Methacrylate (MA), Am-co-MBAAm-co-AMPS, Butyl methacrylate-co-ethylene dimethacrylate (BMA-co-EDMA), PEGDA, Ethylene glycol dimethacrylate (EGDMA), Butyl methacrylate (BMA), 2-Acrylamido-2-methyl-1-propane sulfonic acid (AMPS), Acrylamide (AAm), Poly(lauryl methacrylate-co-ethylene dimethacrylate), Poly(styrene-co-divinylbenzene), Glycidyl methacrylate, Trimethylolpropane trimethacrylate	3-(Trimethoxysilyl)propyl methacrylate (TMSPM), Ethylene diacrylate (EDA), Methyl methacrylate (MMA), Oligonucleotide immobilized, Cu (II) immobilized, Multiple antibodies immobilized, Quaternary ammonium functionalized, Cibacron-blue-3G-A	DNA, BSA, Proteins, Peptides, Lysozyme, Human albumin	Borofloat borosilicate glass, PDMS, Glass, PMMA, Cyclic Polyolefin, Polyimide	[36,54–57]
Nanowires incorporated	Si-nanowires, SnO$_2$ nanowires, ZnO nanowire	Antibodies (anti e-GFP; polyclonal antihemoglobin or anti-cTnT) immobilized	DNA, RNA, Proteins, Troponin T, exosomes	Cr, PDMS, Fused silica	[36,58–67]
Liquid-liquid extraction	Open, Interconnected channels	-	DNA, Proteins, Peptides	PDMS-Glass, PDMS, PMMA, PS, PC, Cyclo olefin copolymer (COC), Glass, Silicon,	[68–73]

users with a new toolbox to design versatile open-channel/open-space microfluidic systems. Kralj et al.[79] have confirmed that boundary-free microfluidic systems enable the user to maintain the liquid-liquid phase separation in small interfacial areas and provide a continuous system with a substantial extracted fraction for separating miscible compounds. In another study, Feng et al.[80] developed an open-space system with fluidic walls for in situ online detection and semi-quantification of proteins through a rolling circle amplification (RCA) reaction. As shown in **Figure 2**a, two aqueous phases, a cell culture drop and a DNA aptamers-containing, drop were loaded individually onto a hydrophilic surface at two locations. Then, an oil phase was used to cover the surroundings of these two drops. Afterward, on–off control of the microfluidic system could be manipulated by sliding a pipette tip between the two aqueous phases. The two aqueous phases could then be selectively connected. This then allows

the separation of the protein (i.e., vascular endothelial growth factor (VEGF)) secreted from the cancer cells treated with deferoxamine (DFO) in situ, its diffusion to the sensor chambers containing DNA aptamers andsemi-quantification online.

A paper-based microfluidic system is a typical open-channel system that provides a powerful and accurate analytical tool for rapid detection of the analyte in chemical, pharmaceutical, and biological samples. Since capillary force is the major driving force to transport fluids and no active pumps are required within paper-based open-channel systems, it offers an easy, minimal, and portable approach to observing the testing results in real-time via the change in colorimetric or electrochemical signals.[81] However, the fluidic transportation in paper-based open-channel systems is limited by the physicochemical and interfacial properties between the fluid and solid phases, which results in difficulties in controlling the flow in multistep sequences.[82] Many
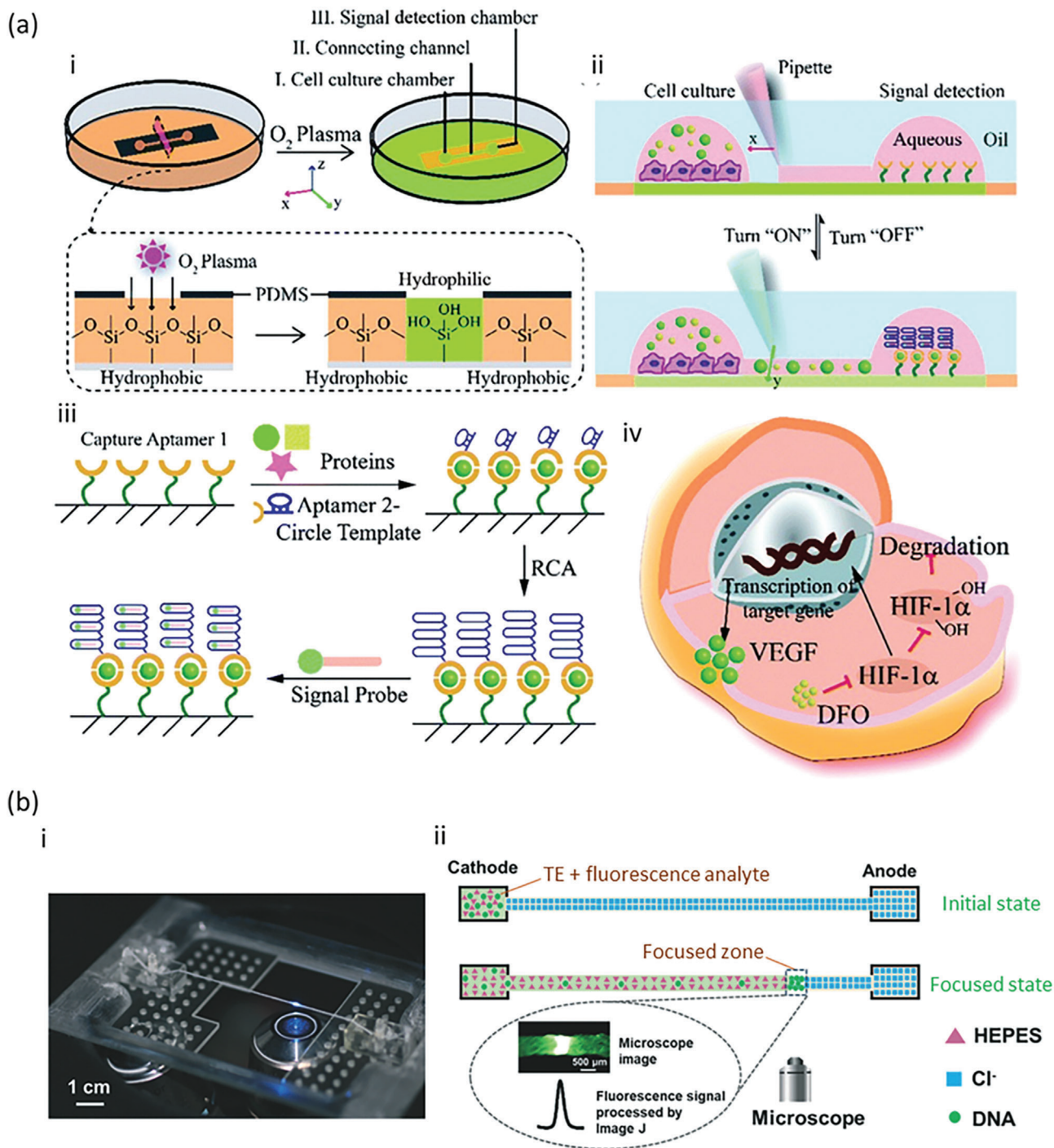
Figure 2. a,i) Schematic figure of an open-space microfluidic chip design with a fluidic wall. ii) The on-off control of the microfluidic system is accomplished by using a pipette tip to create a switchable connection between two chambers. iii,iv) The principle for detecting VEGF through RCA reaction and the mechanism of the hypoxia signaling pathway triggered via DFO. Reproduced with permission.[80] Copyright 2021, Royal Society of Chemistry. b,i) A thread-based, open-channel microfluidic system produced using a nylon material. ii) The illustration of the DNA separation in a thread-based ITP for DNA extraction from the biological samples. Reproduced with permission. [91] Copyright 2021, The Royal Society of Chemistry.

**ADVANCED
SCIENCE NEWS**

www.advancedsciencenews.com

**ADVANCED
MATERIALS
INTERFACES**

Open Access

www.advmatinterfaces.de

next-generation, paper-based, open-channel systems were developed to overcome limitations in programming fluidic behaviors by regulating the topologies and geometries of microchannels.[83–85] For example, Giokas et al.[86] developed a paper-based device to accelerate or delay fluidic transportation. They accomplished this by using a blade to carve thin longitudinal channels along or perpendicular to the flow path on the paper. The channels along the flow path provide a free flow regime for the fluid to accelerate the flow movement. In contrast, the channels perpendicular to the flow path delay the flow movement since the fluid needs to fill the perpendicular channels before moving further.

In chromatographic technologies, thin-layer chromatography (TLC) is widely used to separate proteins, DNA, chemical compounds, etc. Based on the affinities among the components in a mixture of stationary and mobile phases, the target components can be separated by their polarity or size. Similar to TLC, a thread-based microfluidic system is another open-channel system that drives the fluid flow through the wicking of fiber and woven yarns.[87,88] The fluid flow can be driven by capillary forces between fibers or woven yarns and controlled through the specific patterns formed by different geometric textile designs. Additionally, converging more threads to form knots further provides an easy strategy to mix two or more streams.[88] The common materials used in the thread-based microfluidic system are cellulose, polyester, silk, etc.[89] These materials possess strong mechanical properties, which endows the thread-based system with a stable structure and enable the system to transport liquid continuously for a long time. Therefore, thread-based, open-channel systems have been widely applied to portable diagnostic systems and tissue engineering.[90] For example, as shown in Figure 2b, Chen et al.[91] utilized 100% nylon to fabricate a disposable, thread-based open-channel microfluidic system for the application of the isotachophoresis (ITP) process to extract and preconcentrate DNA from a biological sample. They used the nylon stretches overlocking thread (diameter 500 µm), with super electrophoretic performance (electroosmotic flow of 6.09×10^{-8} m^2 V^{-1} s^{-1}), as the microfluidic channels, and both ends of nylon were connected to the buffer reservoirs in the PMMA base. Then, the buffer solution and the DNA samples could be transported and separated in the nylon thread, where the separated DNA could then be observed using a microscope. After the electrophoretic process, the separated DNA on the nylon thread could be cut and collected into an Eppendorf tube for further posterior qPCR analysis. This shows that the thread-based device could be used as a new strategy for electrophoresis to extract DNA from biological samples.

Open microfluidic systems simplify the manufacturing and surface modification processes[92,93] while eliminating the problem of air bubble formation, and enhancing the device's reliability.[94] Moreover, open microfluidic systems offer convenient operation and can access the fluid at any point in the system to add a new sample or collect the processed fluid.[95,96] Therefore, the future direction of open-channel microfluidic systems could be their use as sensors for diagnostics or chemical analysis. For instance, threads possess excellent wicking properties and flexibility, making them promising candidates for creating microfluidic circuits.[90,97] By using nanomaterial-blended conductive threads, these threads could be fabricated as physical

and chemical sensors and further interconnected with electronic circuitry for signal readout, modulation, and wireless transmission. The thread-based sensors could offer a reliable way to detect very small changes in electrical potential, enabling the measurement of ion exchanges in living tissues. Furthermore, open-channel microfluidic systems could be integrated with other analytical tools, such as surface-enhanced Raman spectroscopy.[98] The large surface area of the air-liquid interface in open-channel microfluidic systems allows for rapid molecule exchange between gas and liquid phases, making them suitable for trace detection of small molecules and potential chemical sensors.

Despite the versatile applications provided by open microfluidic systems, some common challenges still need to be overcome. For example, the high evaporation behavior of the air-liquid interface in any open-channel microfluidic system may lead to changes in sample concentration and channel drying, further disrupting the fluidic environment. The exchange of liquid raises concerns about sample or solution leakage into non-channel paths, resulting in sample waste and contamination. Moreover, the flow in open-channel microfluidic systems operates at atmospheric pressure, limiting fluidic pressure and preventing the provision of high pressure in the open-channel system. To address these challenges, common methods for decreasing evaporation include adding water droplets as sacrificial liquid surrounding the microfluidic systems or using humidified containers with 10–15 mL of water. Additionally, the addition of liquid may increase the air-liquid interface, affecting gas solubility in the microfluidic system. To avoid this new challenge, supplying gas concentration to enhance gas exchange is advantageous. Furthermore, placing open-channel microfluidic systems in confined transportation or cartridge cages is another strategy for reducing the effects of both sample evaporation and gas exchange. Therefore, integrating devices with humidified containers or confined cages to overcome the aforementioned challenges offers open microfluidic systems new possibilities for more applications in microfluidic technologies.

2.1.2. Pillar-Structured Microfluidic Chips

Pillar arrays are fabricated by using both top-down and bottom-up fabrication methods. These methods allow the control of the pillar geometries, such as diameter, pitch, height, and shape as well as the total number of pillars. Compared to open-channel microfluidics, pillar arrays significantly increase the internal surface area[99,100]; thus, they have been used for the separation of various biomolecules, such as bacterial DNA,[99] exosome,[101–103] double-stranded DNA,[104] genomic length DNA,[82] different size DNA,[105] albumin,[106] interleukin 6 (IL-6),[107] and hemoglobin.[108]

In one study, silicon micropillars having different geometries were fabricated by etching silicon wafers, and the micropillars were compared in terms of their DNA extraction performance. The device with the highest surface-to-volume ratio exhibited the highest DNA extraction efficiency.[99] In another work based on immunoaffinity, PDMS pillars were fabricated by using photolithography; the pillars were functionalized with multi-walled carbon nanotubes (MWCNTs) and CD63 antibodies to isolate exosomes, which are nanovesicles that are 50–150 nm in diameter

**ADVANCED
SCIENCE NEWS**

www.advancedsciencenews.com

**ADVANCED
MATERIALS
INTERFACES**

www.advmatinterfaces.de

and contain signaling proteins, nucleic acids (mRNA, miRNA, DNA), and a lipid bilayer.[101] Wang et al.[102] demonstrated the integration of micropillars with nanowires, ciliated micropillars, to isolate exosomes. Silicon micropillars were fabricated by using standard lithography and etching. However, the fabrication of the silicon nanowires included a complex silver nanopatterning process. A nanoscale deterministic lateral displacement (DLD) pillar array was fabricated using a silicon etching process. Bioparticles smaller than a critical size follow the laminar flow direction in the zigzag mode, whereas larger bioparticles are displaced laterally by the pillars.[109] In one study, the pillar array could separate double-stranded DNA in 100–10000 base pairs when the fluid velocity was optimized.[104] In another work, to concentrate genomic-length DNA at high flow velocities, a silicon DLD pillar array was fabricated and incorporated with polyethylene glycol (PEG), which compacts the DNA. PEG concentration and flow rate were optimized to purify the DNA in collection channels (**Figure 3**a).[82]

DLD pillar arrays made of PDMS were developed to separate albumin protein and polymer vesicles. Antibody-conjugated 1 µm size beads were loaded with a mixture of human serum albumin or vesicles and then introduced to micron-size pillars containing DLD device. Due to the electrostatic charges and changes in size, different concentrations of target-loaded beads were then separated.[106] In a promising study, PDMS pillars were functionalized with streptavidin. The blood samples from patients were incubated with antibody-coated latex beads to capture interleukin 6 protein, a sepsis biomarker prior to the chip study. The loaded beads were incubated with biotinylated antibody. This sandwich complex was introduced to the pillars and captured in the microfluidic platform.[107] As shown in Figure 3b silicon nanopillars were coated with 8-hydroxypyrene-1,3,6-trisulfonic acid (HPTS) and IgG antibody to capture different target proteins, such as green fluorescence protein (GFP), hemoglobin and cancer antigen 15-3 (CA-15.3). The captured proteins were released by illuminating the nanopillars with light (50 mW/cm^2) at 400 nm wavelength. The light triggering alters the pH of HPTS and, thus, affects the dissociation of the antibody. This light-controlled protein capture and release method has great potential for further protein purification and preconcentration applications.[108] Moreover, another microfluidic platform, including a nanopillar array and incorporating an electric field, was capable of separating larger (48.5 kbp) from smaller DNA (100 bp) fragments (Figure 3c).[105]

Pillar-structured microfluidic platforms require external pumps to control the fluid flow. Even though the microfluidic platforms are portable, and some fabrication methods can be low-cost the required external fluid pumps and signal read-out methods such as microscopes, lock-in amplifiers can be costly. Also, human/animal samples contain several different types of biomolecules other than then the target molecule which would result in clogging and contamination in the pillar structures. As a result of clogging applied fluid pressure can be increased which would result in leakages in the system. As a next step, the developed systems must be tested extensively with human and animal samples for repeatability and reliability. Research articles generally report experiments using patient and healthy samples but testing same sample multiple times and comparing the outputs of the system is lacking. **Table 2** summarizes some

parameters like fabrication methods, surface modification, chip materials, separated molecules, resolution, limit of detcion (LOD), throughput, repeatability, and flow rates used in the pillar-structured microfluidic separation studies.

2.1.3. Resin (Beads) Incorporated Microfluidic Chips

Resin materials generally offer a large surface area and high adsorption potential when integrated into microfluidic channel as stationary phase materials. Among them there are several resin materials used in chromatography; i) natural polysaccharides, including cellulose and agarose; ii) polymers, including trisacryl, polyacrylamide, methacrylate; and iii) stiff adsorbents, including inorganic substances such as alumina and silica, have become more widespread.

Chan et al.[112] presented a pressure-driven microchip for liquid chromatography using mesoporous silica as the stationary phase in high-performance liquid chromatography (HPLC). This device was tested to separate a dye mixture (fluorescein/Rhodamine B) and a biomolecule mixture (10 kDa dextran and 66 kDa BSA) to confirm the chip's performance. The retention time was 45 s for dextran and 120 s for BSA. Notably, the selectivity and resolution were reported to be 3.2 and 10.7, respectively. Shao et al.[113] engineered and tested a pneumatically controlled microfluidic device in one approach for establishing an efficient bead-based assays. This device was composed of a pillar array located concentrically with the fluid channel for capturing beads and also contained a pneumatically actuated elastomeric membrane for releasing the beads. Flow cytometry fluorescence detection verified the uniformity of reactions between packed beads. Further, mouse IgG was used as a model analyte, and a detection limit of 1 ppb confirmed the performance of this system. The authors anticipated that their device might effectively employ DNA and cell-related assays and diagnose diseases. Andar et al.[114] designed a customizable microscale chromatography system for protein purification to achieve therapeutic quality using affinity resins. The group reported the successful separation of comparable protein yields compatible with several different separation platforms, including those operating by ion exchange, size-exclusion, and buffer-exchange chromatography, through adaptations of the resin, design, and volume of the column.

Pinto et al.[115] developed a high-throughput microfluidic device to optimize capturing conditions of an anti-interleukin 8 mAb using CaptoTM MMC (2-benzamido-4-mercaptobutanoic acid) as a commercial multimodal resin. The results confirmed that this resin mainly exhibited electrostatically driven adsorption. The recovery yield value was 94.6% ± 5.2%, which was reported to be comparable with the recovery value of 97.7% ± 1.5% obtained from a conventional system. Furthermore, their approach resulted in the consumption of a very small volume of reagent (<50 µL) and resin (≈70 nL) within a very short assay duration (<1 min). Then, they introduced PDMS microchannels, including four conjugated sections: an inlet, a taller microchannel, a shorter microchannel, and an outlet. An interface section formed by the height difference between the two microchannels promoted the trapping and packing of beads, and this resulted in about 100% trapping efficiency. Nevertheless, a
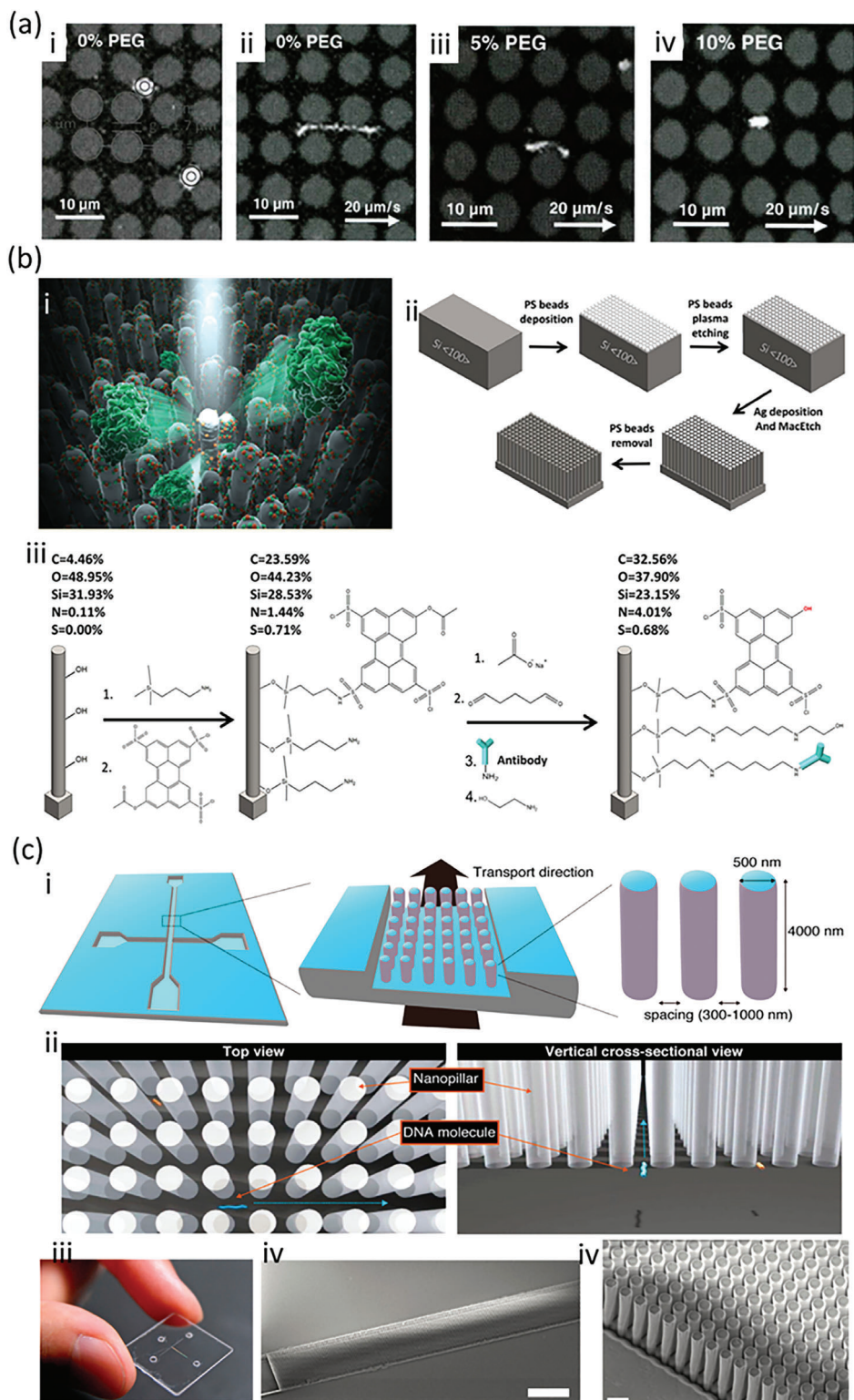
**ADVANCED
SCIENCE NEWS**

www.advancedsciencenews.com

**ADVANCED
MATERIALS
INTERFACES**

www.advmatinterfaces.de

Figure 3. a) The impact of PEG concentrations on the elongation of 166 kbp T4 DNA in a pillar array. Adapted with permission.[82] Copyright 2015, American Physical Society. b,i) Light-controlled collection and release of biomolecules using silicon nanopillars, as well as a ii) schematic representation of the fabrication process and iii) antibody immobilization with X-ray photoelectron spectroscopy (XPS) analysis results. Adapted with permission.[108] Copyright 2019, American Chemical Society. Note: PS (Polystyrene). c) Schematic illustrations of the microfluidics and nanopillars. i) Embedded nanopillars in a microchannel (substrate: fused silica). ii) DNA molecules migration behavior between nanopillars. Blue arrows show the direction of migration). iii) The microchannel Photo of the microfluidics. iv,v) SEM images of the nanopillars (scale bars, 1 µm). Adapted with permission.[105] Copyright 2015, American Chemical Society.

**ADVANCED
SCIENCE NEWS**

www.advancedsciencenews.com

**ADVANCED
MATERIALS
INTERFACES**
Open Access

www.advmatinterfaces.de

Table 2. Pillar-structured microfluidic-based molecular separation.

Fabrication method and surface modification	Chip materials	Biomolecules	Resolution or LOD	Throughput	Repeatability	Flow rate	Ref.
Deposition of polystyrene bead monolayer (PS) on silicon wafer and oxygen plasma treatment to create a porous SiNP array	Silicon wafer and PS, to produce porous Si nanopillars vertical arrays (SiNPs)	Protein eGFP, hemoglobin, CA-15.3,	Selective separation of low abundant proteins from complex biosamples	The separation of specific protein markers from whole blood samples can be performed within <10 min.	High	NR	[108]
Photolithography	PDMS micron sized beads	Protein IL-6,	LOD: 127 pg mL^{-1}	90%	NR	20 µL min^{-1}	[107]
Photolithography, electron beam lithography, and vapor-liquid-solid (VLS) growth technique for growth of the nanowires.	SnO$_2$ (3D nanowire)	DNA, Protein, RNA	DNA 0.93-0.99 Protein: 1.5-1.99 RNA: 0.41-1.38	Analyze DNA mixture in 50s, protein mixture in 5 s, and RNA mixture in 25 s.	NR	NR	[60]
Laser interference lithography and Photolithography (nanofluidic)	Silica nanopillars (Label-free)	DNA(used for proteins, amino acids, extracellular vesicles, and cell)	Requires further investigation for enhancing sensitivity and realizing high throughput.		High	NR	[110]
Electron Beam lithography	Quartz nanopillars (Equilibrium and nonequilibrium transport)	DNA	0.6-0.8 (The narrower spacing provided better resolution)	Separated four different sizes of DNA molecules (48.5, 2.2, 1 kbp, 100 bp) within 60 s	NR	NR	[105]
Iterative lithographic and reactive-ion etch (RIE) processes	Si (Velocity dependence, length-based 100 bp 75% recovery)	double-stranded DNA	size-selective resolution of 200 bp	75%	NR	100–400 µm s^{-1}	[104]
Photolithography and Soflithography	PDMS	Can be used for the separation of, proteins, DNA, RNA and cells.	Quasi-resolution of 34 nm for DLD-S1 and 17 nm for DLD-S2	Method is fast and efficient, with ability to process large number of particles in a short time.	NR	NR	[106]
Photolithography and deep anisotropic etching	Silicon	DNA	NR	Up to 0.25 gL/h (at 40 µm/s	NR	Moderate flow velocities	[111]

limitation of this system was the heterogeneous size distribution of the chromatography beads obtained in suspension since smaller beads may have passed through the gap at the interface of the two microchannels.

The researchers attempted to sieve the beads to address this limitation and get a narrow size distribution. Finally, they successfully identified nucleic acids of the mycotoxin aflatoxin B1; obtained much better detection limits for free prostate-specific antigen (a specific prostate cancer biomarker); and achieved antibody purification.[116] Recently, they studied the development of a portable, microbead-based microfluidic system for providing high-speed screening of chromatography conditions (**Figure 4**).[117] This system evaluated the separation of fluorophore-labeled monoclonal antibodies from a cell culture supernatant. Using soft lithography, they fabricated a PDMS microfluidic chip and integrated Capto-MMC functionalized-

agarose beads (average size: 75 µm) in the micro-columns as the stationary phase. The microfluidic chip had a taller microchannel packed with beads and a shorter microchannel to avoid the movement of these beads during the chromatography process. Additionally, adsorption and elution kinetics were determined successfully in real time by coupling the device with amorphous silicon photodiodes. They claimed that their results were consistent with those obtained from a microscope or conventional chromatography system.[117] Afterward, in a 2019 publication,[118] they designed a microfluidic system composed of three individual chambers packed with different chromatography beads, such as protein A, CM Sepharose, and Q Sepharose, to determine recovery yield and purities quantitatively. Here, an artificial mixture, containing immunoglobulin G (IgG) and BSA, was used to evaluate the quantitative performance of their system. With that, mAb purification with
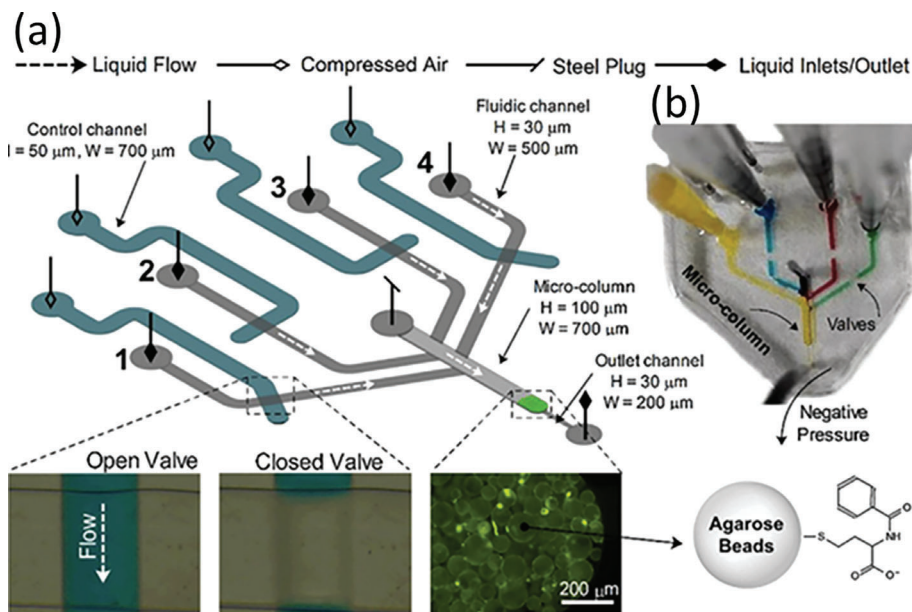
**ADVANCED
SCIENCE NEWS**

www.advancedsciencenews.com

**ADVANCED
MATERIALS
INTERFACES**
Open Access

www.advmatinterfaces.de

Figure 4. a) Functionalized agarose beads were packed into the micro-columns of microfluidic devices, and the capturing efficiency of this device was optimized for the target monoclonal antibody. b) PDMS microchip has selective flow for four colored solutions towards the micro-column. Reproduced with permission.[117] Copyright 2018, Elsevier.

low molecule consumption was achieved within <3 min. Importantly, the minimum detectable mass of labeled IgG was 0.66 ± 0.24 ng nL^{-1} resin and that of BSA was 1.86 ± 1.36 ng nL^{-1} resin. Compatible with the use of complex matrices such as cell culture supernatants, this technique can also be integrated with valves and optical sensors.[118]

Landers et al.[119] introduced a microfluidic device based on the pH-responsive charge of chitosan for low-volume DNA extraction from complex biological fluids, such as human blood. The whole blood DNA extraction efficiency of microchip was found to be $75 \pm 4\%$. This platform may show great potential for combining this device with more advanced on-chip sample processing steps (e.g. PCR) and for the advanced integration of genomic analysis on a microchip. Then, they proposed using chitosan-coated silica beads (average size 15–30 μm) to obtain enhanced RNA extraction efficiency. The use of chitosan-coated silica beads resulted in approximately fourfold increase in the extraction efficiency of RNA for biological samples compared to plain silica beads. Their findings indicated that this system enables higher RNA extraction and purification efficiencies.[52] They fabricated a Borofloat glass microfluidic device packed with MagneSil paramagnetic silica particles. This microdevice successfully purifies human genomic DNA from dilute whole blood samples. Furthermore, it was used to extract mitochondrial DNA from diluted whole blood and degraded blood stains. Their system provided a sample volume reduction of 50-fold and a DNA concentration increase of 15-fold.[120] Afterward, they used silica and chitosan phases in a Borofloat glass microfluidic device. While the silica phase allowed substantial volume reduction, the chitosan phase provided more precise extraction. However, this procedure resulted in 50- and 14-fold reductions in DNA and RNA concentrations, respectively.[120]

Previously, the use of stimuli-responsive polymers was introduced to generate "smart" beads and reversibly to immobilize these smart beads on the walls of microfluidic channels as an effective strategy for biochemical analysis. Malmstadt et al.[121] engineered a heating tool integrated into a microfluidic device to adhere biotin-coated poly(N-isopropylacrylamide) (PNIPAAm) nanobeads (average size 100 nm) within the microchannel. Herein, the beads aggregated and adhered to the microchannel wall when the temperature of the microchannel was higher than the lower critical solution temperature (LCST) of the PNIPAAm nanobeads. Accordingly, a reduction in the temperature to below the LCST of the PNIPAAm allowed a break-up of the aggregates and the release of beads into the fluid.

It is worth mentioning that a high specific surface area, shortened diffusion distances along constricted fluid paths among neighboring particles and high adsorption capacities in microfluidic systems holds great prominence for effective performance. Besides, this technique offers extremely low reagent consumption and extremely fast output of results. However, developing resin-based microfluidic separation systems requires diverse chemistries for materials synthesis, ligand immobilization, and surface functionalization.[36,122] In addition, their use at analytical scale may be limited because of low mechanical strength especially in the case of soft gels, difficulty in packaging, the need of Frits to keep packaged resins intact, generation of high pressure and low mass transfer.[36,122]

Kim et al.[53] developed a microchip with two microchambers integrated by a microchannel loaded with agarose gel for target-binding single-stranded DNA (ssDNA) isolation and enrichment. In addition, human immunoglobulin E (IgE) modified beads were added to the isolation chamber. The temperature in the chamber was increased for the separation of ssDNA from the beads, and DNA was moved to the second chamber by electrophoresis. A higher concentration of DNA was detected in

ADVANCED
SCIENCE NEWS

www.advancedsciencenews.com

ADVANCED
MATERIALS
INTERFACES

Open Access

www.advmatinterfaces.de

Table 3. Summary of resin (beads) incorporated microfluidic chips for separation and/or purification of different biomolecules.

Fabrication method	Chip material and design	Biomolecules	Resolution or LOD	Throughput	Repeatability	Flow rate (and assay time)	Ref.
Photolithography and Soflithography	Three PDMS layers: i. top PDMS layer with number of microfluidic ports and separation capillary, ii. two polyethylene membranes incorporated to second layer of the chip as porous frits to keep silica particles inside HPLC column, iii. silica particles inside the HPLC column.	Dextran (10 kDa) and BSA (66 kDa)	Degree of separation between neighboring solute peaks: 10.7	NR	NR	0.23 µL s^{-1} (Dextran 45 s BSA 120 s)	[112]
Photolithography and Soflithography	The microfluidic PDMS chip including three layers: i) the micro filter and bead chamber layer, ii)the pneumatic control layer and iii)the glass substrate	Mouse IgG	LOD: was 0.1 ppb	NR	Good device reliability and repeatability	Bead injection: 10 µL min^{-1}, Bead flushing: 20 µL min^{-1}, (Total assay time: less than 25 min)	[113]
CO$_2$ laser printer	The microfluidic chip including three PMMA layers: i) A top PMMA layer (1.5-mm thick) with a large circular slot in 6 mm of diameter toward the outlet end that has PTFE frits, ii) A middle PMMA layer (1-mm thick) with the microchannel for accommodating the chromatography resin, and iii) A bottom PMMA (1.5-mm).	Granulocyte colony-stimulating factor (G-CSF)	NR	Similar or better yields compared to conventional columns	NR	0.1-0.4 mL min^{-1} (Purification time 10–20 min)	[114]
photolithography and Soflithography	PDMS microchannels consisted of four sections: i)the inlet, ii) a taller microchannel, iii) a shorter microchannel, and iv) the outlet	An anti-IL8 mAb	NR	A recovery yield of 94.6 ± 5.2%	High	15 µL min^{-1} (Residence time 0.28 s, Assay time 2 min)	[115]
photolithography and Soflithography	The PDMS microchannels consisted of four conjugated sections. i) the inlet, ii) a channel with larger height, iii) a channel with smaller height, iv) the outlet.	Mycotoxin aflatoxin B1 (AFB1)	LOD: 10 ng mL^{-1} PSA.	NR	NR	15 µL min^{-1}	[116]
photolithography and Soflithography	PDMS	Fluorophore-labeled monoclonal antibodies	NR	NR	NR	10 µL min^{-1} (Assay time 3 min)	[117]

the enrichment chamber with an increasing number of enrichments. After the second and third enrichment cycle, the intensities of the bands enhanced by around 72.1% and 153.3%, respectively, than the band of intensity after the first cycle. This system was used successfully for selective ssDNA detection from dilute and complex biological samples. Similarly, a PDMS and printed circuit board (electrodes substrate)-based microchip, including agarose gel, was introduced by Ghanim and Abdullah for DNA separation and detection.[123] The DNA pattern obtained from this microchip was consistent with conventional gel electrophoresis. They then developed a miniaturized microchip for

counter electrode (CE) by utilizing agarose gel as the separation medium. Herein, a glass/ PDMS microchannel equipped with platinum electrodes was used. This device provided very sensitive separation (higher than 100 nA) with a very low electric field of 12 V cm^{-1} using 1.5 µL of sample volume, which was favorable for DNA separation. Furthermore, the sensitivity of this method was higher than 100 nA with a separation time of ≈30 min. **Table 3** summarizes some parameters such as fabrication methods, chip materials and design, separated molecules, resolution, LOD, throughput, repeatability, and flow rates used in the resin (beads) incorporated microfluidic separation studies.

**ADVANCED
SCIENCE NEWS**

www.advancedsciencenews.com

**ADVANCED
MATERIALS
INTERFACES**
Open Access

www.advmatinterfaces.de

2.1.4. Monolith-Incorporated Microfluidic Chips

Research for discovering new chromatography materials led to the development and production of new materials, coined "Monolith". A monolith is a single piece of a stationary phase with a highly interconnected porous network.[124] This continuous, single-structural porous material was first applied in a chromatographic separation technique in the early 1990s.[125] Afterward, the utilization of monolith technology has increased due to the raised demand for materials with micro-nano dimensions in separation, molecular detection, and production.[126] Because of high pore interconnectivity, monoliths cause the high mass transfer of molecules, which leads to the rapid separation of molecules.[127] Moreover, monoliths are an unsurpassed material for separation applications due to high flow rate tolerance and satisfactory back-pressure capacities.[128] Their surface chemistry and porosity can be manipulated with synthesis and surface modification techniques for specific applications.[129] Also, monoliths have technical advantages since they can be fabricated by in situ polymerization and possess adjustable permeability properties, thus propagating the separation of proteins, peptides, nucleic acids, and other biomolecules.[130]

In the production of monolithic microfluidics, photolithography, and soft lithography fabrication techniques are the most employed methods, which can vary depending on the material chosen for the microfluidic chip material and the monolith to be used.[36] Polymers, copolymers, as well as traditional materials like PMMA, glass, and resin, are commonly utilized as chip materials. In particular, materials such as cyclic olefin copolymer (COC) with high UV permeability, which are suitable for the UV polymerization technique used for monolith production, are frequently employed.[131]

Both monolith material composition and synthesis method are significant factors for separating biomarkers in microfluidic devices. Based on the chemical nature of their precursor materials, monoliths can be broadly classified as i) organic polymer, ii) inorganic (silica), and iii) hybrid-based monoliths.[132,133] Organic polymer-based monoliths can be fabricated using UV or thermally-initiated free-radical polymerization of a mixture that contains monomers, cross-linkers, porogens, and radical initiator.[134] The UV-assisted approach offers various benefits, such as a shorter polymerization time, simple site-specific immobilization, and surface modification of the monolith. For the fabrication of inorganic silica-based monoliths, the conventional approach is the sol-gel process, including hydrolysis and polycondensation.[133] These sol-gel monoliths can provide high porosity and excellent mechanical stability since they do not swell in organic solvents. However, thermal treatments required for their preparation limit their usage.[128] On the other hand, hybrid monoliths, which contain both organic and inorganic structures, can be prepared easily within microchannels by combining synthetic routes with chemically reactive substances.[135]

As in chromatography techniques, monolith-based microfluidic chips can separate proteins and peptides. For instance, a mixture of proteins consisting of ribonuclease A, cytochrome c, myoglobin, and ovalbumin, was successfully separated within polyimide microchips packed with a lauryl methacrylate-based (LaMA) monolith.[56] The high porosity of the monolith material ensures higher linear flow velocities and, therefore, pro-

vides faster separations. Octadecylated (C_{18}) silica-based monolith was used to extract six proteins: insulin, cytochrome C, lysozyme, myoglobin, b-lactoglobulin, and hemoglobin, in a glass microchip.[136] A sol-gel process was used to derive the monolithic porous silica, and then this monolith was further modified with C_{18} to enrich protein binding. The proteins were extracted with high recovery rates (94.8–99.7%) using molecular weights and isoelectric points of proteins as a basis for separation within 5.33 min retention time. Monolith-integrated microfluidic devices can also be developed for on-chip sample preparation stages, enhancing sensitivity and shortening separation and analysis time. For instance, a butyl methacrylate-based (BMA) monolith fabricated in a cyclic olefin copolymer (COC) microfluidic device was reported for on-chip labelling and solid-phase extraction (SPE) of heat shock protein 90 (HSP90) and BSA.[14] 1 µg mL^{-1} of protein mixture was rapidly (30-55s) eluted from the monolithic column. This column effectively concentrated the proteins, as indicated by the calculated enrichment factors of 11-fold for HSP90 and sixfold for BSA compared to the absence of pre-concentration. In another approach, the methacrylate-based monolith was synthesized with Glycidyl methacrylate (GMA) monomer using UV-induced graft polymerization to separate the BSA and ovalbumin mixture on chip.[137] The methacrylate monolithic polymer was modified with weak anionic ligands for separating the proteins with respect to their ionic strengths. By doing so, BSA (1 mg mL^{-1}) and ovalbumin (1 mg mL^{-1}) with a 1:1 v/v ratio were separated using anion-exchange liquid chromatography. Furthermore, a thiol-ene (tetrathiol and triallyl) monolith microfluidic chip was fabricated for separating, purifying, and ionizing seven different proteins (insulin, hemoglobin, beta-lactoglobulin, lysozyme, ubiquitin, cytochrome c, and carbonic anhydrase).[138] Two-dimensional separation could also be achieved using monolithic microfluidic devices. For instance, BMA-EDMA-based monolithic polymers, used both as frits and separation media, were fabricated in a microfluidic glass chip to separate five peptides (Gly-Tyr, Val-Tyr-Val, Met-Enkephalin, Leu-Enkephalin, and angiotensin II).[139] Those peptides were separated from the column for at least 50 min at a flow rate of 15 µL min^{-1}.

An alternative construction to provide affinity-based separation could be achieved by integrating molecularly imprinted monolith polymers into the microchip channel.[140] It was also utilized in the formulation of monolith design in addition to being integrated into the composition of dimethyl amino ethyl methacrylate (functional monomer) and hydroxyethyl methacrylate (HEMA) (monomer). For affinity-based separation by imprinted monolith, human serum albumin (HSA) was employed as a target molecule, and ≈85% of imprinted HSA could be successfully recovered. Moreover, it was demonstrated that the designed material exhibited high selective (>98% selectivity) recognition for HSA within a mixture of other proteins from diluted human plasma.

GMA-based monolith, whose surface was immobilized with the antibody specific to ferritin, was also integrated into a 3D-printed microfluidic chip with UV polymerization technique.[141] The ability of this monolith to specifically bind ferritin molecules was tested using a twofold higher concentration of another PTB biomarker, corticotropin-releasing factor (CRF). The results showed that the monolith only gives fluorescence signals

**ADVANCED
SCIENCE NEWS**

www.advancedsciencenews.com

**ADVANCED
MATERIALS
INTERFACES**

www.advmatinterfaces.de

for ferritin molecules, indicating high selectivity for this PTB biomarker. Besides, the recovery rate of this monolithic separation is ∼50% for the extracted sample.

Another microfluidic device with a GMA-based monolith was demonstrated for the extraction of three PTB biomarkers from human blood serum.[142] These PTB biomarkers which are corticotropin-releasing factor, thrombin-antithrombin complex, and tumor necrosis factor-α receptor type 1, were selectively separated from a serum mixture in 10 s with concentrations of 100, 60, and 100 nM, respectively. Furthermore, LaMA-based monolith was successfully used in the 3D printed microfluidic device for SPE and detecting different biomarkers, including ferritin, corticotropin-releasing factor, defensins, lactoferrin, and tumor necrosis factor-α receptor type 1 within 30 min.[143]

Immunoglobulin G (IgG) is a major type of antibody that exists in all body fluids. It is extensively used to detect and treat various diseases.[144] For instance, an IgG-coated GMA-based monolith in a PDMS microchip was used to separate and detect fluorescent-labeled IgG antibodies to as low as 4 ng mL^{-1} concentration levels in phosphate-buffered saline.[145] This limit was 10 ng mL^{-1} for sandwich immunoassay for the same microfluidic device. This system has not required any incubation steps and the assay can be performed within 30 min. IgG was also extracted using monolithic-based metal ion affinity chromatography.[146] The monolith surface constructed from hydroxyethyl methacrylate was immobilized with Cu (II) metal ions and used as a proper chelating agent. The adsorption capacity (27.8 mg g^{-1} monolith) was higher than that for the monolith without metal ions.

Monolithic columns can be implemented in microfluidic chips for pre- or post-processes. For instance, the poly-allyl phenoxyacetate (AP) monolith and lysine-glycine-glycine (KGG) imprinted poly-trimethylolpropane trimethacrylate (poly-TRIM) monolith were used for protein fractionation as the pre-process and peptide extraction as the post-process, respectively, for peptide separation on chip.[147] This platform could remove the MCF-7 proteins with 94.6% separation efficiency and recover 90.8% of the KGG peptide. The platform demonstrated the capability to process an entire cell sample in a significantly shorter duration (≈9.6 h) than traditional processing methods, which typically take ≈13.3 h. Another implemented GMA-based monolith structure to a microfluidic chip was developed for separating N-glycans from serum samples using peptide-N-glycosidase (PNGase).[148] This chip was able to perform chromatographic separation of all types of N-glycans with 90% efficiency and >60% recovery in ≈30 min.

A COC-based microfluidic chip was designed for nucleic acid capture and purification.[149] The microfluidic channels were coated by chitosan-functionalized GMA monolith for pH-modulated DNA capture. Approximately 10% of the DNA was retained in the control monolith during loading and washing steps when compared with the chitosan-functionalized monolith. The loading capacity of the chip was more than 360 µg mL^{-1}, the DNA capture efficiency was <99% and the DNA recovery efficiency was higher than 54.2% ± 14.2% within a 24 min elution time. A polypropylene-based microfluidic chip was used with a GMA and poly(ethyleneglycol) diacrylate (PEGDA) monolith structure for antibiotic resistance gene detection.[150] The polymer monolith was modified with the complementary sequence of the target oligonucleotide (Verona Integron Mediated Metallo-

β-lactamase gene). The device could perform 1 pM target oligonucleotide extraction in a 100 µL sample solution with an 83% recovery efficiency within 12 min. The same technology with different monolith compositions (Poly(lauryl methacrylate-co-ethylene dimethacrylate) and poly(styrene-co-divinylbenzene)) was used for extraction of the target DNA of *Klebsiella pneumoniae* with the carbapenemase antibiotic resistance gene.[151] Capture efficiency is 86% for the target DNA. However, low recovery of the target DNA (2.5%) was achieved within 18 min in 100 µL of the sample solution.

Table 4 summarizes monoliths used for different molecular separations applications. Monolithic microfluidics offers remarkable benefits attributed to its high surface area, porosity, permeability, and selectivity. In addition, monoliths are well suited to surface modifications, easy fabrication, and in situ preparation in micro channels.[128] SPE is the most commonly preferred technique since highly porous monolithic materials enable the passage of solvents by adsorbing the biological molecules on themselves. In addition, affinity and immunoassay-based separation are frequently used techniques, as monolithic structures allow very effective surface modification.[128] Despite its benefits, monolith fabrication is a delicate process, and controlling the porosities of monoliths could be a challenge. If the process parameters do not adjust accurately, this process can result in low surface area or low binding capacity on the monolith structure, and as a result, the separation efficiency can decrease.[152] The monolith synthesis technique can also cause difficulties in ensuring material integrity. Although monolith formation with an in situ polymerization technique is useful for microfluidic chips, the chip material should be chosen precisely for the polymerization.[135] In addition, the chip material must have surface properties suitable for biosample separation and monolith anchoring. Microfluidic chips could be incorporated further with composite/hybrid monolith materials, such as monomers embedded with nanoparticles, nanosheets, nanotubes and graphene, phosphopeptide enriched monomers, and molecularly imprinted monomers, for better extraction properties that could increase their usages.[128,153]

2.1.5. Nanowires Incorporated Microfluidic Chips

Highly stable nanowires can be selectively self-assembled on or attached to the microfluidic system. In one study, nanowire arrays integrated into microfluidic platforms formed 3D nanopore structures to filter DNA molecules (48.5 and 166 kbp). The nanowires were fabricated in a bottom-up approach, whereas a gold catalyst-assisted pulse laser deposition method was used to grow SnO$_2$ nanowires on fused silica microchannels. The size of the nanopores was controlled by regulating the number of nanowire growth cycles. The larger DNA molecules could not pass through the nanowire structure, whereas smaller DNA fragments were capable of migrating under applied electric fields.[62] The same approach was implemented for the separation of RNA and proteins as well (**Figure 5**a).[60]

Protein molecules (20–340 kDa), RNA molecules (100–1000 bases), and DNA molecules (50–1000 bp) showed different mobilities in the nanowire structure, and thus the separation of biomolecules was possible. As explained in the subsection on

Table 4. Summary of monolith incorporated microfluidic chips for separation of different biomolecules.

Monolith type	Preparation of monolith	Monolith surface modification	Microfluidic chip material	Used separation technique	Separated analytes	Efficiency	Recovery	Processing time	Ref.
AP + EDMA, poly-TRIM	Thermally initiated polymerization	Peptides	Glass	Reverse-phase chromatography + SPE	MCF-7 proteins, KGG peptide	94.6% removal efficiency for MCF-7 cell protein	90.8% recovery for KGG	9.6 h	[147]
BMA + EDMA	UV polymerization	–	COC	Affinity SPE	HSP90 and BSA	Enriched 11-fold for HSP90, 6-fold for BSA	NR	30-55 s	[14]
BMA + EDMA	UV polymerization	–	Glass	Reverse-phase chromatography	Gly-Tyr, Val-Tyr-Val, Met-Enkephalin, Leu-Enkephalin, and Angiotensin II	NR	NR	50 min	[139]
BMA, OMA, LaMA+ EDMA	UV polymerization	–	COC	SPE / Electrophoresis	P1, Lactoferrin, and Ferritin	NR	NR	15-20 min	[154]
GMA + BMA + EDMA	UV polymerization	Chitosan	COC	Charge-switch-based nucleic acid capture and purification	PUC 19 plasmid DNA	Capture efficiency <99%,	Recovery efficiency 54.2% ± 14.2%.	24 min	[149]
GMA + EDMA	UV polymerization	A weak anionic ligand (Diethylamine)	PDMS	Ion exchange liquid chromatography	BSA and Ovalbumin	NR	NR	NR	[137]
GMA + EDMA	UV polymerization	Antibodies	COC	Immunoaffinity extraction + Electrophoresis	Ferritin and Lactoferrin	NR	NR	~30 min	[155]
GMA + EDMA	UV polymerization	Antibodies	PEGDA	Immunoaffinity extraction	Corticotropin-releasing factor, thrombin-antithrombin complex and tumor necrosis factor-α receptor type 1	NR	NR	NR	[142]

(Continued)

Table 4. (Continued).

Monolith type	Preparation of monolith	Monolith surface modification	Microfluidic chip material	Used separation technique	Separated analytes	Efficiency	Recovery	Processing time	Ref.
GMA + EDMA	UV polymerization	Antibodies	3D printed resin (Nitrophenyl phenyl sulfide)	Immunoaffinity extraction	Ferritin and Corticotropin-releasing factor	NR	~50% recovery of extracted sample	NR	[141]
GMA + EDMA	UV polymerization	IgG	PDMS	Direct / sandwich immunoassay	IgG and H1N1 influenza virus	NR	NR	30 min	[145]
GMA + EDMA	Thermally initiated polymerization	PNGase F enzyme	–	Liquid chromatography	N-glycans	>90% labeling efficiency	>60% recovery	~30 min	[148]
GMA + EDMA	UV polymerization	Oligonucleotides	Polypropylene	Sequence-specific capture	Klebsiella pneumoniae carbapenemase gene	86% capture efficiency	2.5% recovery	18 min	[151]
GMA + PEGDA	UV polymerization	Oligonucleotide	Polypropylene	SPE	Verona Integron Mediated Metallo-β-lactamase gene	NR	83% recovery	12 min	[150]
HEMA + DMAE* + MBAA* + PPDAA*	UV polymerization	Human serum albumin	PDMS	Molecularly imprinted polymer-based SPE	HSA	NR	~85% recovery	NR	[140]
HEMA + N, N′-DATA* + PPDA*	Thermally initiated polymerization	Cu (II) metal ions	Silica	Affinity chromatography	IgG, Transferrin, and Albumin	NR	NR	NR	[146]
LaMA + EDMA /OMA + EDMA	UV polymerization	–	3D printed resin (Nitrophenyl phenyl sulfide)	SPE	Peptides (1,2,3), Ferritin, Corticotropin-releasing factor, Defensins, Lactoferrin, Tumor necrosis factor-α receptor type 1, and Thrombin antithrombin complex	>70% for ferritin, >60% for TAT, >70% for lactoferritin, >30% for TNF, >20% for CRF	NR	30 min	[143]

(Continued)

Table 4. (Continued).

Monolith type	Preparation of monolith	Monolith surface modification	Microfluidic chip material	Used separation technique	Separated analytes	Efficiency	Recovery	Processing time	Ref.
LaMA + EDMA	Thermally initiated polymerization	–	Polyimide	Liquid chromatography	Ribonuclease A, Cytochrome c, Myoglobin, Ovalbumin, and Peptides	NR	NR	2.5 min	[56]
OMA + EDMA	UV polymerization	–	COC	SPE / Electrophoresis	P1 and Ferritin	Enriched 50-for for single-channel SPE, more 15-fold for integrated electrophoresis	NR	5 min	[156]
Silica-based monolith	Sol-gel method	Octadecylsilyl (C18)	Glass	SPE	Insulin, Cytochrome C, Lysozyme, Myoglobin, b-Lactoglobulin, and Hemoglobin	NR	94.8–99.7%	NR	[136]
Tetrathiol and Triallyl	UV polymerization	–	PMMA	Reverse-phase chromatography	Insulin, Hemoglobin, Beta-lactoglobulin, Lysozyme, Ubiquitin, Cytochrome C, and Carbonic Anhydrase	NR	NR	NR	[138]

*Dimethyl amino ethyl (DMAE), Methylene bisacrylamide (MBAA), Piperazine diacrylamide (PPDAM), diallyltartramide (DATA), Piperazine diacrylate (PPDA).
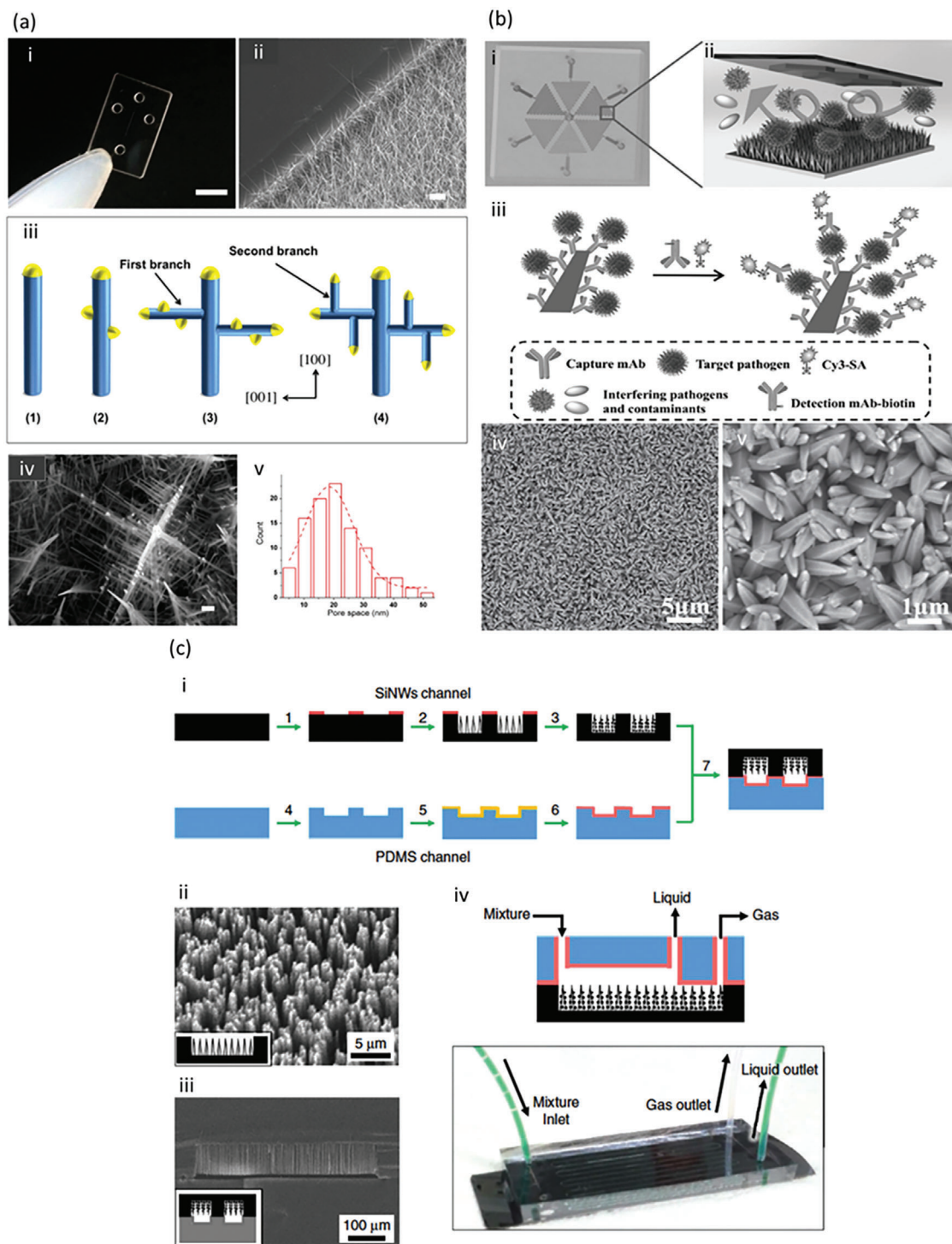
Figure 5. a) 3D nanowire structures. i) Photo of the microfluidic device (scale bar 5 mm). ii) SEM image of the nanowires (SnO$_2$) embedded in a microchannel (scale bar 1 µm), iii) Au catalyst 3D nanowire growth, iv) SEM of 3D nanowires structures (scale bar, 100 nm), and v) pore size distribution. Adapted with permission.[60] Copyright 2015, Springer Nature. b,i–iii) ZnO nanorod-based microfluidic device for pathogen capture: i) Top view of the microfluidic chip. ii) The sandwich immunoassay for pathogen detection on a single ZnO nanorod inside the ZnO-NIM. iii) The pathogen capture process on the 3D nanostructured ZnO surface conjugated with capture monoclonal antibody (mAb). iv,v) SEM images of the synthesized ZnO nanorods on glass slide: iv) low and v) high magnification. Adapted with permission.[67] Copyright 2017, Wiley-VCH. c, i) Schematic illustration of fabrication steps of the SiNW microseparator and the microfluidics. Steps: 1: patterning photoresist layer (Az) on Si. 2: SiNW pattern. 3: superamphiphobic SiNWs pattern. 4: spin-coating polyvinylsilazane on PDMS channel treated with plasma. 5: UV exposure. 6: thermal bonding PDMS channel on the SiNW channel. ii,iii) SEM images of the SiNW, and iv) a photo of the microfluidic device. Adapted with permission.[66] Copyright 2016, Springer Nature.

**ADVANCED
SCIENCE NEWS**

www.advancedsciencenews.com

**ADVANCED
MATERIALS
INTERFACES**

www.advmatinterfaces.de

pillared structures, nanowires were fabricated on pillars to increase the surface area to better trap exosomes.[102]

Zinc oxide (ZnO) materials have promising advantages when used in microfluidic platforms; they can be synthesized in microfluidic reactors and can be used for various applications, such as in trapping and photocatalysis.[63] It was shown that a ZnO nanowire-embedded PDMS microfluidic platform collected urinary extracellular vesicles and enabled miRNA extraction with higher efficiency than traditional ultracentrifugation.[58] A ZnO/Zn(OH)F nanofiber array was fabricated inside a glass capillary to isolate hemoglobin, a histidine-rich protein, from human blood.[64] Three different ZnO nanostructures (sharp, rod, and hexahedral-puncheon) were grown in microfluidic channels and tested for protein capture efficiency after surface functionalization. Sharp ZnO structures presented the highest capture efficiency among the rod and hexahedral ZnO structures.[65] Randomly oriented ZnO nanorods were fabricated on a glass slide and improved the fluorescence signal. The microfluidic platform consists of 6 channels functionalized with different antibodies against viruses (Figure 5b).[67] Another study on silicon nanowires demonstrated the separation of a highly carcinogenic chemical, chloromethylmethyl ether (CMME), from a gas-liquid mixture. This method can be extended for safely handling other carcinogenic and toxic reagents (Figure 5c).[66]

The network of 3D nanowires has a large surface-to-volume ratio, which increases the capture area. Nanowires can be fabricated using both top-down and bottom-up techniques. However, microfabrication of nanowires requires costly methods such as photolithography, electron beam lithography, vapor-liquid-solid growth technique, deposition, and reactive ion etching. **Table 5** summarizes some parameters like fabrication methods, chip materials and design, separated molecules, resolution, LOD, throughput, repeatability and flow rates used in the nanowire incorporated microfluidic separation studies.

2.1.6. Liquid–Liquid Extraction

Hydrometallurgy and liquid–liquid (L/L) extraction serve as the foundation for numerous extractions and refining processes aimed at separating molecules or compounds from mixtures with varying solubility. L/L extraction, characterized by its high level of complexity, presents challenges when studying molecular phenomena at the liquid surface. It is widely recognized that two key factors affecting extraction efficiency are the transmission length and the interfacial area. Therefore, shorter transmission lengths and larger interfacial areas result in increased extraction efficiency. Furthermore, downsizing chemical processes, can offer numerous advantages. This method requires only a small volume, enabling analysis with minimal sample quantities and eliminating the need for costly experiments. Sato et al.[68] studied the microfluidic extraction between two immiscible liquids for the first time. In the following years, microfluidic liquid–liquid extraction has attracted numerous researchers and has been widely used to separate compounds and prepare samples.[69–71,160–164] Ciceri et al.[165] reported that one of the main areas for future development is the direct integration of traditional diagnostics with on chip method. While processes involving mixing and chemical reactions have been successfully down-

sized to the micrometer scale, there are challenges in performing all operations within a single microfluidic device, particularly when separations are required. One reason for this is that gravity-driven phase separation is not feasible due to the predominance of surface over body forces. Therefore, alternative forces must be explored to achieve on-chip separation. L/L extraction has garnered more attention in microchannels because of the short molecular diffusion distances and efficient liquid/liquid contact.[72,166]

L/L Extraction Using Micro-Fluids: Fast and cost-effective studies of L/L extraction processes can be conducted using a fully automated and integrated microfluidic method. Given that the contact and separation of molecules and compounds are closely tied to the multiphase flow pattern, some information on flow patterns will be provided in this section.

- **Parallel Flow**: In microchannels, due to the dominance of surface tension and friction over gravity, two fluids can flow together irrespective of their density.[167] Kitamori's group successfully analyzed the parallel flow in quartz glass microchips using a thermal lens microscope.[168] Liquid-liquid extraction is a standard technique for purifying DNA directly from cells. While DNA remains in the aqueous phase, membrane components migrate to the interfacial area between the phases.[73] In chip-based liquid-liquid extraction, fast velocities stabilize parallel flow patterns, while slow velocities increase segmented flow, resulting to slug flow. Since extraction in microchannels relies solely on diffusion within parallel flow, both interfacial area and diffusion length have a significant impact on the time needed to reach equilibrium.[169] The Intermittent separation walls positioned in the center of the microchannel between the two phases can enhance the extraction efficiency two- or three-fold. This improvement can be attributed to the slight fluctuation of the interface between the partition wall sections that led to improved mixing.[170] In parallel flow, another way to stabilize the interface between the two liquid phases is to add a microporous membrane, which results in very high flow stability without separating the next phase.[171,172]

- **Segmented Flow**: In microfluidic L/L extraction utilizing segmented flow, the transfer rate of the molecules is enhanced by high surface area and internal circulation. During segmentation, the two liquid phases form intermittent sections with the wetting phase enveloping the non-wet phase droplets in a thin-walled layer. This arrangement significantly, increases the surface tension by three to four times.[173]

- **Emulsions**: Micromixers offer a cost-effective alternative to traditional small plant extractors. These devices are commonly employed to generate emulsions that can be utilized in larger-scale systems. The Institut für Mikrotechnik Mainz has developed static micromixers, which have been utilized for extracting liquids from various compounds using the conventional mixer/sedimentation complex.[161] Microfluidic extractors are classified into three main groups based on the flow arrangement of two immiscible liquids:[174]

1) *Stop-Flow Microfluidic Extractors*: The "stop-flow" indicates that the acceptor liquid phase is stationary, while the conduction phase is always moving.[175] One of the key advantages of this method is the utilization of very small sample volumes. Microfluidic membrane liquid-phase

Table 5. Summary of nanowire incorporated microfluidic chips for separation and/or purification of different biomolecules.

Fabrication method	Chip materials and design	Biomolecules	Resolution	Repeatability	Reproducibility	Flow rate	Ref.
Photolithography and soft lithography	PDMS microchannels and Silicon Nanowire inside the microchannels	Chloromethyl methyl ether (as a carcinogenic model)	NR	Yields over 96%	High degree of control and reproducibility	100 µL min⁻¹	[66]
Photolithography and soft lithography	PDMSbased Chip with two symmetric chambers, connecting channels, and inlet/outlet. The substrate of silicon nanowire arrays is aligned and bonded to the PDMS device.	Circulating Tumor Cell	NR	The capture efficiency of cancer cells was mostly higher than 80%.	NR	1 mL h⁻¹	[157]
Photolithography and soft lithography	PDMS chip consists of five microfluidic channels, with the local synthesis of different types of ZnO nanowires	Streptavidin and Anti-mouse IgG	LOD: Streptavidin 417 fM Anti-mouse IgG 4.17 pM	NR	NR	750 µL h⁻¹	[65]
Seed ZnO layer in the inner surface of Silica glass cappillaries	Silica glass cappillaries seed by ZnO layer and then ZnO/Zn(OH)F nanofibers	Histidine-rich protein (hemoglobin)	LOD: 0.5 mg mL⁻¹ for hemoglobin	NR	NR	NR	[64]
Photolithography and soft lithography, electron beam lithography and vapor liquid-solid growth	Quartz glass microchannels, SnO₂ nanowire, Au particles, Cr and SiO₂ layers	DNA (λDNA and T4 DNA)	NR	High throughput	NR	NR	[62]
Photolithography, electron beam lithography, and vapor-liquid-solid (VLS) growth technique for growth of the nanowires.	SnO₂ (3D nanowire)	DNA, Protein, RNA	DNA 0.93-0.99 Protein: 1.5-1.99 RNA: 0.41-1.38	Analyze DNA mixture in 50s, protein mixture in 5 s, and RNA mixture in 25 s.	NR	NR	[60]
Photolithography, soft lithography, sputtering	ZnO nanoviers embedded on Cr layer sputtered inside PDMS microchannel	Exosomes Microvesicles EV-free miRNAs	LOD: 0.194 ± 0.028 ng/m	NR	NR	50 µL min⁻¹	[158]
Photolithography, soft lithography	ZnO nanoviers seeded on glass + PDMS microchannels	Proteins (human α-fetoprotein (AFP), carcinoembryonic antigen (CEA))	LOD: AFP 1 pg mL⁻¹ CEA 100 fg mL⁻¹	High-throughput	NR	2-10 µL min⁻¹	[159]

extractors represent advantages in single-drop microfluidic extraction. In this technique, the droplet suspended at the tip of the needle is continuously washed by the moving phase, which may cause the droplet to fall. Consequently, to enhance the droplet stability, some researchers introduced a membrane into the single droplet microfluidic extractors.[176–178] Microfluidic membrane liquid-phase extractors do not contain droplets, resulting in a relatively stable system. The centrifugal microfluidic extractor employs a centrifugal force field to maintain the aqueous phase in a steady states, allowing organic phase droplets to flow through the static aqueous phase. A prominent example of this method, called liquid-liquid counter-current chromatography (L/L-CCC), was developed by Ito.[179–183] L/L-CCC employs the aqueous phase as the stationary phase, while the organic phase serves as a mobile phase. The primary challenge of this method lies in maintaining a stationary liquid phase. It is important to note that these microfluidic extractors are not operated in the counter-current flow mode. According to Bertoud et al.[184] the name of this technique is inappropriate since the two liquid phases do not have opposite currents. Fang et al.[185] developed two new approaches based on a flow-stopped extraction technique using microfluidic chips. In the first method, known as droplet extraction mode, the organic solvent was trapped inside the hollows produced in the channel walls of the microfluidic chips, and the analytes were transferred to them via the water streams that flowed onto the droplets, affecting a preconcentration. In the second approach, by stopping the flow of the organic phase, a stable interface was formed between the static organic phase and the aqueous phase with continuous flow. Both approaches made molecular separation possible with high efficiency.

2) *Concurrent microfluidic extractors*: Concurrent microfluidic extractors lack a fixed liquid phase and both immiscible fluids flow in the same direction, allowing continuous extraction. Based on the flow pattern, concurrent microfluidic extractors are divided into four groups. These are the laminar flow microfluidic extractors, droplet flows microfluidic extractors, slug flow microfluidic extractors, and chaotic flow microfluidic extractors. In laminar flow microfluidic extractors, both immiscible liquids flow continuously in the same direction without dispersion. Therefore, molecular diffusion facilitates the transfer of molecules from one liquid phase to another. Published studies indicate that all membrane-free microchannels used in these extractors are less than 7 cm wide.[186–189] Consequently, the contact time between the two liquids is limited in laminar flow microfluidic extractors. The mechanisms of the microfluidic droplet and slug extraction methods are similar. The only distinction between the two methods is that, in the droplet method, the dimensions of the droplets are smaller than those of the microchannel and exhibit no deformation. On the other hand, the slugs are larger than the depth or width of the microchannel and must undergo deformation within the microchannel. The transfer of molecules in droplet flow is more effectively achieved in a tortuous microchannel due to the chaotic internal recirculation of each droplet caused by the secondary currents.[190,191]

There are four methods to generate droplets in microchannels (**Figure 6**): **Cross-flow**: The dispersed phase enters through the branch entrance and is sheared by the continuous phase entering through the horizontal entrance. **Co-current**: The current pattern is determined by the combined action of shear force, surface tension, and inertial force. **Focusing current**: In this device, the continuous phase vertically compresses the dispersed phase on both sides, and then both phases pass through the focusing aperture together. **Step emulsion**: This method relies on the confinement of a liquid in a narrow channel, causing it to experience high curvature. By introducing an expanded region in the channel, the liquid accelerates, forming a necked region behind the droplet as the continuous phase flows upwards.

In chaotic advection micromixers, transverse flows are generated, which include a component of vertical velocity to the mainstream. These transverse flows disrupt regular parallel flows between different liquids and enable microfluidic masses to be split, stretched, folded, and broken up.[192,193] Concurrent microfluidic extractors can achieve high efficiency in continuous liquid-liquid extraction processes, while Chaotic flow microfluidic extractors particularly well-suited for high-throughput applications.

3) **Countercurrent Microfluidic Extractors**: In countercurrent extraction, it is necessary to ensure that the light and heavy liquid phases have opposite flows. However, achieving this on a small scale is challenging due to the dominance of the viscous and the surfaces over the inertial and gravitational forces. Therefore, ongoing investigations are being conducted to address this particular challenge. These studies are divided into three groups based on the molecule transfer mode and flow arrangement details: multi-stage counter-current, continuous counter-current, and hybrid counter-current. **Multi-stage countercurrent microfluidic extractor**: In this system, the three methods of phase separation gravity, surface wettability, and delay are often collectively employed to enhance droplet integration.[194,195] **Continuous counter-current microfluidic extractor**: Continuous counter-current microfluidic extractors are highly suitable for analytical chemistry due to their passive nature, ease of miniaturization, and high enrichment factors. Furthermore, unlike multi-stage counter-current microfluidic extractors, they do not require phase mixing for molecule transfer enabling them to separate the intermediate phase.[196–198] **Hybrid countercurrent microfluidic extractor**: Multi-stage counter-current microfluidic extractors are relatively strong; however, they are not inactive and are not miniaturized simply owing to their intermediate pumps and/or valves. Each liquid phase is transferred in the opposite direction without inter-stage pumps or check valves in a hybrid countercurrent microfluidic extractor. This problem is solved using intermittent pulse feeding of both phases and the accumulation of internal droplets.[199]

Microfluidic L/L extraction offers several advantages and faces certain limitations. Enhancing the mass transfer, reducing the sample and reagent consumption, high selectivity, ease of
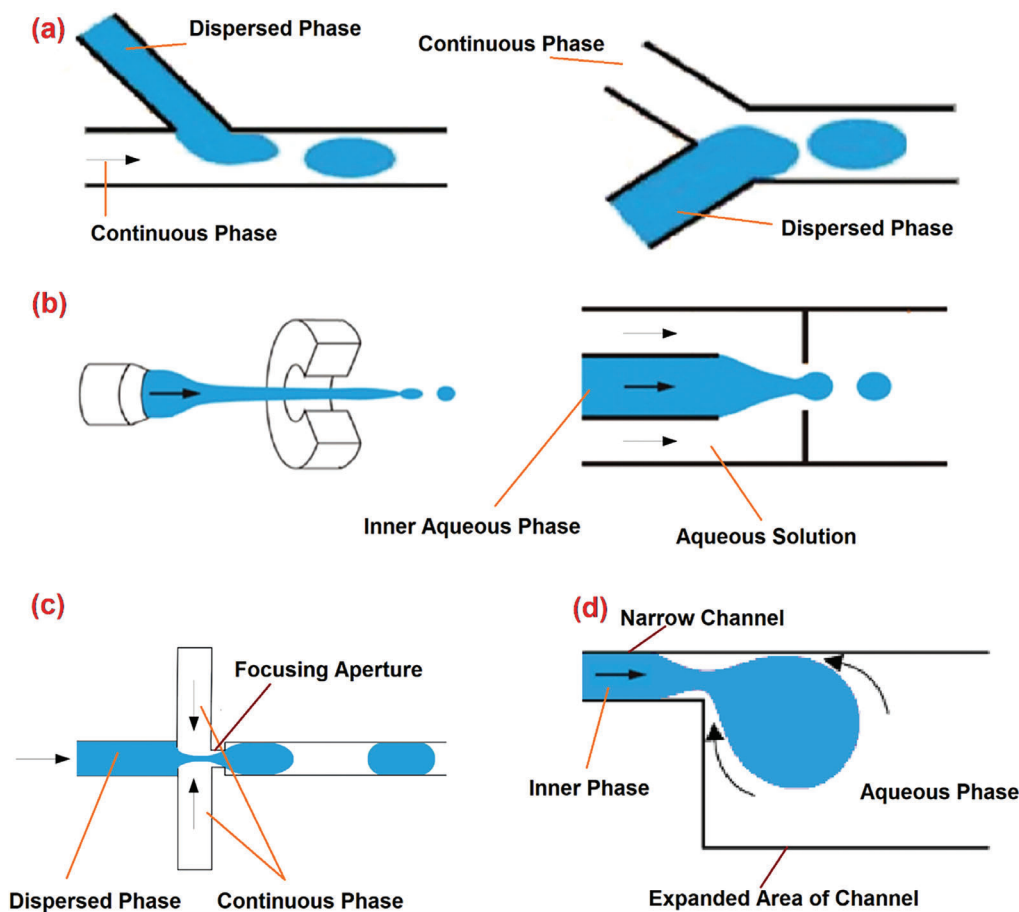
Figure 6. Schematic of droplet generation in a microfluidic device. a) Cross-flow, b) co-current, c) focusing current, and d) step emulsification.

integration and automation are some of the advantages of L/L extraction. Scaling up microfluidic liquid-liquid extraction from laboratory-scale to industrial-scale, compatibility of complex sample with microfluidic materials, and initial setup costs for L/L extraction with microfluidic systems are some of the limitations of this method.

2.2. Active Separation Methods

Active microfluidic separation methods use external force for the separation of analytes. Here, the most common methods used for molecular separation in last decade are discussed. **Table 6** summarizes important parameters, like separation mechanism, separation criteria, molecules, and chip materials for active microfluidic-based molecular separation methods.[19,27,29,31,200–246]

2.2.1. Dielectrophoresis

Powerful analysis techniques are necessary to solve complicated biology problems, even at the molecular level. Dielectrophoresis (DEP) has emerged as one of the most impressive techniques for addressing those problems. DEP is an effective analysis method

that polarizes particles in a non-uniform electric field and causes attractive or repulsive forces to transpire. DEP devices are especially powerful for selective purification, separation, and fractionation. Recently, DEP units utilizing microfluidic devices have garnered significant interest from researchers since DEP has no disruptive or toxic effect on the structural properties of biological materials. Therefore, scientists can unearth vital information about the characteristics of biological materials under the DEP effect. This part will evaluate the most recent research focusing on the impact of DEP on subcellular molecules (<10 μm). DEP is deeply studied with nucleic acids, especially for separation, trapping, deflection, purification, and self-assembly.[200,259] Viefhues et al.[200] reported that the employment of DEP can be used to manipulate the large segments (large kbp strands) of DNA structures, especially for separation and reassembly processes. This study proved that using DEP for DNA manipulation could be useful for sample preparation. Viefhues et al.[201,202] also reported an orifice with a DEP microfluidic device to trap and separate DNA strands (**Figure 7**a). Based on the orifice and DNA characteristics, DNA structures drag and flow through the orifices or become trapped. This process causes the separation of the DNA strands.

Viefhues and his co-workers, of course, were not the only researchers that focused on DNA manipulation by using DEP. There have been several attempts to achieve this goal. Shunbo

**ADVANCED
SCIENCE NEWS**

www.advancedsciencenews.com

**ADVANCED
MATERIALS
INTERFACES**
Open Access

www.advmatinterfaces.de

Table 6. Active microfluidic-based molecular separation methods.

Method	Mechanism	Separation criteria	Biomolecule	Chip materials	Ref.
Dielectrophoresis (DEP)	Inhomogeneous electric field	Size, Density, Polarizability	DNA, RNA, Proteins, Peptides	PDMS, PDMS-glass, SiO$_2$-graphene, Fused silica-carbon, Si/SiO$_2$-PDMS/quartz, Fused silica, Quartz-Graphene	[200–214]
Micro-free flow electrophoresis (μ-FFE)	Homogeneous electric field	Size, Charge density	BSA, DNA, Proteins, Peptides, Amino acids	Glass, PDMS, Glass-Cr, silicon, Trichlorosilane (TPM)-coated glass, Fused silica,	[27,29,31,215–221]
Magnetic separation	Magnetic field	Size, Magnetic susceptibility	DNA, Proteins, Antibody, Antigen, Exosomes	PDMS, PDMS-Glass, Glass, Silicon, PMMA	[222–236]
Acoustic separation	Ultrasonic standing waves	Size, Density	DNA, RNA, Proteins	PDMS, PDMS-Glass, PMMA	[19,237–246]
Centrifugal channel	Open, Centrifugal channels	Differential sedimentation of molecules based on their size, density, etc. under the influence of centrifugal forces	Proteins	Polycarbonate (PC), PDMS, PMMA, PMMA- polyolefin, Polyvinyl chloride pressure-sensitive adhesive (PVC-PSA), COP, Polystyrene (PS)	[247–251]
Thermophoresis	Temperature gradient	Differential movement of molecules in response to temperature gradients.	DNA	PDMS, silicon, Glass	[252–258]

et al. also focused on DNA manipulation using Au-covered nano-electrodes (Figure 7b).[203] In the same research study, the conductivity of DNA was analyzed at low electric fields of 10 V cm^{-1}, and DEP characteristics were investigated.[203] Sonnenberg et al.[204,260] developed a DEP microelectronic device to isolate DNA, and viruses. When used to investigate blood plasma, the method could be applied to separate DNA molecules and viruses from erythrocytes. The mentioned DEP microelectronic device relies on Pt electrodes. It creates various electric fields, accumulating targeted molecules on selected electrodes, thus separating the desired molecules from undesired ones. Barik et al.[205] developed a graphene-incorporated DEP device, generating higher electric fields than metal electrodes at low voltages (<1 V) to manipulate nanodiamonds, nanoparticles, and DNA molecules. Martinez-Duarte et al.[206] developed a carbon electrode-containing DEP microelectronic device that can manipulate λ-DNA (48.5 kbp). This DEP device can attract DNA molecules at 50 kHz and repel them at 250 kHz.

Giraurd et al.[207] focused on ribosomal RNA using a DEP device that attracts RNA molecules between 3 kHz to 1 MHz frequency and repulses RNA molecules over 9 MHz (Figure 7c). The DEP microfluidic devices rely on microelectrodes, which cause powerful repulsive or attractive DEP forces around them. This technology is mainly referred to as electrodes-based DEP, or simply eDEP. Another major technique exploits aqueous solutions that contain non-conductive constrictions, thus creating heterogeneous electrical fields when electrical potentials are applied to the fluid. This technique is called insulator-based DEP, or simply iDEP.[208] Many impressive research studies focus on manipulat-

ing subcellular molecules by employing iDEP. Gan et al.[209,210] used an iDEP-based microfluidic device to analyze DNA migration and trapping frequencies (Figure 7d). In addition, Chaurey et al.[211] also used an iDEP device to trap and manipulate DNA, ssDNA, and protein molecules.

Numerous DEP devices that take advantage of proteins have been reported and described here. Gencoglu et al.[208] reported the linear relationship between protein trapping and electric field in DEP devices. Liao et al.[212] used nanoscale structures and merged DEP and electrokinetic forces to cultivate streptavidin. Streptavidin was cultivated over 10^5 with the help of the technique used in this study. Rohani et al.[261] developed a DEP device to cultivate prostate-specific antigens (PSA). Zhang et al.[214] advanced a nanoscale-constructed iDEP microfluidic device to cultivate BSA. These properties may help researchers to understand how to develop treatments in personalized medicine in the future. **Table 7** summarizes some parameters like related DEP methods, mechanism, separation criteria, separated molecules, nd chip materials, used in the DEP-based microfluidic molecular separation studies.

2.2.2. Micro Free-Flow Electrophoresis (μ-FFE)

In recent years, the electromigration phenomenon, due to several extensive developments, has emerged with numerous successes in separation processes, in the ways of diagnosis assays,[28] cancer cell detection methods,[262,263] and also food-borne pathogen determination techniques.[264] In addition, state-of-the-art strategies combined with modern devices have been substituted for
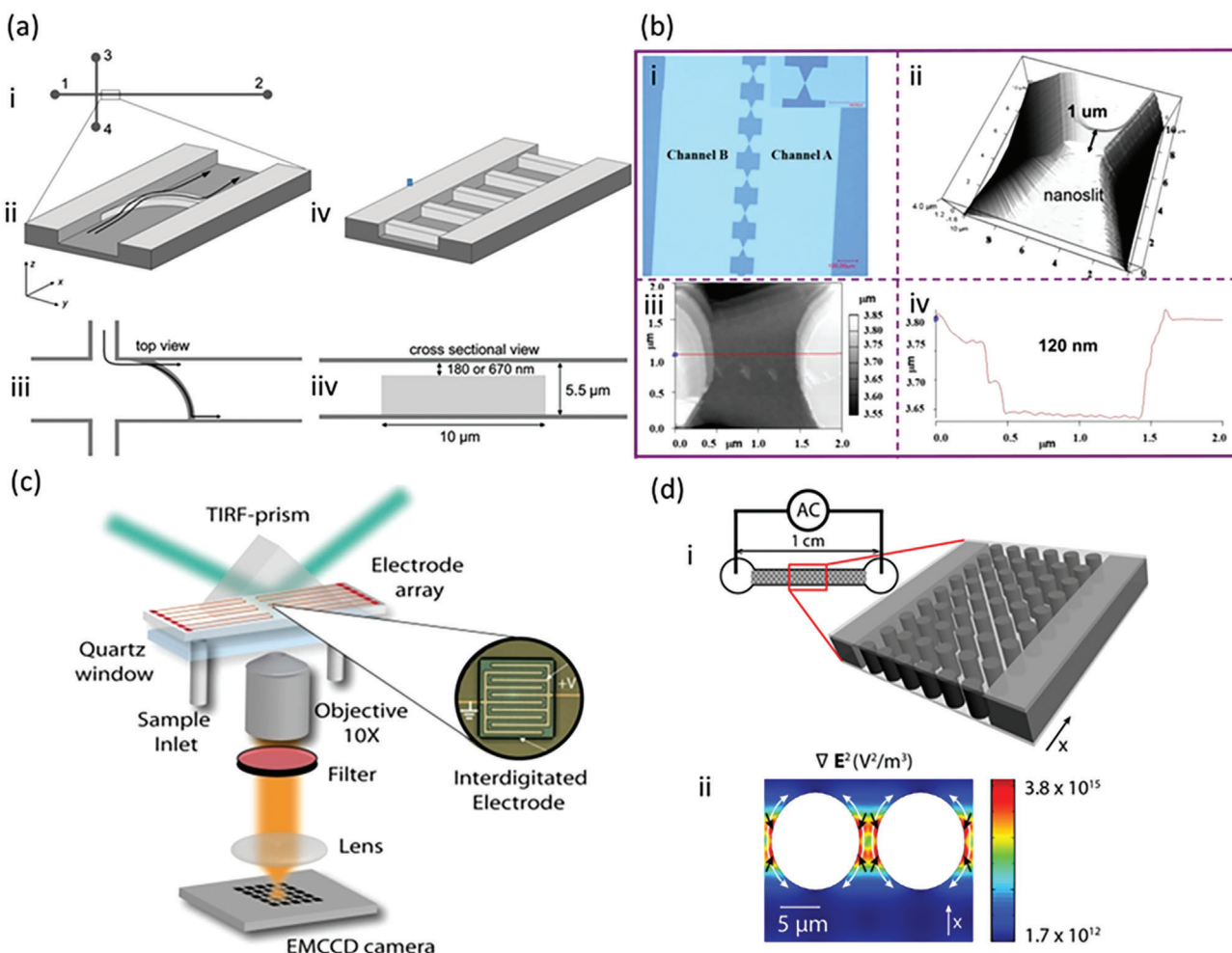
Figure 7. a,i) Schematic layout of the microfluidic device (not to scale). ii) Central element of the microfluidic separation device. iii) Top view of the bowed ridge. iv) Scheme of the microstructure used for determining polarizabilities. v) Cross-sectional view of a single ridge. Reproduced with permission.[201] Copyright 2013, Royal Society of Chemistry. b) Illustration of the nanofluidic device for DNA trapping: i) the optical image of the channel layout consists of two microchannels and nano-slits. ii) The 3D image of a nano-slit with the size of 1 µm. iii) The 2D image of the slit. iv) The height profile of the red line in (b-iii). Reproduced with permission.[203] Copyright 2015, AIP Publishing. c) Experimental setup for live monitoring of rRNA dielectrophoretic activity. Reproduced with permission.[207] Copyright 2011, AIP Publishing. d,i) iDEP device consisting of a linear microchannel molded with PDMS. ii) ∇E^2 around two posts and the dimensions of the posts are outlined. Reproduced with permission.[210] Copyright 2015, American Chemical Society.

Table 7. DEP-based molecular separation methods.

Method	Mechanism	Separation criteria	Biomolecules	Chip materials	Reference
DEP	Inhomogeneous electric field	Dielectric Constant, Conductivity, Frequency of the Electric Field, Particle Size and Shape, Medium Properties	DNA, Protein, Streptavidin, Prostate Specific Antigens, Avidin	PDMS, PDMS-glass, SiO$_2$-graphene, Fused silica-carbon, Si/SiO$_2$-PDMS/quartz, Fused silica, Quartz- Graphene	[200–214]
e-DEP	Patterned electrodes create Inhomogeneous electric fields	Electrode Configuration, Frequency of the Electric Field, Applied Voltage, Dielectric Properties, Particle Size and Shape, Buffer Conditions	DNA, Viruses, Ribosomal RNA, λ-DNA, nanoparticles, neuropeptides, BSA	PDMS, PDMS-glass, SiO$_2$-graphene, Fused silica-carbon, PMMA, Polycarbonate, Si/SiO$_2$-PDMS/quartz, Fused silica, Quartz- Graphene, gold, platinum, silver, PEDOT:PSS, graphene, carbon nanotubes	[27,29,31,215–221]
iDEP	Electrokinetic Concentration Polarization	Insulator Configuration, Surface Charge, Applied Voltage, Dielectric Properties, Particle Size and Shape, Buffer Conditions	DNA, ssDNA, Proteins, BSA	PDMS, PDMS-glass, SiO$_2$-graphene, Fused silica-carbon, PMMA, Polycarbonate, Si/SiO$_2$-PDMS/quartz, Fused silica, Quartz- Graphene, SU-8	[222–236]

**ADVANCED
SCIENCE NEWS**

www.advancedsciencenews.com

**ADVANCED
MATERIALS
INTERFACES**

www.advmatinterfaces.de

conventional protocols in electro-separation and tracking of proteins, nucleic acids, and other biomoieties. In all categories of these techniques, the bioelectric properties of the biological matter or biomolecules must be considered.[265] Furthermore, recent electromigration methods provide highly efficient separation, especially with applications in genetic engineering and forensic serology;[266] the advanced medical sciences; medical biotechnology; nano-biotechnology; and biomedicine.[267] Conventional protocols include western blots with SDS-PAGE and Northern and Southern blot techniques. Electrophoresis is a ubiquitous separation technique based on the integral compartments' electrical charges and mass differences. Proteins, DNA, RNA, and microorganisms (or their antigens) are the diverse biomolecules appropriate for being separated by this technique. The benefits of electrophoresis compared to conventional methods (such as culture media and biochemical assessments) are the consumption of lower volumes of biofluid samples, accuracy, simplicity, and fast implementation. Electrophoresis systems can also be cheap and capable of providing consumer-friendly assessments for diagnosis. Micro-free-flow electrophoresis separation will be introduced as an attractive separation strategy for the subgroups of electrophoresis. The μFFE (micro free-flow electrophoresis) method was introduced during the last few years with continuous separation potency. It differed from the other protocols, which required the charging of samples through batch processes. The μFFE technique has been applied to proteins, DNA, RNA, and peptides.

Furthermore, μFFE has been used in coalescence with lab-on-a-chip techniques to detect biological living moieties and biomolecules. In the past, drawbacks related to the channels, spatial sample feeding, and other problems in FFE have led to the substitution of FEE by μFFE.[29] Most μFFE devices, with few exceptions, possess an open-accessed channel mechanism that allows the fluid to flow along the microchannel in the micron (volume) scales.[215] As in conventional electrophoresis, the principles in μFFE are based on mass differences and hydrodynamic broadening, which cause velocity gradients of the different materials along the travel paths. The main problem in using μFFE is that bubbles are trapped in the microchannels of μFFE devices, which causes surface adsorption in the channels.[31] The other challenging area in the μFFE devices is governing the surface electrostatically. Scientists continuously try to find the materials that dissolve the problems related to the nature of μFFEs, which are generally made of glass, silicon, or other polymer-based easy-to-fabricate materials. Several studies apply μFFE in separating and purifying DNA, RNA, and proteins, in the analysis of synthetic moieties, such as peptides, aptamers, biomolecules,[31] and in proteomics.[268] The critical structural units in the fabrication of microfluidic free-flow electrophoresis devices are microchannels which could be fabricated by different techniques such as laser-assisted micromachining, microwire molding, 3D printing,[269] mechanical tools assisted micromilling, microdrilling[270] and imprinting techniques. Recently, the light incorporation (femtosecond laser) protocols have been more attractive than others relying on light energy so-called "micro- stereolithography" or "laser microfabrication".[216,271,272]

Laser modular techniques such as laser-induced plasma-assisted ablation[273] and monolithic digital patterning with subsequent laser pyrolysis[274] could be introduced to the μFFE device. Nevertheless, the turn of quality in the performance in engraved microchannels will be made after optimization, a complementary step in the fabrication process. The main functions in the output accuracy in the microfabrication of microchannels in μFFE are the nature or type of engraved material, the tool(s) used and the accuracy of the applied instrumentation. The fluid applied as an air-jet in cryogenic abrasive air-jet machining (CAAJM) is a novel micro-milling technique.[275–277] Zhang et al.[278] used the cryogenic micromachining technique for preparing microchannels on a PDMS substrate and obtained satisfactory results. The considerable role of microchannels in the μFFE devices is due to their innate capacity to withstand pressure rises. Other factors that influence separations in μFFE devices are the different strategies of bonding used during the fabrication of microchannels, which can be tuned to provide sufficient separation efficiency of biological macromolecules (proteins, DNA, RNA, etc.) in the μFFE.[279] **Table 8** summarizes the μFFE modalities.[280] The comprehensive studies in the field of μFFE separation reveals abundant advantages compared to the other orthogonal methods (i.e. HPLC and CE) of the separation techniques. The low expert labor need, implementation in a very short time, (100-fold faster in analytical evaluation) compared to the conventional FFE method. Also, a high surface area to volume ratio in this method is highly considerable because it increases the speed of separation and prevents heat losses produced by the applied electric field. All these advantages lead to the use of μFFE as a method for high-level purification (%) of proteins in the proteomics investigations. In contrast to the mentioned advantages expressed previously, gas bubbles generated by electrolysis, choosing appropriate (high quality) material for fabrication of μFFE device, perturbation in applied electric field can be considered as disadvantages of μFFE technique. Furthermore, low resolution and that districts the application of this technique.

Free Zone or Capillary Zone Electrophoresis: Free zone electrophoresis (FZE) is a continuous electrophoretic separation process without a stationary phase, such as a gel or mobile environment. Free zone electrophoresis was originally based on methods for purifying cells and bacteria. Zone electrophoresis (ZE), by default, is an appropriate method for separating[27] small molecules, proteins,[281,282] biomolecules,[283] peptides,[217,284] DNA,[285,286] viruses,[218,287] and membranes. In capillary zone electrophoresis (CZE), the electrophoretic separation of glycoproteins and glycopeptides can be performed by consideration of the m and z differences among the input ingredients, where m is the mass and z is the charge of the compartments. The enantiomers and organelles are other groups of biomoieties for electrophoretic separation through CZE. Buszewski et al.[218] reported a study on diagnosing pathogens by CZE. Buszewski illustrated that CZE could be considered an appropriate method for identifying pathogen moieties, such as those on viruses. Though PCR is traditionally the gold standard technique for identifying pathogenic moieties, often, false results are a major drawback associated with this strategy. The hyphenated zone electrophoresis system could be a precise method for separating, tracking, identifying, and characterizing bacterial cells and other biological microorganisms due to its fast, accurate, and reliable results.[288] The issue described in this

Table 8. The µFFE modalities.[280]

Name of FFE Modality	Biomolecules	Resolution	Throughput	Repeatability	pH gradient	Economic	Detection
Zone electrophoresis (ZE)	Cells, Bacteria, Proteins, Peptides, DNA, Viruses, Membranes, Enantiomers, Organelles	3% EPM	40 mg h^{-1}** 50 mg h^{-1}***	Weak	–	Weak	Good
Isotachophoresis (ITP)	Proteins, Membranes, Peptides, Organelles, Viruses, Enantiomers, Bacteria	1% EPM	150 mg h^{-1}***	Middle	Good	Mıddle	Good
Isoelectric Focusing (IEF)	Proteins, Peptides, Membranes, Organelles, Viruses	0.03 pI	500 mg h^{-1}***	High	Good	Good	Excellent
Field step electrophoresis (FSE)	preconditioning of any sample	30% EPM	5 g h^{-1}***	Weak	Excellent	Weak	Excellent

*Attainable at optimal conditions, **Eukaryotic cells, ***Proteins or peptides, EPM (Electrophoretic Mobilities).

section demonstrated that this technique differs with common electrophoresis manners due to the electrophoretic mobilities of analytes that are related to the charge-to-size ratio. As benefits (advantages) of capillary zone electrophoresis are its high accuracy and high detection borders. Three is another type of CZE which is introduced as Correlation Capillary Zone Electrophoresis (CCZE). The difference and main problem of this technique compared to general CZE method is only its injection system. The advantage of the CCZE is its easy modification in the injection system which this section is electrically rather than pressure-driven.

Micellar Electrokinetic Chromatography: Micellar Electrokinetic Chromatography (MEKC) is a micro-free-flow electrophoresis technique that separates the non-electrically charged specimens between two phases.[289] The stationary and dynamic phases are the bases for separation mechanisms by MEKC. There are different classifications of electrokinetic separation protocols, such as CE and capillary electrochromatography (CEC).[290] The surfactants play a crucial role in determining the separation ratio, and often, the application of stable micelles (MEs) is preferred.[291] Micelles are polymeric micro-vesicles that are used in different applications of science, and they are often applied to assist in the propagation of biochemistry approaches, as are they used in biology and different fields of the advanced medical sciences. The critical task of micelles in the MEKC technique is based on their highly charged properties, which enable their migration in an electric field. This mechanism of transportability brings a few benefits in different applications of medicine, such as in bio-separations (by applying smart bio-separation materials),[292,293] biomolecule quantification,[294] and many other uses.[295,296] The micelles can interact with segments of the analyte during neutral associations. Salido-Fortuna and his research group investigated the method fundamentals and characteristics of chiral separation in micellar electrokinetic chromatography.[297] The separation rules, with different polarities and characteristics regarding enantiomeric separations, were considered the bases of Salido-Fortuna's study. The investigation focused on the micellar surfaces or the electrochemical polar property of surfactants, which extensively af-

fect the separation rate. In MEKC, the solute is embedded into the core of the micelle. In another study, Bernando-Bermejo investigated the diastereoisomers in chiral separation (analysis) using electrokinetic chromatography.[298] They conjectured the cost-effectiveness and sufficient flexibility of chiral EKC, which is a technique that is often used for the separation of different biomolecules.

Isoelectric Focusing: Isoelectric focusing (IEF) is one of the subgroups in micro-free-flow electrophoresis based on the isoelectric point (pI), which is specific for each microorganism.[299] This method transports a low electrical current between the cathode and anode in the low molecular weight ampholytes.[219,300,301] The significant factors affecting the performance of this technique include the stable pH gradient within monovalent buffers being used,[302,303] the charge-to-mass ratio, and the isoelectric point. Density gradient, polyacrylamide gel, and zone convection electrofocusing are three modalities of the isoelectric focusing method in electrophoresis. All the techniques mentioned above are considered in human health for diagnosing diseases and, generally, for tracking, separation, and treatment. The isoelectric focusing method is commonly used for the accurate tracking and separation of proteins[304] and peptides[220]; and in viral capsid evaluation[282] by the surveying of genetic materials (mRNA, DNA fragments).[305] A wide range of applications of trillions of microorganisms (microbiome) living in the human body can be uncovered using this technology. Zhang et al.[304] reported a novel research study in which imaged capillary isoelectric focusing analysis (iCIEF) was performed using PEGylated proteins. The novel matrix of glycine and taurine helped Zhang and his colleagues to accurately identify pI charge variants in PEGylated proteins and effectuate their separation. The significant improvements associated with this method enabled substantial separation yields. However, a 50% improvement was seen in the separation efficiency of PEGylated proteins compared to the non-PEGylated proteins. This observation suggests that any progress in separation processes on the basis of pI extensively depends on the matrix composition (Glycine (40 mM), Taurine (50 mM)) used in the iCIEF procedure. **Figure 8**a illustrates the electropherogram of PEGylated proteins passed through an iCIEF device
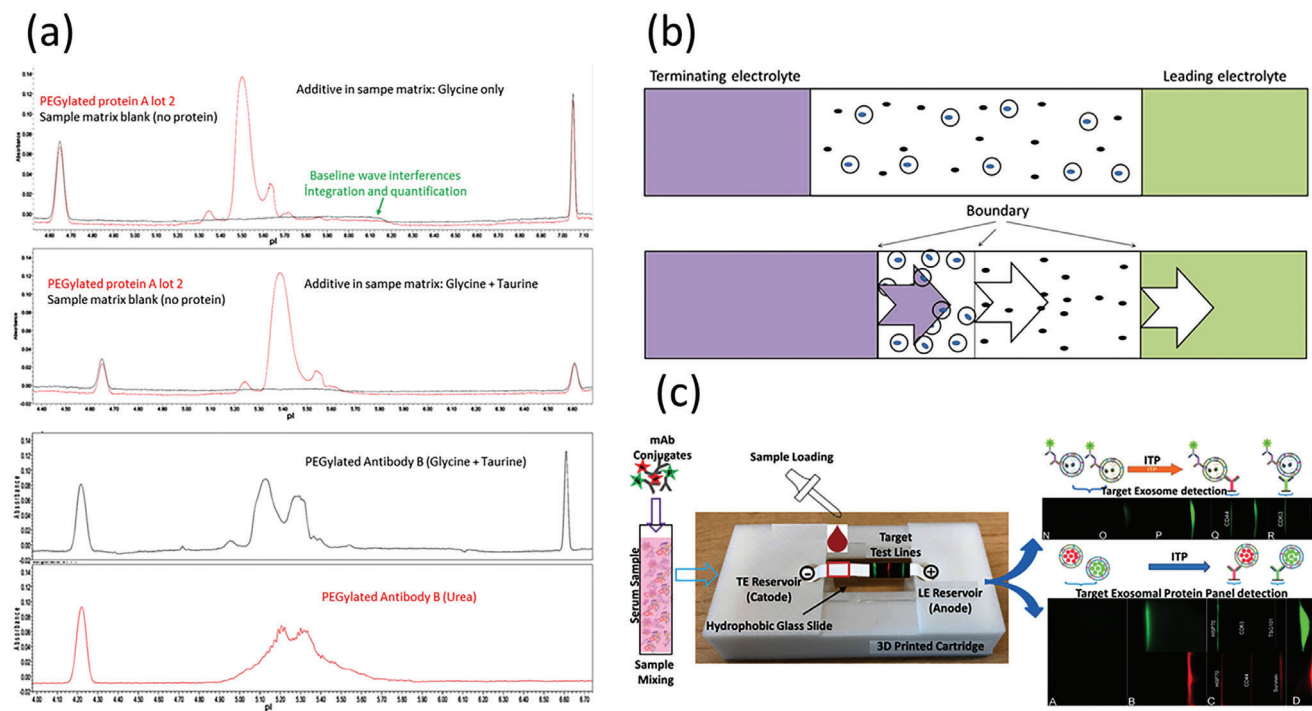
Figure 8. a) An illustration of the electropherograms obtained in the case of separation and detection of PEGylated protein A, in a blank, Glycine only, and Glycine+Tuarine environment (Upper), or of PEGylated antibody B, in Glycine+Tuarine and pure Urea environment (Bottom). Reproduced with permission.[304] Copyright 2020, Electrophoresis. b) Schematic illustration of the capillary isotachophoresis (cITP) mechanism by considering separation speed in the terminating and leading phases. c) The schematic illustration of cancer-derived exosomal protein separation by ITP, followed by depictions, by fluorescence microscopy, of mouse mAb against CD81 (a universal surface protein biomarker for all exosomes) plus a rabbit anti-mouse secondary antibody labeled with Alexa Fluor 488. Reproduced with permission.[221] Copyright 2020, Biosensors and Bioelectronics.

in the blank, Glycine, and Glycine/Taurine environments.[304] The significant incremental changes in the peak values of pI in curves, shown in Figure 8a, verify the effect of the medium on the rate and separation accuracy of proteins, as presented in the study by Zhang et al. By applying the IEF protocol, separating the combined entities and analyzing their co-migrating peaks for charge variants of PEGylated proteins proved to be impossible in this study.

Isotachophoresis: Isotachophoresis (ITP), one of the subgroups in free-flow electrophoresis, is commonly used for selective separation in concentrated ionic analytes. Like the other strategies in free-flow electrophoresis, ITP is also used to identify and separate microorganisms, proteins and peptides; DNA; RNA; and other biomoieties. Based on the mobility of the ionic fragments of the analyte and their differences, the migration of different constituents of the sample can be determined. The capillary isotachphoresis (cITP) method is a subset of ITP, whereby the solutes (anaytes) for the separation process flow along a capillary. The terminating and leading electrolytes are identified according to the slow or fast movement of the different constituents. Principle of cITP that is applied to separate solutes is shown in Figure 8b.

Cancer presents a significant public health challenge on a global scale. There is a pressing need for novel diagnostic techniques that can effectively track the potent symptoms of cancer cells or the detection of biomarkers with sufficient precision, rapidity, and high accuracy. Novel diagnosis methods are highly crucial and valuable in cancer diseases due to their prevent ion regarding the metastatic spreading of cancer or forming massive tumor tissue. Cancer is a severe public health difficulty worldwide, and applying an accurate, rapid isolation and detection method for cancer is one of the most severe problems in medicine. Advanced diagnosis protocols are needed to track the cancer cells at early stages, even before their complex functions appear. Guo et al.[221] reported one applicable study, which elaborated on cancer detection using the paper-based ITP method in conjunction with cancer-derived exosomes. Exosomes are biopolymeric vehicles that carry the identifying genetic information of the cells of origin. Their use is becoming prevalent in disease diagnostics and sensing technologies. According to Guo's study, the diagnosis of cancer cells through exosomes could be realized, even at $2.0–3.0 \times 10^{-18}$ M limits, within 10 min, by running the paper-based ITP. Figure 8c (above, right) shows thatanionic ITP was performed with unlabelled intact exosomes. The fluorescently red-labeled cancer exosomes (50 ng mL^{-1}) and green-labeled normal exosomes (40 ng mL^{-1}) that were separated or obtained weremixed with mouse mAb against CD81 (a universal surface protein biomarker for all exosomes).[221] To the mixture, a rabbit anti-mouse secondary antibody labeled with Alexa Fluor 488 was added to stain the captured cancer exosomes.

The studies reveal that Isotachophoresis has different benefits such as no preparation stages necessary for sample, rapid implementation and applicability regarding a wide range of samples simultaneously, and automated high-performance as well. Unlike the advantages of the mentioned method, the disadvantages of this protocol can be considered as selecting of suitable buffer type.

As a conclusion and regarding the µFFE, the following reasons provide a clear landscape to the researchers and scientists to choose a suitable separation protocol whether described in the past part and regarding the comparable parameters. The studies in this field reveal that µFFZE and µFFIEF are the most general scenarios in the separation of protein compared to the other techniques. The micron scale platforms supplies opportunity to be used lesser amount of expensive chemicals and reagents. Also, large-scale separation, rapid and real-time separation with high efficiency is obtainable. In the micro scale separation of proteins isolation and characterization issues of target are expectable.

2.2.3. Magnetic Separation

Magnetic particles can be manipulated with an external magnetic field[306]; this unique property makes them attractive for separating biomolecules from biological fluids. A magnetic particle has a magnetic core (Fe, Co, Ni, metal oxides, ferrites, or alloys) encapsulated by an outer shell, and various receptors can be linked to this outer shell.[307,308] The magnetic particles can be functionalized with oligonucleotides, antibodies, avidin, peptide sequences, or enzymes.[309] Magnetic manipulation and functional coating properties of magnetic particles enable them to be integrated with microfluidic platforms.[222] Magnetic particles have been synthesized in various shapes and sizes ranging from a few nanometers to micrometers; they also can possess varying degrees of magnetism.[310,311] An external magnetic field can be applied using permanent magnets[312] or electromagnets.[313] Also, to increase the magnetic field gradient inside the microfluidics, soft magnetic materials may be integrated inside the microfluidic platform.[223] Microfluidics incorporated with functionalized magnetic particles have been developed to separate various targets, such as DNA from blood (**Figure 9a**),[224,225] DNA from foodborne bacteria,[226] circulating cell-free DNA (cfDNA,[227] and protein (interleukin-8) from undiluted serum.[228]

Fluid flow and magnetic force inside the microfluidics are simulated using finite element method-based software to improve and optimize the system's performance before fabrication.[229] To simultaneously detect multiple influenza HA subtypes, two different sizes of magnetic particles (10 or 5 µm) were functionalized with anti-H7N9 and H9N2 antibodies. The PDMS microfluidic platform consisted of two channels with 7 and 4 µm heights acting as barriers for different-sized magnetic particles.[230] It was reported that antibody-coated magnetic beads captured exosomes shed by tumor cells of breast cancer patients (Figure 9b)[231] and derived from plasma of ovarian cancer patients, which were then separated in a microfluidic platform (Figure 9c).[232]

One advantage of magnetic separation combined with microfluidics is controlling the concentration of the sample by adjusting the buffer volume; for instance, the sample volume was reduced to 60 nL to separate human interleukin-6 (IL-6), which is an approximately 15 × reduction in the sample volume compared with conventional ELISA.[233] Another study reported a 10× decrease in sample volume for separating interleukin-8 from serum samples.[228] In another design, magnetic nanochains were functionalized with three different antibodies against three cancer markers: prostate-specific antigen (PSA), carcinoembryonic antigen (CEA), and α-fetoprotein (AFP) (Figure 9d).[234] In a PDMS microfluidic platform, mixing and separation processes were performed.

Magnetic nanoparticles were functionalized with probe DNAs to capture target DNA sequences. The PDMS microfluidic platform consists of three channels, and a permanent magnet was designed to capture the magnetic particles in the reaction area.[235] It was reported that H7N9 was detected with a detection limit of 8.4 ng mL^{-1} using 10 µm magnetic beads coated with antibodies. The 3-D microfluidic platform consisted of glass and PDMS layers. The inside of the glass capillary channel was also functionalized with antibodies to form a sandwich assay.[236]

The magnetic particles can separate the target biomolecule (DNA, protein, RNA, cells, pathogens) from the complex medium such blood or serum and then the captured target biomolecule can be suspended in a friendly buffer which can be conveniently used with microfluidics or microstructures.[314] Various magnetic particles are commercially available and can be purchased easily. The main advantage is applying an external magnetic field (permanent magnets and/or electromagnets) to move or manipulate the magnetic particles. The main disadvantage is that unloaded magnetic particles present in the buffer can aggregate with the loaded particles due to the magnetic interaction and create sort of a noise signal. **Table 9** summarizes some parameters like fabrication methods, chip materials and design, separated molecules, resolution, LOD, throughput, repeatability, and flow rates used in magnetic separation studies.

2.2.4. Acoustic Separation

As a result of theoretical studies and published reports, the principle of separating many biomolecules or cells exposed to acoustic flow and acoustic radiation forces according to their properties, such as size, shape, compressibility or density differences, is frequently used in microfluidic technology.[237] Because of their distinct advantages, such as excellent biocompatibility, controllability, and non-invasive and label-free qualities, acoustic microfluidic separation techniques are well-suited for biological material applications. However, drawbacks such as reliance on external equipment and insufficient throughput make laboratory-based prototypes unsuitable for commercialization.

In the acoustic microfluidic separation method, both the drag force and the acoustic radiation force (ARF) can generally be mentioned as driving the mechanism of action. The sample to be separated is subjected to an ARF (Fr) and a Stokes drag force when it enters the microchannel (Fd). Mathematical expressions describing the forces to which these particles are subjected derived from the publication of Gao et al.[19] The acoustic
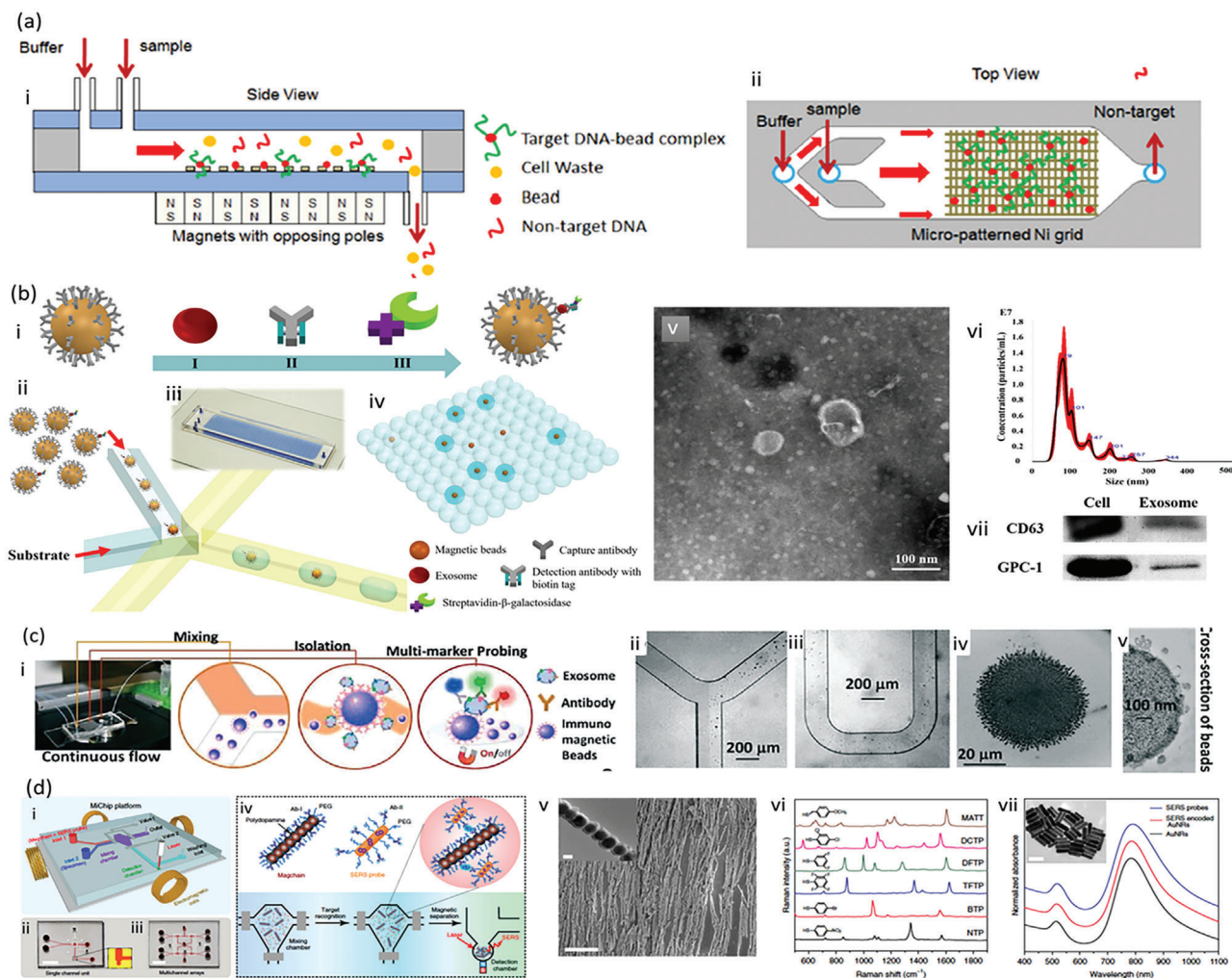
ADVANCED
SCIENCE NEWS

www.advancedsciencenews.com

ADVANCED
MATERIALS
INTERFACES
Open Access

www.advmatinterfaces.de

Figure 9. a) Schematic illustration of the microfluidic chip for DNA isolation. Adapted with permission.[225] Copyright 2014, AIP Publishing. b,i) Schematic illustration of the microfluidic system for exosome separation: a) Exosome immunocomplex constructed on a magnetic bead. b,ii) Exosome encapsulation in microdroplets. iii) Droplet digital ExoELISA chip. iv) Fluorescent counting of the positive droplets with the exosomes. v) TEM images of exosomes. vi) NTA analysis and vii) Western blot analysis. Adapted with permission.[231] Copyright 2018, American Chemical Society. c,i) Photo of the microfluidic device and schematics of the detection of circulating exosomes. c,ii and b,iii) Bright-field microscope images of the channels and aggregated immunomagnetic beads. iv,v) TEM image of an exosome-bound immunomagnetic bead. Adapted with permission.[232] Copyright 2016, Royal Society of Chemistry. d) Schematic illustration of the magnetic nanochain integrated microfluidic chip (MiChip). i) MiChip assay platform. ii,iii) Photo of MiChip (scale bar: 0.5 cm): ii) single channel unit, iii) multichannel arrays. iv) The MiChip assay for the detection of biomarkers. v) Magnetic nanochains SEM image (scale bar: 20 μm, Inset: magnetic nanochain. scale bar: 200 nm). vi) SERS spectra of 6 representative SERS-encoded AuNRs. vii) UV–vis spectra of original AuNRs, SERS-encoded AuNR, and antibody-conjugated SERS probes (Inset: TEM image of the AuNRs. Scale bar: 100 nm). Adapted with permission.[234] Copyright 2018, Springer Nature. Note: 4-nitrothiophenol (NTP), 4-bromothiophenol (BTP), 2,3,5,6-tetrafluorothiophenol (TFTP), 3,5-difluorothiophenol (DFTP), 2,4-dichlorothiophenol (DCTP), and 4-methoxy-α-toluenethiol (MATT).

microfluidic device is created by positioning a pair of interdigital transducers (IDTs) on a piezoelectric substrate with PDMS and altering the 15° inclination angle between the IDT and the microchannels. Oblique alignment guarantees that pressure nodes and antinodes develop at an angle to the flow direction.[238] Bulk acoustic waves (BAW) and surface acoustic waves (SAW), used to manipulate biomolecules or cells in the microfluidic field, may be divided or denoted into as two main categories of techniques.

Bulk Acoustic Waves (BAWs)-Based Separation: BAWs, usually created using chip materials with high acoustic reflectance properties, such as silicon and glass, are connected to the piezoelectric transducer microchannels and driven by an AC power source

to produce ultrasonic standing waves within the microchannel. BAWs spread through the mass of the material[19] In their study, Petersson et al.[239] successfully separated lipids and erythrocytes with high efficiency using the BAW device. As a result of their research, they reported that separation efficiencies of over 80% were obtained for triglyceride emulsions.

- **Microbubble-Based BAW Separation**: In recent years, microbubble-based separation, a biomolecule separation technique used frequently in microfluidic applications, has been utilized with excitations at a relatively low frequency in the kHz level. Acoustic bubble-based BAW devices are

**ADVANCED
SCIENCE NEWS**

www.advancedsciencenews.com

**ADVANCED
MATERIALS
INTERFACES**

www.advmatinterfaces.de

Table 9. Summary of magnetic microfluidic chips for separation and/or purification of different biomolecules.

Fabrication and Separation method	Chip design and materials	Biomolecules	Resolution or LOD	Throughput	Repeatability	Flow rate	Ref.
Lithographically fabricated antiferromagnetic nanoparticles	Synthetic antiferromagnetic nanoparticles (SAFs)	Biotinylated substrates, DNA	LOD: 10 pм	High-throughput	NR	NR	[310]
FeCo nanoparticles	FeCo nanoparticles	Protein	LOD: 2.08×10^6 molecules of IL-6	NR	NR	NR	[311]
Superparamagnetic, by depositing and patterning an array of thin nickel stripes on a glass substrate	Glass, nickel, polyimide: i) Glass substrate with nickel grid, ii) Fluidic channels were cut into a double-sided polyimide film, iii) Glass substrate	DNA	Purity of 1.8 or higher	Volumetric throughput of up to 50 mL h^{-1}	Likely to be high.	10-50 mL h^{-1}	[225]
Superparamagnetic, Photolithography (Printing digital microfluidics (DMF) electrodes, applying coatings to the top and bottom plates)	2 electrodes each one consists of: i) glass layers, ii) ITO electrodes, iii) Dielectric layer, iv) Teflon layer	DNA	NR	Automation of the DNA extraction process is possible	NR	NR	[224]
Superparamagnetic beads Fabrication method NA	Polycarbonate substrate	ctDNA	NR	NR	NR	NR	[312]
Superparamagnetic green-fluorescent beads, photolithography, and soft lithography	PDMS microchannel bonded to glass layer with a NiFe layer and permanent magnet.	Cells (red blood cells) and bacteria	Separation process has high efficiency	Cell throughput is 10000 cell s^{-1} (s: second)	Likely to be high.	25-40 μL h^{-1}	[223]

being developed based on size or density. In this regard, Rogers et al. developed a method that can be used to separate silica beads and polystyrene particles of the same size. This result shows that it is promising for biological applications in separation.[19,240]

Surface Acoustic Waves Based Separation: Lord Rayleigh discovered surface acoustic waves (SAWs), also known as Reynolds SAWs, in 1885, which were generated via IDT.[238] SAWs spread across the material's piezoelectric substrate surface and work in essentially the same way that BAWs do. The technique of using SAWs has recently been adopted and is a reasonably new method for microfluidic devices. SAW devices are divided into two subclasses: moving (or traveling) surface acoustic waves (TSAWs) and standing surface acoustic waves (SSAWs).

- **Traveling SAWs, TSAW-Based Separation**: The TSAW-based separation technique has been utilized to separate particles of various sizes, including PS, fused silica (FS), and PMMA. The particles are exposed to both acoustic radiation and friction forces in this separation process. However, it is necessary to calculate the value of a dimensionless factor (k_{tr}) derived by Skowronek et al. to define which force the particles are subjected to.[19,241] Ma et al.[242] used the TSAW technique to separate PS and PMMA microspheres using only mechanical properties (**Figure 10**a). During acoustophoresis (AP), PS and PMMA particles with the same diameter showed nonlinear and different trends related to the applied TSAW frequency and the mechanical features of the particles under an applied

ARF. Although this technique shows promise for biological applications, it needs further investigation.

Separation with TSAW is used not only for separating polymeric particles but also for separating cells and biomolecules, such as proteins and DNA, as well as viral and bacterial bodies or antigens. The microfluidic chip makes separation possible even at low infection levels. Afzal et al.[315] successfully simultaneously segregate three proteins, such as thrombin (th), IgE, and mCardinal2, via TSAW-guided ARF in an acoustic fluid device.

- **Standing SAWs, SSAW-Based Separation**: Based on the principle that two acoustic waves propagating in opposite directions occur at the surface, numerous pressure and anti-pressure nodes are used on the substrate surface in SSAW microfluidic separation.[19] When AC signals are applied to the IDTs, two identical frequency SAWs are produced. These SAWs are opposing and radiate toward the main channel in the device. These two opposing SAWs propagating towards the channel produce constructive interferences, resulting in SSAWs forming in the region where the micro-channels are connected.[243] The density and compressibility of the particles in the medium determine the acoustic contrast factor (ϕ). This has an impact on particle migration to pressure nodes or antinodes. Positive substances will migrate toward pressure nodes and negative substances will move toward pressure antinodes for ϕ values that are negative for lipids and gas bubbles and positive for biological cells and solid particles.[19,243] Particles in the SSAW field are subjected to four different forces. These forces are,
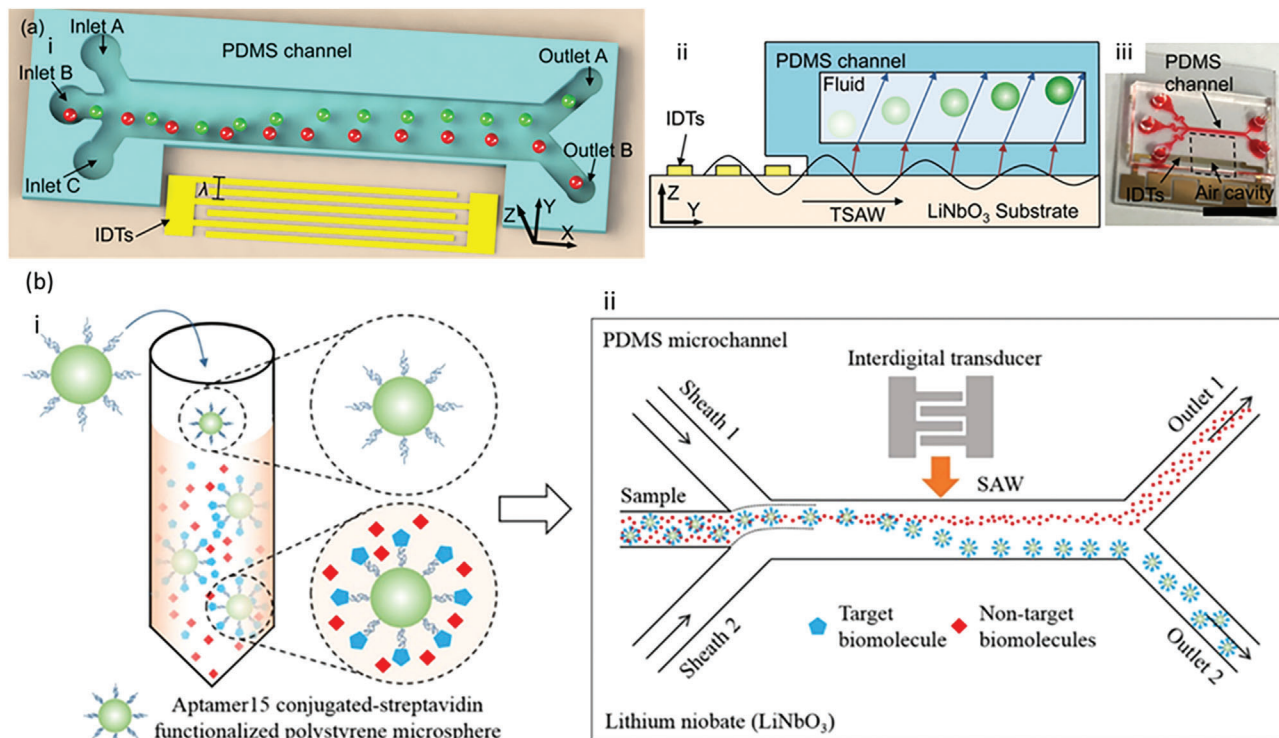
ADVANCED
SCIENCE NEWS

www.advancedsciencenews.com

ADVANCED
MATERIALS
INTERFACES
Open Access

www.advmatinterfaces.de

Figure 10. a) The acoustophoretic microfluidic system utilized for particle separation is depicted. a,i) Illustration of 3D perspective. ii) The device's cross-section. The PDMS channel is placed on a TSAW transducer with IDTs connected to the microchannel. The PDMS channel is disposable. These particles have different mechanical properties and are translated by different distances while flowing through the channel. In this way, it is collected from different outputs. iii) A photograph of the completed apparatus. The scale bar measures 5 mm. Reproduced with permission.[242] Copyright 2017, American Chemical Society. b) Diagram depicting the target biomolecule–microparticle combination creation and the acoustofluidic separation device used to extract the targeted protein using SSAWs. b,i) A biotin-labeled aptamer coupled to previously synthesized Streptavidin-functionalized microparticles preferentially collected target biomolecules (blue) from a complex mixture (green). b,ii) Target biomolecules (blue) and non-target biomolecules (red) in a sample fluid from sheaths 1 and 2 with hydrodynamic focusing are laterally deflected from laminar flow streamlines by the SAW, originating from the IDT. In this way, target biomolecules are isolated. The separated biomolecules are collected separately from sheaths 1 and 2. Reproduced with permission.[246] Copyright 2017, American Chemical Society.

respectively, the lateral acoustic force along the x-axis; the viscous force in the direction opposite to the flow direction of the particles; the gravitational force in the negative y-axis direction of the coordinate plane; and the buoyant force in the positive y-axis direction.[243–245]

Since the magnitudes of the gravitational and buoyancy forces are equal and opposite, they balance each other, and the particles move along the direction of the viscous force and acoustic force in the microfluidic channels. For this reason, the mathematical expressions of the primary acoustic force (Fr) and the viscous force (Fn) acting on the particles have been derived and are reported here:[242]

$$Fr = -\left(\frac{\pi p_0^2 V_p \beta_m}{2\lambda}\right) \phi(\beta, p) \, \sin(2kx) \tag{1}$$

$$\phi(\beta\sigma, p) = \frac{5p_p - 2p_m}{2p_p + p_m} - \frac{\beta_p}{\beta_m} \tag{2}$$

$$Fn = -6\pi\eta R_p \nu \tag{3}$$

where p_0, acoustic pressure; λ, SAW wavelength; V_p, volume of the particle; k, wave vector; x, distance from a pressure node; ρ_p, density of the particle; ρ_m, density of the medium; β_p, compressibility of the particle; β_m, compressibility of the medium; η, viscosity of the medium; R_p, radius of the particle; and ν, relative velocity of the particle.

Nam et al.[244] used SSAWs and a microfluidic device to extract platelets from undiluted whole blood. They reported that with the developed method, an RBC clearance rate of over 99% and a purity of platelets close to 98% could be obtained from whole blood. Ahmad et al.[246] developed an acoustofluidic separation device using functionalized microparticles to isolate particle-conjugated target biomolecules using high-frequency SAWs on chip (Figure 10b). They developed a biotin-labeled aptamer with streptavidin-functionalized microparticles that could selectively capture the target model protein, thrombin. The formed biomolecule–a continuous flow regimen successfully separated microparticle complexes within a microchannel.

In general, acoustic-based microfluidic separation of biomolecules enables continuous flow operation and compatibility with small sample volumes while providing gentle, label-free manipulation with great precision and selectivity. Its integration capability, low danger of cross-contamination,

2300492 (30 of 45)

**ADVANCED
SCIENCE NEWS**

www.advancedsciencenews.com

**ADVANCED
MATERIALS
INTERFACES**
Open Access

www.advmatinterfaces.de
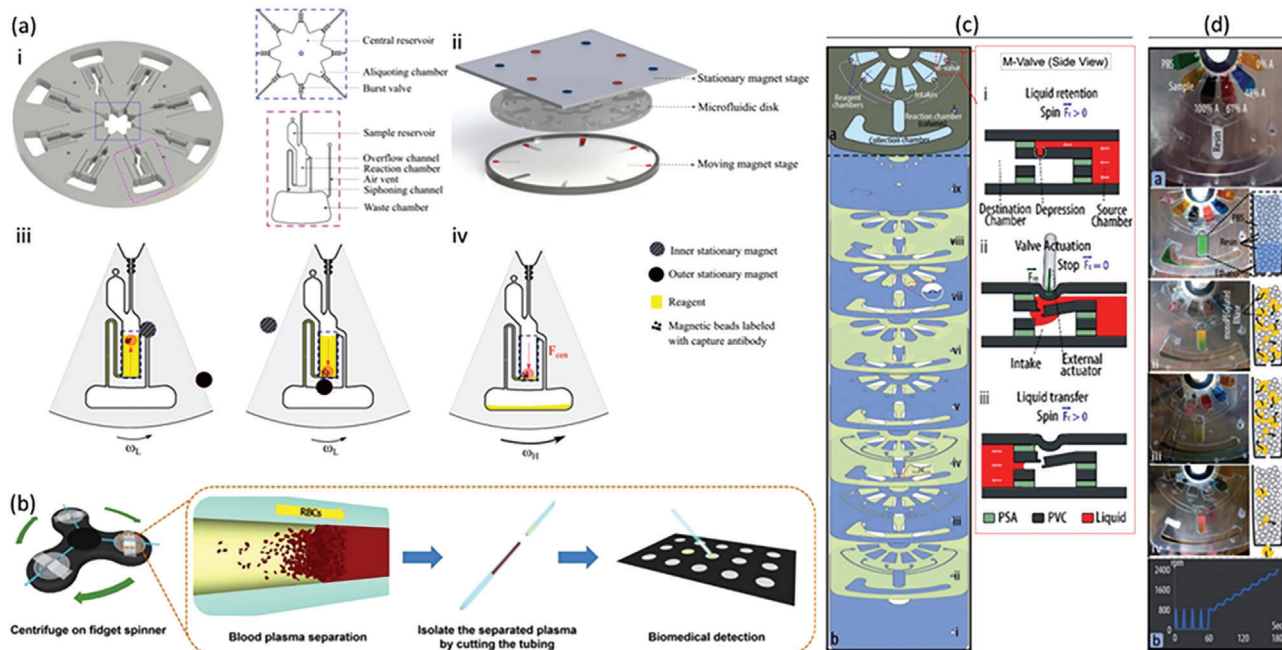
Figure 11. a, i) The design of the aliquoting fluidic disk. ii) The illustration of the centrifugal microfluidic disk containing a magnetic module. iii) The magnet alternatively moves in the reaction chamber when the rotational speed is low during incubation. iv) In the washing process, the magnetic beads were kept in the reaction chamber at high rotational speed for transferring the liquid into the waste chamber. Reproduced with permission.[249] Copyright 2021, AIP Publishing LLC. b) The schematic figure uses the centrifuge fidget spinner to separate plasma. Reproduced with permission.[250] Copyright 2021, American Chemical Society. c) The schematic figure of the nine-layered centrifugal microfluidic disk with the M-valves for chromatographic separation. d) The chip morphology contains six sample reservoirs, a column chamber, and one collection chamber. The spin procedure of the chip for each step includes four cycles at low speed (i.e., 800 rpm) for one minute and a continuous high-speed cycle (i.e., 2400 rpm) during the next two minutes to incubate the sample and resin and remove the waste solution. The illustration of four main steps, i: washing, ii: sample addition, iii: elution, and iv: collection, in the centrifugal chromatographic chip during RNase isolation, is also shown. Reproduced with permission.[251] Copyright 2021, The Royal Society of Chemistry.

customizable parameters, and low energy consumption make it a versatile and efficient approach for a variety of biomolecule separation applications. Size dependence, difficulties with complex sample mixtures, sensitivity to frequency and environmental factors, a small number of applicable biomolecule types, device complexity, potential for clogging and trapping, constrained throughput, potential biomolecule conformation changes, sample pre-processing requirements, a lack of standardization, and limited commercial availability are some of the drawbacks of this method.

2.2.5. Centrifugal Microfluidic Chip

Centrifugal microfluidic chips are widely used in immune analyses, protein purification, clinical diagnosis, food/chemical compounds analysis, and other areas. A centrifugal microfluidic chip is a microfluidic disk that integrates many microfluidic functions for flow control, fluid distribution, mixing, separation, etc.[247] Generally, the driving forces for a centrifugal microfluidic chip include capillary action, the Coriolis Effect, the Euler force, and the centrifugal forces. The centrifugal force could pump the fluid flow and cause it to emanate from the center to the edge of a spinning disk. In addition, the Coriolis Effect, Euler force, and centrifugal force can be controlled by regulating the angular acceleration and the rotational speed of the disk, which provides a

convenient way to conduct fluid transportation from one reservoir to another.

Moreover, valves play an indispensable role in designing a microfluidic system because they offer the "on" and "off" control of fluid transportation in microfluidic systems. The function of valves could be regulated via the geometry and surface properties of the microchannels. By changing the cross-section or the surface properties of microchannels, a pressure barrier could be formed, which can be used to control the transportation of fluids.[248] Therefore, the combination of the control over the rotational disk speed and the geometry of the microchannels enables the conceptualization of centrifugal microfluidic systems with versatile functions for different purposes. For example, an enzyme-linked immunosorbent assay (ELISA) protocol usually involves multiple steps for reagent addition and wash processes. Wu et al.[249] proposed a protocol on a centrifugal microfluidic disk to perform enzyme-linked immunosorbent assays (**Figure 11**a). In their design (Figure 11a(i)), the reagent was evenly distributed in the aliquoting chamber and then transferred into different reaction chambers to mix with the samples. During the incubation period, the rotational speed was kept at a low speed so that the capillary force could overcome the centrifugal force, and the liquid advanced to the exit of the siphoning channel. In the meantime, the low centrifugal force also favored the movement of the magnetic beads in the reaction chamber, which resulted in the excellent mixing of samples

**ADVANCED
SCIENCE NEWS**

www.advancedsciencenews.com

**ADVANCED
MATERIALS
INTERFACES**

www.advmatinterfaces.de

and reagents during the incubation process. After incubation, the reagent could be removed from the reaction chamber by increasing the disk's rotational speed through a siphoning channel. An ELISA protocol can be completed by repeating the liquid addition and removal processes. Since the liquid removal process can reduce the amount of the remaining reagents in the previous step, the signal-to-noise ratio of assays could be enhanced (Figure 11a(ii–iv)).

Centrifugal microfluidic systems have also been applied to separate the compounds in human blood samples. Lu et al.[250] integrated a polyethylene tube with a fidget spinner, performed as a centrifugal separator for isolating the plasma compounds (Figure 11b). This design only requires an ultralow volume blood sample (5–15 µL) from a finger-prick and reduces the risk of contamination from using pumps. In addition, the fidget spinner separator provided a rapid separation process (less than 7 min) and recovered 99% plasma purity. The biological activity of yield plasma approached 98%, which was validated by a paper-based protein ELISA. This shows that the platform provides an inexpensive and rapid method for blood-related applications in resource-limited regions.

In addition, Aeinehv et al.[251] reported a chromatography cartridge device in a multi-layered centrifugal microfluidic disk for isolating RNase A. In the fluidic design, the disk that contained one reaction column and six reagent chambers for storage of samples, elution buffers, and the washing solution was fabricated by multiple layers of PVC and PSA (Figure 11c). Active mechanical valves (M-valves) were made by creating a breakable thin wall in one layer, which was conducted by cutting the PVC layer to less than its total thickness. Notably, the M-valves play indispensable roles since they were tested at the rotational speed of 7000 rpm without leakage while they can be opened easily by an external mechanical force. In the assay protocol, the reaction chamber was first filled with the PEG resin in ethanol solution. By increasing the rotational speed to 2400 rpm, the PEG resin could be compressed and stacked to form a column in the reaction chamber, and the ethanol could be subsequently drained from the chamber. In the washing step, the first M-valve was actuated and PBS flowed into the column to wash out the residual ethanol. The PBS solution was incubated in the column for one minute under a low rotational speed (800 rpm) and the centrifugation was brought to a stop. Then the rotational speed was raised to 2400 rpm during the next two minutes to move (or shift) the waste solution from the reaction chamber into the collection chamber. In the next step, the second M-valve was actuated to convey the suspended PEGylated RNase sample into the column. After the protein absorption step, the waste liquid in the collection chamber was collected for further analysis. Similar procedures were performed for the four elution buffers. The four elution buffers were passed through the column sequentially and then collected in the collection chamber for further analysis. The success of this design indicates that centrifugal microfluidic chips offer a next-generation strategy for miniaturizing chromatographic devices and reducing chromatographic analysis time.

In summary, these reports indicate that centrifugal microfluidic systems provide a new perspective for designing the next-generation portable microfluidic system for various applications. Compared with pump-driven microfluidic systems, centrifugal microfluidic systems show advantages, such as low-cost

fluid transportation by the rotation of the disk and the integration of fluidic components, such as pumps, valves, flow mixers/rectifiers, and others. In addition, a wide range of the sample volume (from nanoliters to milliliters) can be processed by centrifugal microfluidic systems, and parallelization tests can be conducted to validate the efficacy and performance of the test systems. Compared to conventional capillary forces, the liquid driving forces from the centrifugal system show more stable flow behaviors. Moreover, the liquid driving force can be regulated by changing the direction of rotation (clockwise or counter-clockwise), the magnitude of the angular acceleration, and the rotational speeds. Furthermore, a process integration of multiple-step analysis on a disk can be achieved with the combination of fluidic functions, which can be controlled with the rotation of the disk and the geometry of the microstructure on the disk. Therefore, the features mentioned above indicate that the centrifugal microfluidic systems, or the "lab-on-a-disk" platforms, provide a programmable and portable design for various applications.

2.2.6. Thermophoresis

Since it was recognized that a temperature gradient causes a redistribution of species in a mixture, thermodiffusion in liquids has been intensively studied. Thermal diffusion (The Ludwing–Soret effect) was a significant breakthrough since it allowed for the investigation of the partial separation of components in a mixture using a temperature gradient.[252,253] As a temperature gradient phenomenon thermophoresis is when molecules, particles, or cells suspended in a media migrate through a channel as a result of an applied heat gradient. Because it can only be seen at extremely small scales (less than 1 mm), it can be used in conjunction with Brownian motion to control cells or other particles according to their characteristics even in systems lacking pressure gradients.[254]

Different techniques such as laser beam, hot/cold liquid, or a heater can be used to create the temperature gradient to force and manipulate molecules or particles.

Vigolo et al. demonstrate that thermophoresis, or mass flow driven by thermal gradients, may be utilized to drive particle motion in microfluidic devices using appropriate temperature control tactics. Thermophoresis offers significant advantages in terms of selectivity over typical particle manipulation techniques due to its strong sensitivity to particle/solvent interfacial characteristics. Furthermore, they show that by adding certain electrolytes and utilizing the additional thermoelectric effect resulting from their differential thermal responsiveness, it is possible to selectively drive particles to the cold or hot side.[316]

The viability of employing thermophoresis to separate submicroparticles of varying sizes in a thermophoretic sorter with an expansion-contraction microchannel is investigated by Ruijin et al. The chip has two inlets, A and B, as well as a separation channel, sub-outlets, a Plate heater, and an enlarged region. The 0.5 lm and 1.0 lm fluorescent particles are only fed into the system through inlet B, and the tracer particles are equally distributed in deionized water. The researchers used numerical simulations to determine the particle trajectories at various

**ADVANCED
SCIENCE NEWS**

www.advancedsciencenews.com

**ADVANCED
MATERIALS
INTERFACES**
Open Access

www.advmatinterfaces.de

inlet velocity, sheath flow rates, channel expansion-contraction ratio, and wall temperature differential. The results suggest that thermophoresis can be used to sort submicroparticles of varying sizes, and that smaller inlet velocity, bigger wall temperature differential, lower sheath flow rate, and higher channel expansion-contraction ratio can improve separation efficiency. The study also analyses numerical and experimental results and supports the thermophoretic sorter's preferable parameters based on numerical and experimental results.[255]

Geelhoed et al. described a microfluidic system that separates particles using thermophoresis. The microfluidic device is constructed of silicon, with a silicon-etched integrated thermophoretic separator channel. Because the thermal resistance across the channel must be high, a slit is carved from the lower side of the wafer to separate the chip's hot and cold sides. A heater is placed on top of a silicon nitride layer, which is an efficient thermal insulator, to provide a 1 mm thin transparent layer that allows the channel to be lighted from both sides. The system separates 83% of particles in ≈100 s while requiring minimum electrical power. The study compares experimental data to theoretical expectations and discovers a good fit. They also examine potential applications for this technology and mention that more research is needed to fully comprehend the increased separation speed. The research reveals a revolutionary particle separator that can be applied on-chip and has the potential to transform lab-on-a-chip systems.[256]

Duhr and Braun offer a thermophoresis-based approach for capturing and aggregating single particles on a PDMS-based microfluidic chip. The authors show how opposing fluid flow and a temperature gradient can capture and accumulate DNA molecules. The authors demonstrate how a radially converging temperature field can limit DNA to a narrow region.[257] Duhr et al. describe a microfluidic all-optical approach for measuring DNA thermophoresis. The authors used a narrow chamber sandwiched between glass covers or PDMS slides, and a moderately focused infrared laser was used to heat the center of the chamber locally. They discovered that the temperature and concentration profiles across the chamber had the same parabolic shape, and that fluorescence imaging averaging across the chamber produces no artifact. The authors additionally accounted for fluorescence dye bleaching and inhomogeneous fluorescence illumination. The observed results and parameters open up new avenues for monitoring thermophoresis at the single-molecule, near-boundary, and complex mixture levels.[258]

Thermophoresis, which has been studied extensively since the discovery of the influence of temperature gradients on species dispersion, has resulted in key advances such as the Ludwing-Soret effect. This small-scale phenomenon permits precise manipulation of particles, cells, or molecules within microfluidic systems, showing promise for a wide range of applications. The benefits include selectivity based on interfacial properties that outperform previous approaches. Using thermophoresis, researchers demonstrated particle motion control, separation, and accumulation in microfluidic devices. However, limitations include the inability to apply at extremely tiny sizes and the requirement for optimization. To summarize, thermophoresis has the potential for precise manipulation, but further research is needed to fully exploit its powers.

2.3. Hybrid Techniques

Isolation of biomolecules and cells from heterogeneous samples is one of the highest steps of diagnostic and pharmaceutical research.[317–319] Microfluidic chips offer several advantages over centrifuges and cytometers, including high speed, easy transportation, simple operation, reduced costs, and the ability to handle high volumes of reactions.[34,320] Biomedical samples typically consist cells, viral residues, proteins, and many other molecules. These molecules often present challenges due to their minimal numbers and small sizes compared to the surrounding environment.[321] In the past decade, hybrid microfluidic system have emerged as an attractive approach for obtaining more accurate results. Hybrid techniques in microfluidic chips for separation often integrate both passive and active approaches to enhance separation efficiency and selectivity.[322] The combination of these strategies leverages the inherent physical and chemical properties of the components being separated while also applying external energy or forces. As previously mentioned, the active methods involve the application of external physical forces such as magnetic, electrical, acoustic, light, and thermal forces,[322–325] and in passive methods, the shapes of channels and the flow velocity play a crucial role in the separation process.[21,326,327] While the active methods offer high accuracy in molecular and cellular isolation, it can be slow at times. In contrast, the passive approach generally offers greater speed and convenience. Therefore, the integration of active and passive enables enhanced control over the separation process.[328]

Integration of passive and active separation strategies within hybrid techniques enables synergistic effects and improved separation performance. For example, combining size-based filtration with electrophoresis can enhance separation efficiency by selectively driving charged particles through size-exclusion membranes.[329] In addition, according to the study by Petersson et al. in Analyst (2004), the integration of adsorption-based separation with acoustophoresis enables improved capture and release of target molecules by leveraging acoustic modulation of surface affinity.[330] Also, controlled diffusion-based separation can be combined with magnetophoresis for sorting and separation of magnetically labeled targets with different diffusion rates.[331] These examples highlight the possibilities of integrating passive and active separation strategies in hybrid techniques for microfluidic chips. By combining these approaches, researchers can achieve enhanced separation efficiency, improved selectivity, and precise control over separation processes.

Hybrid methods can be categorized into five parts based on the physical principles involved in the isolation process, as illustrated in Figure 1:

(a) Electrophoresis-assisted hybrid techniques (EP-assisted Hybrid techniques)

(b) Dielectrophoresis-assisted hybrid techniques (DEP-assisted techniques)

(c) Magnetophoresis-assisted hybrid techniques (MP-assisted technique)

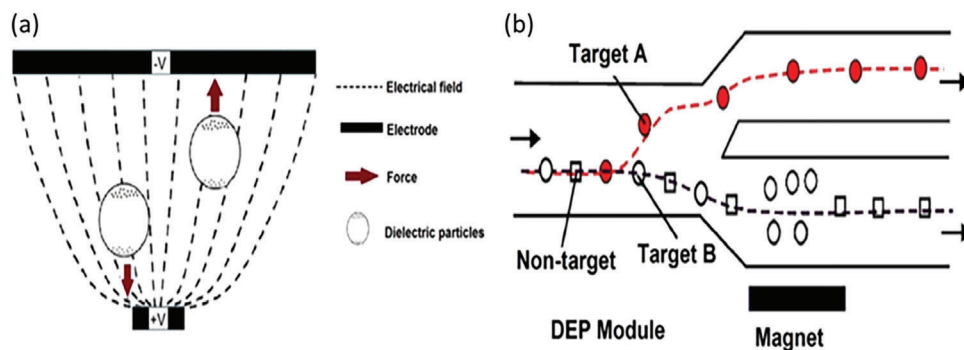(d) Acoustophoresis-assisted hybrid techniques (AP-assisted technique)

2300492 (33 of 45)

of the molecule, the density of the magnetic flux, the gradient of the magnetic field, and the permeability of space. The application of external magnetic fields enables precise control over the movement and positioning of magnetic particles, directing them to desired locations within the microfluidic device. This hybrid approach combines the advantages of magnetic manipulation with other separation mechanisms, allowing for enhanced separation performance and improved selectivity[336–340] Ying Xu et al.[337] utilized magnetophoresis method to isolate free extracellular DNA. First, free DNAs were labeled with magnetic particles and then subsequently washed using appropriate methods. The separation of molecules was achieved through a combined method of magnetophoresis and viscoelasticity. This process was performed in two steps. In the first step, the magnetic and nonmagnetic particles were concentrated in a straight rectangular channel by leveraging fluid viscoelasticity. In the second step, the channel was exposed to the magnetic field, causing the magnetic particles to deviate from the main flow and allowing for the separation of non-magnetic molecules. Currently, most of the magnetophoresis-assisted devices rely on the attachment of molecules to magnetic particles to achieve precise results. The passive compartment is positioned in the initial stage to consolidate the particles and molecules within a single flow. In the active stage, a magnetic field is applied to manipulate and separate the molecules labeled with immunomagnetic particles.[341]

2.3.4. AP-Assisted Hybrid Technique

AP is a technique that utilizes acoustic waves to manipulate particles within a fluidic environment. When integrated as a hybrid technique in microfluidic chips, AP provides a powerful means of separation and manipulation. By exploiting the properties of particles, such as size, density, and acoustic properties, AP enables precise control over their movement, resulting in efficient separation and enrichment. Acoustic flow is generated by stimulating a microfluidic channel with ultrasound, bringing it to a resonant state. Sound waves have a proportional effect on nano-sized bioparticles, such as DNA, proteins, viruses, and exosomes, based on their sizes. Therefore, larger molecules experience stronger forces compared to small molecules. Molecule density also play a role in this phenomenon with the dimensions of molecules.[320] Acoustic forces generated by the interaction between particles and acoustic waves can be utilized to position, trap, and separate particles within the microfluidic device. By applying different frequencies, modes, and spatial patterns of acoustic waves, researchers can achieve fine-tuned control over particle motion, enhancing the capabilities of microfluidic systems for molecular separation. Deterministic lateral displacement (DLD) is a passive method proposed by Huang et al.[327] that enables the precise separation of beads as small as 20 nm. Additionally, it can be used to separate bioparticles from plasma.[342] while this method is effective for accurate bioparticle separation, it lacks the required flexibility to accommodate changes. To address these limitations, DLD needs to be combined with an active method.[343] Compared to DEP, which requires electrodes inside the chip and a special buffer, AP is a non-contact and biocompatible method for biomolecule isolation that offers more flexibility for passive components. Furthermore, ultrasound of varying in-

tensities is safe for biological samples[344]; making it widely applicable in various biomedical processes.[345] Since the common problem with these devices is low-power AP, combining AP with other passive techniques can provide additional benefits to AP-assisted methods. Optophoresis-assisted Hybrid Techniques

Besides electric, magnetic, and acoustic fields, the utilization of highly concentrated light beam have rapidly advanced in recent decades. Optophoresis (OP) is a technique that utilizes light-induced forces to manipulate particles within a microfluidic chip.[346] When OP is integrated as a hybrid technique, it provides precise control over particle motion by leveraging their optical properties, such as refractive index or absorption. This technique facilitates efficient separation and manipulation of molecules within microscale environments. Optical methods offer the advantages of not interfering with the functions of biological cells and possess the capability to manipulate smaller targets, including cells and biomolecules. As a result, they are considered more promising than other techniques.[347] By leveraging optical trapping or gradient forces, OP allows for the selective positioning and manipulation of particles. Optical traps, created using focused laser beams, can immobilize or trap particles at specific locations within the microfluidic device. A focused laser beam can manipulate biomolecules based on the difference in refractive index between a molecule and its environment. This manipulation is achieved through the generation of scattering forces and gradients. The scattering forces cause the biomolecule to move away from the center of the beam, while the gradient forces pull the molecules towards the region of maximum beam intensity.[348,349] Optical forces can be used to sort molecules by active and passive methods.[350] The passive method for separation was introduced by MacDonald et al.[351] A wide, interconnected, reconfigured 3D optical network, similar to DLD, was utilized to sort protein microcapsules based on the refractive index by the size of colloidal particles. As the mixture passes through the network, the molecules deviate from their original positions while the rest particles remain in place. The efficiency of this separation method primarily relies on the response of the biomolecules to their optical potential. In their study, Yamada et al.[326] employed the pinched flow fraction (PFF) method, a straightforward passive method for separating DNA in a micro-channel using spreading flow. It can be easily combined with active systems due to the simple structure of this system. The integration of OP with other separation principles in hybrid systems enhances separation performance and expands the capabilities of microfluidic chips. By combining optical forces with other techniques, such as size-based filtration or electrokinetic separation, researchers can achieve improved selectivity and efficiency in molecular separation processes.

Hybrid microfluidics has received significant attention since its emergence in recent years. It combines the advantages of different techniques, allowing for enhanced performance and versatility in the separation of biomolecules. The continuous separation of biomolecules in hybrid microfluidic devices has shown promising results, demonstrating the potential for various applications in diagnostics, pharmaceuticals, and other areas of research. However, despite the progress made in the field, there are still significant challenges that need to be solved to fully realize the practicality and widespread adoption of hybrid microfluidics. One major challenge lies in the commercialization of hybrid

ADVANCED
SCIENCE NEWS

www.advancedsciencenews.com

ADVANCED
MATERIALS
INTERFACES
Open Access

www.advmatinterfaces.de

technologies, ensuring that they can be effectively implemented in industrial and clinical settings. While the field remains attractive and dynamic; it is important to bridge the gap between the prototype stage and clinical applicability. Many of the microfluidic technologies investigated in current studies are still in the early stages of development and have limited clinical use.

To advance the field of hybrid microfluidics, researchers need to focus on finding effective ways to translate these technologies into practical and impactful medical applications. This requires exploring innovative strategies and developing robust systems that can be seamlessly integrated into existing healthcare infrastructure. By addressing the practical challenges and establishing reliable and scalable solutions, hybrid microfluidics has the potential to revolutionize medicine and significantly improve diagnostics, therapeutics, and patient care. With continued innovation and collaboration, hybrid microfluidics can pave the way for groundbreaking advancements in various healthcare applications.

3. Conclusions

Molecular separation and precise identification of biomolecules, like nucleic acids, proteins, and polysaccharides from complex biological fluids are vital to numerous medical applications. Selective separation and identification of target analytes at molecular levels are more difficult because of the limited sample quantities. CE is a reasonably quick micro-level separation method and requires lower sample quantities. However, it can only separate biomolecules based on charge-to-size ratio. Passive and active methods are also capable separating of biomolecules. Passive methods drive channel structures, forces, and interactions between the molecules, and the flow field to manipulate the target biomolecules. Open microfluidic systems make surface customization and manufacturing simpler while increasing dependability by doing away with air bubble problems, providing promise as sensors for diagnostics, and facilitate fluid access for adding samples. They can be used in a wider range of technologies by addressing problems like evaporation, sample leakage, and restricted pressure control with techniques including sacrificial liquids, humidified containers, and enclosed cages. Pillar arrays microfluidic systems that are produced by both top-down and bottom-up techniques, allowing for more interior surface area for biomolecule separation. However, these systems need expensive external pumps for fluid control, and leakage from probable biomolecule blockage is a possibility. Additional investigation is required to validate the repeatability and comparability of system outputs with human and animal samples. Resin (beds) incorporated microfluidic channels were used in chromatography because of their strong adsorption potential and huge surface area. Different types of resin materials are used, including polymers, inorganic compounds, and natural polysaccharides. While resin-based microfluidic systems have advantages like low reagent consumption and quick results, they also come with difficulties like material synthesis, immobilization, and mechanical strength restrictions, particularly for soft gels, which can affect packaging and pressure generation. Monolithic microfluidics characteristics such as high surface area, porosity, and ease of fabrication make them ideal for methods like SPE and affinity-based separations. However, to maintain surface area and separation effec-

tiveness during production, precise control of porosity is essential. Challenges include the requirement for careful chip material selection for in-situ polymerization, which might affect material integrity and potential reductions in binding capacity caused by inadequate porosity adjustment. Microfluidic chip applications could be expanded and extraction properties improved by using composite or hybrid monolith materials, such as those imprinted with molecules or nanoparticles. Nanowires incorporated microfluidic systems have high potential for filtering DNA due to its high surface-to-volume ratio, and the resulting nanowire network improves capture area and may be used to separate proteins and RNA. However, using expensive methods such as photolithography, electron beam lithography, vapor-liquid-solid growth, deposition, and reactive ion etching, for microfabrication of nanowires is the drawback of these systems. L/L extraction microfluidic systems have advantages like improved mass transfer, decreased consumption, selectivity, and ease of integration. However, scaling it up from the lab to industry, working with complicated materials, and initial setup expenses are drawbacks.

Active methods use external forces such as acoustic, magnetic, and electric fields to manipulate the target biomolecules. DEP devices are useful for the selective purification, separation, and investigation of the properties of biological materials without causing structural damage, especially in microfluidic systems. The effect of DEP on subcellular molecules, in particular nucleic acids, for applications in separation, trapping, purification, and self-assembly is also highlighted in literature. μFFE is useful for proteomics protein purification due to advantages like decreased labor requirements, quick implementation, and improved separation speed; however, difficulties like gas bubble generation, material selection, and sensitivity to electric field perturbations may occasionally prevent resolution. In magnetic separation systems, magnetic particles rapidly remove target biomolecules from complex media such as blood, allowing for easy integration with microfluidics and manipulation with an external magnetic field; nevertheless, the presence of unloaded particles in the buffer might cause aggregation and noise. Acoustic microfluidic separation approaches provide label-free and non-invasive separation of biomolecules based on features such as size and density, but their dependency on external equipment and low throughput make commercialization difficult. Centrifugal microfluidic systems are a low-cost solution to portable microfluidic designs that integrate components and enable steady fluid transfer via disk rotation. These systems can handle a wide range of sample volumes, have steady flow characteristics, and can allow multi-step analysis via disk rotation and microstructure geometry control, making them versatile platforms for a variety of applications. Thermophoresis allows for precise manipulation of particles, cells, or molecules within microfluidic devices, with benefits such as increased selectivity; however, size constraints and optimization requirements exist. More research is required to fully realize its potential.

In the case of the complex biological samples, precise separation with a single-module microfluidic device (either passive or active) seems to have difficulty. Therefore, hybrid microfluidics are emerging techniques that combine active and passive methods, and provide advances in reaching stability of performance, convenience, and versatility. Hybrid microfluidics, which combines several approaches, has the potential to improve biomolecule separation for applications in diagnostics and

pharmaceuticals. However, commercialization and clinical integration of them remain hurdles. Hybrid microfluidics make it possible to process multi-target samples; enhance the ability for multiplexed separation, adjustability for a wider working range, and higher sensitivity. To maximize the impact of these technologies, researchers should concentrate on translating them into practical medical applications, addressing practical challenges, and developing robust, scalable systems that can seamlessly integrate with healthcare infrastructure, potentially revolutionizing medicine and improving diagnostics, therapeutics, and patient care. The key to unleashing the revolutionary potential of hybrid microfluidics in healthcare is continued innovation and collaboration. Nevertheless, the separation methods elucidated here have a great potential for use in biological research and clinical practices by determining the technique depending on the need. Although much progress in microfluidic-based molecular separation methods has been reported, there are numerous questions about their integration with other components. In this regard, research should focus on integrating multiple functions into a single microfluidic system to be used in biological analysis systems more efficiently.

Conflict of Interest

The authors declare no conflict of interest.

[1] F. A. Vicente, I. Plazl, S. P. M. Ventura, P. Znidarsic-Plazl, *Green Chem.* **2020**, *22*, 4391.

[2] E. Chiesa, R. Dorati, S. Pisani, B. Conti, G. Bergamini, T. Modena, I. Genta, *Pharmaceutics* **2018**, *10*, 267.

[3] R. R. Alexander, J. M. Griffiths, M. L. Wilkinson, *Basic Biochemical Methods, Wiley*, John Wiley & Sons, Chichester **1985**.

[4] M. Sonker, V. Sahore, A. T. Woolley, *Anal. Chim. Acta* **2017**, *986*, 1.

[5] K. M. Horsman, J. M. Bienvenue, K. R. Blasier, J. P. Landers, *J Forensic Sci* **2007**, *52*, 784.

[6] S. R. Shin, Y. S. Zhang, D.-J. Kim, A. Manbohi, H. Avci, A. Silvestri, J. Aleman, N. Hu, T. Kilic, W. Keung, M. Righi, P. Assawes, H. A. Alhadrami, R. A. Li, M. R. Dokmeci, A. Khademhosseini, *Anal. Chem.* **2016**, *88*, 10019.

[7] S. R. Shin, T. Kilic, Y. S. Zhang, H. Avci, N. Hu, D. Kim, C. Branco, J. Aleman, S. Massa, A. Silvestri, J. Kang, A. Desalvo, M. A. Hussaini, S.-K. Chae, A. Polini, N. Bhise, M. A. Hussain, H. Lee, M. R. Dokmeci, A. Khademhosseini, *Adv. Sci.* **2017**, *4*, 1600522.

[8] S. A. M. Shaegh, A. Pourmand, M. Nabavinia, H. Avci, A. Tamayol, P. Mostafalu, H. B. Ghavifekr, E. N. Aghdam, M. R. Dokmeci, A. Khademhosseini, Y. S. Zhang, *Sens. Actuators, B* **2018**, *255*, 100.

[9] R. Mohammadigharehbagh, Ö. Tomsuk, H. Ghorbanpoor, A. Ebrahimi, N. Abdullayeva, N. Gasimzade, Y. Koç, C. Özel, A. Ghorbani, B. Demir, O. Uysal, F. Dogan Guzel, A. Eker Sarıboyacı, H. Avci, in *11th International Fiber and Polymer Research Symposium*, Gebze, Turkey **2022**, pp. 222–226.

[10] Y. S. Zhang, J. Aleman, S. R. Shin, T. Kilic, D. Kim, S. A. Mousavi Shaegh, S. Massa, R. Riahi, S. Chae, N. Hu, H. Avci, W. Zhang, A. Silvestri, A. Sanati Nezhad, A. Manbohi, F. De Ferrari, A. Polini, G. Calzone, N. Shaikh, P. Alerasool, E. Budina, J. Kang, N. Bhise, J. Ribas, A. Pourmand, A. Skardal, T. Shupe, C. E. Bishop, M. R. Dokmeci, A. Atala, *Proc. Natl. Acad. Sci. USA* **2017**, *114*, E2293.

[11] C. Özel, Y. Koç, A. Topal, A. Ebrahimi, T. Sengel, H. Ghorbanpoor, F. Dogan Guzel, O. Uysal, A. Eker Sariboyaci, H. Avci, *Eskişehir Technical University Journal of Science and Technology A-Applied Sciences and Engineering* **2021**, *22*, 85.

[12] C. Özel, Y. Koç, A. E. Topal, A. Ebrahimi, T. Şengel, H. Ghorbanpoor, F. Doğan Güzel, O. Uysal, A. Eker Sariboyaci, H. Avci, in *8th International Fiber and Polymer Research Symposium*, **2021**, pp. 53–54.

[13] L. Gorgannezhad, H. Stratton, N.-T. Nguyen, *Micromachines* **2019**, *10*, 408.

[14] P. N. Nge, J. V. Pagaduan, M. Yu, A. T. Woolley, *J. Chromatogr. A* **2012**, *1261*, 129.

[15] H. Ghorbanpoor, D. Corrigan, F. Dogan Guzel, *Sakarya University Journal of Science* **2022**, *26*, 120.

[16] Y. Meng, M. Asghari, M. K. Aslan, A. Yilmaz, B. Mateescu, S. Stavrakis, A. J. Demello, *Chem. Eng. J.* **2021**, *404*, 126110.

[17] N.-T. Nguyen, M. Hejazian, C. Ooi, N. Kashaninejad, *Micromachines* **2017**, *8*, 186.

[18] M. Bayareh, *Chem. Eng. Process.* **2020**, *153*, 107984.

[19] Y. Gao, M. Wu, Y. Lin, J. Xu, *Micromachines* **2020**, *11*, 921.

[20] W. Al-Faqheri, T. H. G. Thio, M. A. Qasaimeh, A. Dietzel, M. Madou, A. Al-Halhouli, *Microfluid. Nanofluid.* **2017**, *21*, 1.

[21] J. Mcgrath, M. Jimenez, H. Bridle, *Lab Chip* **2014**, *14*, 4139.

[22] H. Jeon, S. Kim, G. Lim, *Microelectron. Eng.* **2018**, *198*, 55.

[23] Z. Wu, K. Hjort, *Micro and Nanosystems* **2009**, *1*, 181.

[24] R.-J. Yang, H.-H. Hou, Y.-N. Wang, L.-M. Fu, *Sens. Actuators, B* **2016**, *224*, 1.

[25] J. De Jong, R. G. H. Lammertink, M. Wessling, *Lab Chip* **2006**, *6*, 1125.

[26] X. Chen, J. Shen, *Journal of Chemical Technology & Biotechnology* **2017**, *92*, 271.

[27] M. Piotrowska, K. Ciura, M. Zalewska, M. Dawid, B. Correia, P. Sawicka, B. Lewczuk, J. Kasprzyk, L. Sola, W. Piekoszewski, B. Wielgomas, K. Waleron, S. Dziomba, *J. Chromatogr. A* **2020**, *1621*, 461047.

**ADVANCED
SCIENCE NEWS**

www.advancedsciencenews.com

**ADVANCED
MATERIALS
INTERFACES**
Open Access

www.advmatinterfaces.de

[28] A. Ramachandran, D. A. Huyke, E. Sharma, M. K. Sahoo, C. Huang, N. Banaei, B. A. Pinsky, J. G. Santiago, *Proc Natl Acad Sci U S A* **2020**, *117*, 29518.

[29] K. L. Saar, T. Müller, J. Charmet, P. K. Challa, T. P. J. Knowles, *Anal. Chem.* **2018**, *90*, 8998.

[30] V. Kasicka, *Electrophoresis* **2022**, *43*, 82.

[31] W.-W. Sun, R.-J. Dai, Y.-R. Li, G.-X. Dai, X.-J. Liu, B. Li, X.-F. Lv, Y.-L. Deng, A.-Q. Luo, *Acta Astronaut.* **2020**, *166*, 573.

[32] X. Lu, C. Liu, G. Hu, X. Xuan, *J. Colloid Interface Sci.* **2017**, *500*, 182.

[33] A. Dalili, E. Samiei, M. Hoorfar, *Analyst* **2019**, *144*, 87.

[34] A. A. S. Bhagat, H. Bow, H. W. Hou, S. J. Tan, J. Han, C. T. Lim, *Med. Biol. Eng. Comput.* **2010**, *48*, 999.

[35] B. C. Giordano, D. S. Burgi, S. J. Hart, A. Terray, *Anal. Chim. Acta* **2012**, *718*, 11.

[36] K. K. R. Tetala, M. A. Vijayalakshmi, *Anal. Chim. Acta* **2016**, *906*, 7.

[37] M. Karle, S. K. Vashist, R. Zengerle, F. Von Stetten, *Anal. Chim. Acta* **2016**, *929*, 1.

[38] M. Antfolk, T. Laurell, *Anal. Chim. Acta* **2017**, *965*, 9.

[39] P. Sajeesh, A. K. Sen, *Microfluid. Nanofluid.* **2014**, *17*, 1.

[40] H. S. Santana, J. L. Silva, B. Aghel, J. Ortega-Casanova, *SN Applied Sciences* **2020**, *2*, 1.

[41] M. Viefhues, R. Eichhorn, E. Fredrich, J. Regtmeier, D. Anselmetti, *Lab Chip* **2012**, *12*, 485.

[42] M. Dawod, N. E. Arvin, R. T. Kennedy, *Analyst* **2017**, *142*, 1847.

[43] L. Sun, G. Zhu, X. Yan, M. M. Champion, N. J. Dovichi, *Proteomics* **2014**, *14*, 622.

[44] S. F. Berlanda, M. Breitfeld, C. L. Dietsche, P. S. Dittrich, *Anal. Chem.* **2021**, *93*, 311.

[45] H. Tang, J. Niu, H. Jin, S. Lin, D. Cui, *Microsyst. Nanoeng.* **2022**, *8*, 1.

[46] V. Gubala, J. Siegrist, R. Monaghan, B. O'reilly, R. P. Gandhiraman, S. Daniels, D. E. Williams, J. Ducrée, *Anal. Chim. Acta* **2013**, *760*, 75.

[47] F. Kitagawa, K. Kubota, K. Sueyoshi, K. Otsuka, *J. Pharm. Biomed. Anal.* **2010**, *53*, 1272.

[48] J-J. Feng, A.-J. Wang, J. Fan, J.-J. Xu, H.-Y. Chen, *Anal. Chim. Acta* **2010**, *658*, 75.

[49] K.-Y. Hwang, J-H. Kim, K.-Y. Suh, J. S. Ko, N. Huh, *Sens. Actuators, B* **2011**, *155*, 422.

[50] L. Zhang, S. M. Rafei, L. Xie, M. B.-R. Chew, H. M. Ji, Y. Chen, R. Rajoo, K.-L. Ong, R. Tan, S.-H. Lau, V. T. K. Chow, C.-K. Heng, K.-H. Teo, T. G. Kang, *Sens. Actuators, B* **2011**, *160*, 1557.

[51] C. N. Hughes-Chinkhota, M. Banda, J. M. Smolinski, R. A. Thomas, D. M. Petibone, J. D. Tucker, G. W. Auner, *Sens. Actuators, B* **2011**, *155*, 437.

[52] K. A. Hagan, W. L. Meier, J. P. Ferrance, J. P. Landers, *Anal. Chem.* **2009**, *81*, 5249.

[53] J. Kim, J. P. Hilton, K-A. Yang, R. Pei, M. Stojanovic, Q. Lin, *Sens. Actuators, A* **2013**, *195*, 183.

[54] J. Wen, C. Guillo, J. P. Ferrance, J. P. Landers, *Anal. Chem.* **2007**, *79*, 6135.

[55] A. Bhattacharyya, C. M. Klapperich, *Anal. Chem.* **2006**, *78*, 788.

[56] P. A. Levkin, S. Eeltink, T. R. Stratton, R. Brennen, K. Robotti, H. Yin, K. Killeen, F. Svec, J. M. J. Fréchet, *J. Chromatogr. A* **2008**, *1200*, 55.

[57] C. Li, K. H. Lee, *Anal. Biochem.* **2004**, *333*, 381.

[58] T. Yasui, S. Rahong, K. Motoyama, T. Yanagida, Q. Wu, N. Kaji, M. Kanai, K. Doi, K. Nagashima, M. Tokeshi, M. Taniguchi, S. Kawano, T. Kawai, Y. Baba, *ACS Nano* **2013**, *7*, 3029.

[59] S. Rahong, T. Yasui, T. Yanagida, K. Nagashima, M. Kanai, A. Klamchuen, G. Meng, Y. He, F. Zhuge, N. Kaji, T. Kawai, Y. Baba, *Sci. Rep.* **2014**, *4*, 1.

[60] S. Rahong, T. Yasui, T. Yanagida, K. Nagashima, M. Kanai, G. Meng, Y. He, F. Zhuge, N. Kaji, T. Kawai, Y. Baba, *Sci. Rep.* **2015**, *5*, 1.

[61] V. Krivitsky, L.-C. Hsiung, A. Lichtenstein, B. Brudnik, R. Kantaev, R. Elnathan, A. Pevzner, A. Khatchtourints, F. Patolsky, *Nano Lett.* **2012**, *12*, 4748.

[62] S. Rahong, T. Yasui, T. Yanagida, K. Nagashima, M. Kanai, G. Meng, Y. He, F. Zhuge, N. Kaji, T. Kawai, Y. Baba, *Anal. Sci.* **2015**, *31*, 153.

[63] N. Hao, M. Zhang, J. X. J. Zhang, *Biomater. Sci.* **2020**, *8*, 1783.

[64] D. Zhao, Z. He, G. Wang, H. Wang, Q. Zhang, Y. Li, *Sens. Actuators, B* **2016**, *229*, 281.

[65] C.-H. Sang, S.-J. Chou, F. M. Pan, J.-T. Sheu, *Biosens. Bioelectron.* **2016**, *75*, 285.

[66] A. K. Singh, D.-H. Ko, N. K. Vishwakarma, S. Jang, K-I. Min, D.-P. Kim, *Nat. Commun.* **2016**, *7*, 1.

[67] X. Yu, Y. Xia, Y. Tang, W.-L. Zhang, Y.-T. Yeh, H. Lu, S.-Y. Zheng, *Small* **2017**, *13*, 1700425.

[68] K. Sato, M. Tokeshi, T. Sawada, T. Kitamori, *Anal. Sci.* **2000**, *16*, 455.

[69] E. Kamio, Y. Seike, H. Yoshizawa, H. Matsuyama, T. Ono, *Ind. Eng. Chem. Res.* **2011**, *50*, 6915.

[70] A. B. Theberge, F. Courtois, Y. Schaerli, M. Fischlechner, C. Abell, F. Hollfelder, W. T. S. Huck, *Angew Chem Int Ed Engl* **2010**, *49*, 5846.

[71] A. Alrifaiy, O. A. Lindahl, K. Ramser, *Polymers* **2012**, *4*, 1349.

[72] H. Chen, Q. Fang, X.-F. Yin, Z.-L. Fang, *Lab Chip* **2005**, *5*, 719.

[73] V. Reddy, J. D. Zahn, *J. Colloid Interface Sci.* **2005**, *286*, 158.

[74] W. Zhang, Y. S. Zhang, S. M. Bakht, J. Aleman, S. R. Shin, K. Yue, M. Sica, J. Ribas, M. Duchamp, J. Ju, R. B. Sadeghian, D. Kim, M. R. Dokmeci, A. Atala, A. Khademhosseini, *Lab Chip* **2016**, *16*, 1579.

[75] J. Abatemarco, M. F. Sarhan, J. M. Wagner, J.-L. Lin, L. Liu, W. Hassouneh, S-F. Yuan, H. S. Alper, A. R. Abate, *Nat. Commun.* **2017**, *8*, 332.

[76] E. K. Sackmann, A. L. Fulton, D. J. Beebe, *Nature* **2014**, *507*, 181.

[77] P. K. Sharma, M. J. Gibcus, H. C. Van Der Mei, H. J. Busscher, *Appl. Environ. Microbiol.* **2005**, *71*, 3668.

[78] E. A. Vogler, *Biomaterials* **2012**, *33*, 1201.

[79] J. G. Kralj, H. R. Sahoo, K. F. Jensen, *Lab Chip* **2007**, *7*, 256.

[80] S. Feng, S. Mao, J. Dou, W. Li, H. Li, J.-M. Lin, *Chem. Sci.* **2019**, *10*, 8571.

[81] B. D. Kevadiya, J. Machhi, J. Herskovitz, M. D. Oleynikov, W. R. Blomberg, N. Bajwa, D. Soni, S. Das, M. Hasan, M. Patel, A. M. Senan, S. Gorantla, J. Mcmillan, B. Edagwa, R. Eisenberg, C. B. Gurumurthy, S. P. M. Reid, C. Punyadeera, L. Chang, H. E. Gendelman, *Nat. Mater.* **2021**, *20*, 593.

[82] S. F. Cheung, S. K. L. Cheng, D. T. Kamei, *J Lab Autom* **2015**, *20*, 316.

[83] M. Naseri, G. P. Simon, W. Batchelor, *Anal. Chem.* **2020**, *92*, 7307.

[84] H. Lim, A. T. Jafry, J. Lee, *Molecules* **2019**, *24*, 2869.

[85] V. Soum, S. Park, A. I. Brilian, O.-S. Kwon, K. Shin, *Micromachines (Basel)* **2019**, *10*,.

[86] D. L. Giokas, G. Z. Tsogas, A. G. Vlessidis, *Anal. Chem.* **2014**, *86*, 6202.

[87] A. Nilghaz, D. R. Ballerini, W. Shen, *Biomicrofluidics* **2013**, *7*,.

[88] J. Berthier, K. A. Brakke, D. Gosselin, E. Berthier, F. Navarro, *Medical Engineering & Physics* **2017**, *48*, 55.

[89] M. Reches, K. A. Mirica, R. Dasgupta, M. D. Dickey, M. J. Butte, G. M. Whitesides, *Abstracts of Papers of the American Chemical Society* **2010**, *240*, 1722.

[90] P. Mostafalu, M. Akbari, K. A. Alberti, Q. Xu, A. Khademhosseini, S. R. Sonkusale, *Microsyst. Nanoeng.* **2016**, *2*, 16039.

[91] L. Chen, J. M. Cabot, B. Paull, *Lab Chip* **2021**, *21*, 2565.

[92] U. N. Lee, X. Su, D. J. Guckenberger, A. M. Dostie, T. Zhang, E. Berthier, A. B. Theberge, *Lab Chip* **2018**, *18*, 496.

[93] L. J. Barkal, A. B. Theberge, C.-J. Guo, J. Spraker, L. Rappert, J. Berthier, K. A. Brakke, C. C. C. Wang, D. J. Beebe, N. P. Keller, E. Berthier, *Nat. Commun.* **2016**, *7*, 10610.

[94] W. Zheng, Z. Wang, W. Zhang, X. Jiang, *Lab Chip* **2010**, *10*, 2906.

[95] T. E. De Groot, K. S. Veserat, E. Berthier, D. J. Beebe, A. B. Theberge, *Lab Chip* **2016**, *16*, 334.

[96] J. J. Lee, J. Berthier, K. A. Brakke, A. M. Dostie, A. B. Theberge, E. Berthier, *Langmuir* **2018**, *34*, 5358.

[97] I. Lewinska, L. F. Capitán-Vallvey, M. M. Erenas, *Talanta* **2023**, *253*, 124094.

[98] R. Panneerselvam, H. Sadat, E.-M. Höhn, A. Das, H. Noothalapati, D. Belder, *Lab Chip* **2022**, *22*, 665.

[99] S. Petralia, E. L. Sciuto, S. Conoci, *Analyst* **2017**, *142*, 140.

[100] N. C. Cady, S. Stelick, C. A. Batt, *Biosens. Bioelectron.* **2003**, *19*, 59.

[101] J. Wang, W. Li, L. Zhang, L. Ban, P. Chen, W. Du, X. Feng, B.-F. Liu, *ACS Appl. Mater. Interfaces* **2017**, *9*, 27441.

[102] Z. Wang, H.-J. Wu, D. Fine, J. Schmulen, Y. Hu, B. Godin, J. X. J. Zhang, X. Liu, *Lab Chip* **2013**, *13*, 2879.

[103] B. H. Wunsch, J. T. Smith, S. M. Gifford, C. Wang, M. Brink, R. L. Bruce, R. H. Austin, G. Stolovitzky, Y. Astier, *Nat. Nanotechnol.* **2016**, *11*, 936.

[104] B. H. Wunsch, S.-C. Kim, S. M. Gifford, Y. Astier, C. Wang, R. L. Bruce, J. V. Patel, E. A. Duch, S. Dawes, G. Stolovitzky, J. T. Smith, *Lab Chip* **2019**, *19*, 1567.

[105] T. Yasui, N. Kaji, R. Ogawa, S. Hashioka, M. Tokeshi, Y. Horiike, Y. Baba, *Nano Lett.* **2015**, *15*, 3445.

[106] K. K. Zeming, T. Salafi, S. Shikha, Y. Zhang, *Nat. Commun.* **2018**, *9*, 1.

[107] E. Valera, J. Berger, U. Hassan, T. Ghonge, J. Liu, M. Rappleye, J. Winter, D. Abboud, Z. Haidry, R. Healey, N.-T. Hung, N. Leung, N. Mansury, A. Hasnain, C. Lannon, Z. Price, K. White, R. Bashir, *Lab Chip* **2018**, *18*, 1461.

[108] E. Borberg, M. Zverzhinetsky, A. Krivitsky, A. Kosloff, O. Heifler, G. Degabli, H. P. Soroka, R. S. Fainaro, L. Burstein, S. Reuveni, H. Diamant, V. Krivitsky, F. Patolsky, *Nano Lett.* **2019**, *19*, 5868.

[109] T. Salafi, Y. Zhang, Y. Zhang, *Nano-Micro Lett.* **2019**, *11*, 1.

[110] T. Ajiri, T. Yasui, M. Maeki, A. Ishida, H. Tani, J. Nishii, Y. Baba, M. Tokeshi, *ACS Appl. Nano Mater.* **2020**, *3*, 8810.

[111] Y. Chen, E. S. Abrams, T. C. Boles, J. N. Pedersen, H. Flyvbjerg, R. H. Austin, J. C. Sturm, *Phys. Rev. Lett.* **2015**, *114*, 198303.

[112] A. S. Chan, M. K. Danquah, D. Agyei, P. G. Hartley, Y. Zhu, *J. Anal. Methods Chem.* **2014**, *2014*, 1.

[113] G. Shao, D. Lu, Z. Fu, D. Du, R. M. Ozanich, W. Wang, Y. Lin, *Analyst* **2016**, *141*, 206.

[114] A. U. Andar, S. Deldari, E. Gutierrez, D. Burgenson, M. Al-Adhami, C. Gurramkonda, L. Tolosa, Y. Kostov, D. D. Frey, G. Rao, *Biotechnol. Bioeng.* **2019**, *116*, 870.

[115] I. F. Pinto, R. R. G. Soares, S. A. S. L. Rosa, M. R. Aires-Barros, V. Chu, J. P. Conde, A. M. Azevedo, *Anal. Chem.* **2016**, *88*, 7959.

[116] I. F. Pinto, C. R. F. Caneira, R. R. G. Soares, N. Madaboosi, M. R. Aires-Barros, J. P. Conde, A. M. Azevedo, V. Chu, *Methods* **2017**, *116*, 112.

[117] I. F. Pinto, D. R. Santos, R. R. G. Soares, M. R. Aires-Barros, V. Chu, A. M. Azevedo, J. P. Conde, *Sens. Actuators, B* **2018**, *255*, 3636.

[118] I. F. Pinto, R. R. G. Soares, M. R. Aires-Barros, V. Chu, J. P. Conde, A. M. Azevedo, *Biotechnol. J.* **2019**, *14*, 1800593.

[119] W. Cao, C. J. Easley, J. P. Ferrance, J. P. Landers, *Anal. Chem.* **2006**, *78*, 7222.

[120] C. R. Reedy, J. M. Bienvenue, L. Coletta, B. C. Strachan, N. Bhatri, S. Greenspoon, J. P. Landers, *Forensic Sci Int Genet* **2010**, *4*, 206.

[121] N. Malmstadt, P. Yager, A. S. Hoffman, P. S. Stayton, *Anal. Chem.* **2003**, *75*, 2943.

[122] A. Kecskemeti, A. Gaspar, *Talanta* **2018**, *180*, 211.

[123] M. H. Ghanim, N. Najimudin, K. Ibrahim, M. Z. Abdullah, *IET Nanobiotechnol* **2014**, *8*, 77.

[124] F. R. Mansour, S. Waheed, B. Paull, F. Maya, *J. Sep. Sci.* **2020**, *43*, 56.

[125] F. Svec, J. M. J. Frechet, *Anal. Chem.* **1992**, *64*, 820.

[126] A. Namera, A. Nakamoto, T. Saito, S. Miyazaki, *J. Sep. Sci.* **2011**, *34*, 901.

[127] I. Nischang, I. Teasdale, O. Brüggemann, *Anal. Bioanal. Chem.* **2011**, *400*, 2289.

[128] M. R. Gama, F. R. P. Rocha, C. B. G. Bottoli, *Trends Analyt Chem* **2019**, *115*, 39.

[129] M. Araya-Farias, S. Dziomba, N. T. Tran, in *Handbook on Miniaturization in Analytical Chemistry*, Elsevier, **2020**, pp. 35–75.

[130] R. Knob, V. Sahore, M. Sonker, A. T. Woolley, *Biomicrofluidics* **2016**, *10*, 032901.

[131] Y. Ladner, A. Bruchet, G. Crétier, V. Dugas, J. Randon, K. Faure, *Lab Chip* **2012**, *12*, 1680.

[132] L. F. Ribeiro, J. C. Masini, F. Svec, *Trends Analyt Chem* **2019**, *118*, 606.

[133] M. Vergara-Barberán, E. J. Carrasco-Correa, M. J. Lerma-García, E. F. Simó-Alfonso, J. M. Herrero-Martínez, *Anal. Chim. Acta* **2019**, *1084*, 1.

[134] M. Vázquez, B. Paull, *Anal. Chim. Acta* **2010**, *668*, 100.

[135] S. Dziomba, M. Araya-Farias, C. Smadja, M. Taverna, B. Carbonnier, N. T. Tran, *Anal. Chim. Acta* **2017**, *955*, 1.

[136] E. Alzahrani, K. Welham, *Analyst* **2012**, *137*, 4751.

[137] A. S. Chan, M. K. Danquah, D. Agyei, P. G. Hartley, Y. Zhu, *Sep. Sci. Technol.* **2014**, *49*, 854.

[138] R. R. Svejdal, D. Sticker, C. Sønderby, J. P. Kutter, K. D. Rand, *Anal. Chim. Acta* **2020**, *1140*, 168.

[139] N. Abdulhussain, S. H. Nawada, S. A. Currivan, P. J. Schoenmakers, *J. Sep. Sci.* **2022**, *45*, 1400.

[140] R. Mehta, T. A. Van Beek, K. K. R. Tetala, *J. Chromatogr. A* **2020**, *1627*, 461415.

[141] E. K. Parker, A. V. Nielsen, M. J. Beauchamp, H. M. Almughamsi, J. B. Nielsen, M. Sonker, H. Gong, G. P. Nordin, A. T. Woolley, *Anal. Bioanal. Chem.* **2019**, *411*, 5405.

[142] H. M. Almughamsi, M. K. Howell, S. R. Parry, J. E. Esene, J. B. Nielsen, G. P. Nordin, A. T. Woolley, *Analyst* **2022**, *147*, 734.

[143] A. V. Bickham, C. Pang, B. Q. George, D. J. Topham, J. B. Nielsen, G. P. Nordin, A. T. Woolley, *Anal. Chem.* **2020**, *92*, 12322.

[144] K. B. Megha, P. V. Mohanan, *Int. J. Biol. Macromol.* **2020**, *169*, 28,.

[145] Q.-S. Kang, X.-F. Shen, N.-N. Hu, M.-J. Hu, H. Liao, H.-Z. Wang, Z-K. He, W.-H. Huang, *Analyst* **2013**, *138*, 2613.

[146] A. Khaparde, K. K. R. Tetala, *J. Pharm. Biomed. Anal.* **2020**, *181*, 113099.

[147] Z.-H. Wei, X. Zhang, X. Zhao, Y.-J. Jiao, Y.-P. Huang, Z.-S. Liu, *Talanta* **2021**, *224*, 121810.

[148] Y. Wu, Y. Zhang, W. Li, Y. Xu, Y. Liu, X. Liu, Y. Xu, W. Liu, *Talanta* **2022**, *249*, 123652.

[149] E. L. Kendall, E. Wienhold, D. L. Devoe, *Biomicrofluidics* **2014**, *8*, 044109.

[150] R. Knob, D. B. Nelson, R. A. Robison, A. T. Woolley, *J. Chromatogr. A* **2017**, *1523*, 309.

[151] R. Knob, R. L. Hanson, O. B. Tateoka, R. L. Wood, I. Guerrero-Arguero, R. A. Robison, W. G. Pitt, A. T. Woolley, *J. Chromatogr. A* **2018**, *1562*, 12.

[152] Z. Li, E. Rodriguez, S. Azaria, A. Pekarek, D. S. Hage, *Electrophoresis* **2017**, *38*, 2837.

[153] B. Fresco-Cala, S. Cárdenas, *Anal. Chim. Acta* **2018**, *1031*, 15.

[154] M. Sonker, R. Yang, V. Sahore, S. Kumar, A. T. Woolley, *Anal. Methods* **2016**, *8*, 7739.

[155] M. Sonker, E. K. Parker, A. V. Nielsen, V. Sahore, A. T. Woolley, *Analyst* **2018**, *143*, 224.

[156] M. Sonker, R. Knob, V. Sahore, A. T. Woolley, *Electrophoresis* **2017**, *38*, 1743.

[157] C. Wang, M. Ye, L. Cheng, R. Li, W. Zhu, Z. Shi, C. Fan, J. He, J. Liu, Z. Liu, *Biomaterials* **2015**, *54*, 55.

[158] T. Yasui, T. Yanagida, S. Ito, Y. Konakade, D. Takeshita, T. Naganawa, K. Nagashima, T. Shimada, N. Kaji, Y. Nakamura, I. A. Thiodorus, Y. He, S. Rahong, M. Kanai, H. Yukawa, T. Ochiya, T. Kawai, Y. Baba, *Sci. Adv.* **2017**, *3*, e1701133.

[159] L. Guo, Y. Shi, X. Liu, Z. Han, Z. Zhao, Y. Chen, W. Xie, X. Li, *Biosens. Bioelectron.* **2018**, *99*, 368.

[160] D. Janasek, J. Franzke, A. Manz, *Nature* **2006**, *442*, 374.

[161] K. Benz, K.-P. Jäckel, K.-J. Regenauer, J. Schiewe, K. Drese, W. Ehrfeld, V. Hessel, H. Löwe, *Chem. Eng. Technol.* **2001**, *24*, 11.

[162] J. Leng, J.-B. Salmon, *Lab Chip* **2009**, *9*, 24.

[163] R. Didarian, A. Ebrahimi, H. Ghorbanpoor, A. Dizaji, H. Hashempour, F. Guzel, H. Avci, in *International Fiber and Polymer Research Symposium*, **2021**, p. 19.

[164] R. Didarian, A. Ebrahimi, H. Ghorbanpoor, H. Bagheroghli, F. D. Güzel, M. Farhadpour, N. Lotfibakhshayesh, H. Hashempour, H. Avci, *Turk. J. Chem.* **2023**, *47*, 253.

[165] D. Ciceri, J. M. Perera, G. W. Stevens, *J. Chem. Technol. Biotechnol.* **2014**, *89*, 771.

[166] T. Barri, S. Bergström, J. Norberg, J. Å. Jönsson, *Anal. Chem.* **2004**, *76*, 1928.

[167] A. Hibara, M. Tokeshi, K. Uchiyama, H. Hisamoto, T. Kitamori, *Anal. Sci.* **2001**, *17*, 89.

[168] T. Kitamori, M. Tokeshi, A. Hibara, K. Sato, *Anal. Chem.* **2004**, *76*, 52A.

[169] A. Hibara, S. Iwayama, S. Matsuoka, M. Ueno, Y. Kikutani, M. Tokeshi, T. Kitamori, *Anal. Chem.* **2005**, *77*, 943.

[170] T. Maruyama, T. Kaji, T. Ohkawa, K.-I. Sotowa, H. Matsushita, F. Kubota, N. Kamiya, K. Kusakabe, M. Goto, *Analyst* **2004**, *129*, 1008.

[171] W. E. Tegrotenhuis, R. J. Cameron, M. G. Butcher, P. M. Martin, R. S. Wegeng, *Sep. Sci. Technol.* **1999**, *34*, 951.

[172] A.-L. Dessimoz, L. Cavin, A. Renken, L. Kiwi-Minsker, *Chem. Eng. Sci.* **2008**, *63*, 4035.

[173] J. R. Burns, C. Ramshaw, *Lab Chip* **2001**, *1*, 10.

[174] C. Xu, T. Xie, *Ind. Eng. Chem. Res.* **2017**, *56*, 7593.

[175] S. Liu, P. K. Dasgupta, *Anal Chem* **1995**, *67*, 2042.

[176] J. M. Kokosa, *Anal. Chem.* **2015**, *71*, 194.

[177] S. Pedersen-Bjergaard, K. E. Rasmussen, *Anal. Chem.* **1999**, *71*, 2650.

[178] K. E. Rasmussen, S. Pedersen-Bjergaard, M. Krogh, H. Grefslie Ugland, T. Grønhaug, *J. Chromatogr. A* **2000**, *873*, 3.

[179] Y. Ito, R. L. Bowman, *Science* **1970**, *167*, 281.

[180] T. Tanimura, J. J. Pisano, Y. Ito, R. L. Bowman, *Science* **1970**, *169*, 54.

[181] Y. Ito, R. L. Bowman, *Science* **1971**, *173*, 420.

[182] Y. Ito, *Sep. Purif. Rev.* **2005**, *34*, 131.

[183] Y. Ito, M. Knight, T. M. Finn, *J. Chromatogr. Sci.* **2013**, *51*, 726.

[184] A. Berthod, T. Maryutina, B. Spivakov, O. Shpigun, I. A. Sutherland, *Pure Appl. Chem.* **2009**, *81*, 355.

[185] Q. Fang, H. Chen, Z. X. Cai, *Chem. J. Chinese Univ.* **2004**, *25*, 261.

[186] S. A. Bowden, P. B. Monaghan, R. Wilson, J. Parnell, J. M. Cooper, *Lab Chip* **2006**, *6*, 740.

[187] Y. Zhao, G. Chen, Q. Yuan, *AIChE J.* **2006**, *52*, 4052.

[188] P. Guillot, A. Colin, *Phys Rev E Stat Nonlin Soft Matter Phys* **2005**, *72*, 066301.

[189] A. Smirnova, K. Mawatari, A. Hibara, M. A. Proskurnin, T. Kitamori, *Anal. Chim. Acta* **2006**, *558*, 69.

[190] H. Song, M. R. Bringer, J. D. Tice, C. J. Gerdts, R. F. Ismagilov, *Appl. Phys. Lett.* **2003**, *83*, 4664.

[191] M. N. Kashid, Y. M. Harshe, D. W. Agar, *Ind. Eng. Chem. Res.* **2007**, *46*, 8420.

[192] A. D. Stroock, S. K. W. Dertinger, A. Ajdari, I. Mezic?, H. A. Stone, G. M. Whitesides, *Science* **2002**, *295*, 647.

[193] L.-M. Fu, W.-J. Ju, C.-H. Tsai, H.-H. Hou, R.-J. Yang, Y.-N. Wang, *Chem. Eng. J.* **2013**, *214*, 1.

[194] Y. Okubo, M. Toma, H. Ueda, T. Maki, K. Mae, *Chem. Eng. J.* **2004**, *101*, 39.

[195] X. Chen, H. Lu, W. Jiang, L. Y. Chu, B. Liang, *Ind. Eng. Chem. Res.* **2010**, *49*, 9279.

[196] A. Aota, A. Hibara, Y. Sugii, T. Kitamori, *Anal. Sci.* **2012**, *28*, 9.

[197] A. Aota, M. Nonaka, A. Hibara, T. Kitamori, *Angew Chem Int Ed Engl* **2007**, *46*, 878.

[198] A. Hibara, M. Nonaka, H. Hisamoto, K. Uchiyama, Y. Kikutani, M. Tokeshi, T. Kitamori, *Anal. Chem.* **2002**, *74*, 1724.

[199] C. Xu, S. Jing, Y. Chu, *AIChE J.* **2016**, *62*, 3685.

[200] M. Viefhues, R. Eichhorn, *Electrophoresis* **2017**, *38*, 1483.

[201] M. Viefhues, J. Regtmeier, D. Anselmetti, *Analyst* **2013**, *138*, 186.

[202] M. Viefhues, D. Anselmetti, *Mater Today Proc* **2017**, *4*, S208.

[203] S. Li, Z. Ye, Y. S. Hui, Y. Gao, Y. Jiang, W. Wen, *Biomicrofluidics* **2015**, *9*, 054115.

[204] A. Sonnenberg, J. Y. Marciniak, R. Krishnan, M. J. Heller, *Electrophoresis* **2012**, *33*, 2482.

[205] A. Barik, Y. Zhang, R. Grassi, B. P. Nadappuram, J. B. Edel, T. Low, S. J. Koester, S.-H. Oh, *Nat. Commun.* **2017**, *8*, 1.

[206] R. Martinez-Duarte, F. Camacho-Alanis, P. Renaud, A. Ros, *Electrophoresis* **2013**, *34*, 1113.

[207] G. Giraud, R. Pethig, H. Schulze, G. Henihan, J. G. Terry, A. Menachery, I. Ciani, D. Corrigan, C. J. Campbell, A. R. Mount, P. Ghazal, A. J. Walton, J. Crain, T. T. Bachmann, *Biomicrofluidics* **2011**, *5*, 024116.

[208] S. K. Srivastava, A. Gencoglu, A. R. Minerick, *Anal. Bioanal. Chem.* **2011**, *399*, 301.

[209] L. Gan, T.-C. Chao, F. Camacho-Alanis, A. Ros, *Anal. Chem.* **2013**, *85*, 11427.

[210] L. Gan, F. Camacho-Alanis, A. Ros, *Anal. Chem.* **2015**, *87*, 12059.

[211] V. Chaurey, C. Polanco, C-F. Chou, N. S. Swami, *Biomicrofluidics* **2012**, *6*, 012806.

[212] K.-T. Liao, C-F. Chou, *J. Am. Chem. Soc.* **2012**, *134*, 8742.

[213] B. J. Sanghavi, W. Varhue, J. L. Chávez, C-F. Chou, N. S. Swami, *Anal. Chem.* **2014**, *86*, 4120.

[214] P. Zhang, Y. Liu, *Biofabrication* **2017**, *9*, 045003.

[215] R. T. Turgeon, M. T. Bowser, *Anal. Bioanal. Chem.* **2009**, *394*, 187.

[216] S. Jezierski, L. Gitlin, S. Nagl, D. Belder, *Anal. Bioanal. Chem.* **2011**, *401*, 2651.

[217] V. Kasicka, *Electrophoresis* **2020**, *41*, 10.

[218] B. Buszewski, E. Maslak, M. Zloch, V. Railean-Plugaru, E. Klodzinska, P. Pomastowski, *Trends Analyt Chem* **2021**, *139*, 116250.

[219] B. Buszewski, E. Klodzinska, *Trends Analyt Chem* **2016**, *78*, 95.

[220] L. Farmerie, R. R. Rustandi, J. W. Loughney, M. Dawod, *J. Chromatogr. A* **2021**, *1651*, 462274.

[221] S. Guo, J. Xu, A. P. Estell, C. F. Ivory, D. Du, Y. Lin, W-J. Dong, *Biosens. Bioelectron.* **2020**, *164*, 112292.

[222] K. IçöZ, O. Mzava, *Appl. Sci.* **2016**, *6*, 394.

[223] N. Xia, T. P. Hunt, B. T. Mayers, E. Alsberg, G. M. Whitesides, R. M. Westervelt, D. E. Ingber, *Biomed. Microdevices* **2006**, *8*, 299.

[224] P-Y. Hung, P.-S. Jiang, E.-F. Lee, S.-K. Fan, Y.-W. Lu, *Microsyst. Technol.* **2017**, *23*, 313.

[225] C. Hale, J. Darabi, *Biomicrofluidics* **2014**, *8*, 044118.

[226] K. Kwon, H. Gwak, K.-A. Hyun, B.-S. Kwak, H-I. Jung, *Sens. Actuators, B* **2019**, *294*, 62.

[227] T. M. Dias, F. A. Cardoso, S. A. M. Martins, V. C. Martins, S. Cardoso, J. F. Gaspar, G. Monteiro, P. P. Freitas, *Anal. Methods* **2016**, *8*, 119.

[228] H. Zirath, G. Schnetz, A. Glatz, A. Spittler, H. Redl, J. R. Peham, *Anal. Chem.* **2017**, *89*, 4817.

[229] M. A. Maleki, M. Soltani, N. Kashaninejad, N.-T. Nguyen, *Phys. Fluids* **2019**, *31*, 032001.

[230] S. Wang, Z. Ai, Z. Zhang, M. Tang, N. Zhang, F. Liu, G. Han, S-L. Hong, K. Liu, *Sens. Actuators, B* **2020**, *308*, 127675.

[231] C. Liu, X. Xu, B. Li, B. Situ, W. Pan, Y. Hu, T. An, S. Yao, L. Zheng, *Nano Lett.* **2018**, *18*, 4226.

[232] Z. Zhao, Y. Yang, Y. Zeng, M. He, *Lab Chip* **2016**, *16*, 489.

[233] Y. Liu, I. Papautsky, *Micromachines* **2019**, *10*, 107.

[234] Q. Xiong, C. Y. Lim, J. Ren, J. Zhou, K. Pu, M. B. Chan-Park, H. Mao, Y. C. Lam, H. Duan, *Nat. Commun.* **2018**, *9*, 1.

[235] R.-Q. Zhang, S-L. Hong, C.-Y. Wen, D.-W. Pang, Z.-L. Zhang, *Biosens. Bioelectron.* **2018**, *100*, 348.

[236] S-L. Hong, N. Zhang, L. Qin, M. Tang, Z. Ai, A. Chen, S. Wang, K. Liu, *Analyst* **2021**, *146*, 930.

[237] G. Destgeer, H. J. Sung, *Lab Chip* **2015**, *15*, 2722.

[238] M. Wu, A. Ozcelik, J. Rufo, Z. Wang, R. Fang, T. J. Huang, *Microsyst. Nanoeng.* **2019**, *5*, 1.

[239] F. Petersson, A. Nilsson, C. Holm, H. Jönsson, T. Laurell, *Lab Chip* **2005**, *5*, 20.

[240] P. Rogers, A. Neild, *Lab Chip* **2011**, *11*, 3710.

[241] V. Skowronek, R. W. Rambach, L. Schmid, K. Haase, T. Franke, *Anal. Chem.* **2013**, *85*, 9955.

[242] Z. Ma, D. J. Collins, J. Guo, Y. Ai, *Anal. Chem.* **2016**, *88*, 11844.

[243] J. Shi, H. Huang, Z. Stratton, Y. Huang, T. J. Huang, *Lab Chip* **2009**, *9*, 3354.

[244] J. Nam, H. Lim, D. Kim, S. Shin, *Lab Chip* **2011**, *11*, 3361.

[245] J. Shi, D. Ahmed, X. Mao, S.-C. S. Lin, A. Lawit, T. J. Huang, *Lab Chip* **2009**, *9*, 2890.

[246] R. Ahmad, G. Destgeer, M. Afzal, J. Park, H. Ahmed, J. H. Jung, K. Park, T.-S. Yoon, H. J. Sung, *Anal. Chem.* **2017**, *89*, 13313.

[247] M. J. Madou, L. J. Lee, S. Daunert, S. Lai, C.-H. Shih, *Biomed. Microdevices* **2001**, *3*, 245.

[248] D. C. Duffy, H. L. Gillis, J. Lin, N. F. Sheppard, G. J. Kellogg, *Anal. Chem.* **1999**, *71*, 4669.

[249] H.-C. Wu, Y.-H. Chen, C.-H. Shih, *Biomicrofluidics* **2018**, *12*, 054101.

[250] C.-H. Liu, C-A. Chen, S.-J. Chen, T.-T. Tsai, C.-C. Chu, C.-C. Chang, C-F. Chen, *Anal. Chem.* **2019**, *91*, 1247.

[251] M. M. Aeinehvand, P. Magaña, M. S. Aeinehvand, O. Aguilar, M. J. Madou, S. O. Martinez-Chapa, *RSC Adv.* **2017**, *7*, 55400.

[252] S. Srinivasan, M. Z. Saghir, *Int J Therm Sci* **2011**, *50*, 1125.

[253] A. Martin-Mayor, M. M. Bou-Ali, M. Aginagalde, P. Urteaga, *Int J Therm Sci* **2018**, *124*, 279.

[254] H. Afsaneh, R. Mohammadi, *Talanta Open* **2022**, *5*, 100092.

[255] R. Wang, S. Sun, W. Wang, Z. Zhu, *Int. J. Heat Mass Transfer* **2019**, *133*, 912.

[256] P. F. Geelhoed, R. Lindken, J. Westerweel, *Chem. Eng. Res. Des.* **2006**, *84*, 370.

[257] S. Duhr, D. Braun, *Phys. Rev. Lett.* **2006**, *97*, 038103.

[258] S. Duhr, S. Arduini, D. Braun, *Eur Phys J Spec Top* **2004**, *15*, 277.

[259] E.-M. Laux, F. F. Bier, R. Hölzel, *Bioelectrochemistry* **2018**, *120*, 76.

[260] A. Sonnenberg, J. Y. Marciniak, J. Mccanna, R. Krishnan, L. Rassenti, T. J. Kipps, M. J. Heller, *Electrophoresis* **2013**, *34*, 1076.

[261] A. Rohani, B. J. Sanghavi, A. Salahi, K.-T. Liao, C-F. Chou, N. S. Swami, *Nanoscale* **2017**, *9*, 12124.

[262] K. Y. Tan, A. E. Herr, *Analyst* **2020**, *145*, 3732.

[263] D. Y. Butylskii, N. D. Pismenskaya, P. Y. Apel, K. G. Sabbatovskiy, V. V. Nikonenko, *J. Membr. Sci.* **2021**, *635*, 119449.

[264] A. Saravanan, P. S. Kumar, R. V. Hemavathy, S. Jeevanantham, R. Kamalesh, S. Sneha, P. R. Yaashikaa, *Environ. Chem. Lett.* **2021**, *19*, 189.

[265] M. Mozneb, E. Mirtaheri, A. O. Sanabria, C.-Z. Li, *Biosens. Bioelectron.* **2020**, *167*, 112441.

[266] R. S. Murch, B. Budowle, *Applications of isoelectric focusing in forensic serology*, **1987**, *31*, https://doi.org/10.1520/JFS11096J.

[267] W. Schütt, N. Hashimoto, M. Shimizu, in *Cell Electrophoresis*, CRC Press, Boca Raton, **2020**, pp. 255–266.

[268] Y. Lee, J.-S. Kwon, *J Ind Eng Chem* **2022**, *109*, 79.

[269] S. K. Anciaux, M. Geiger, M. T. Bowser, *Anal. Chem.* **2016**, *88*, 7675.

[270] S. Rawal, A. M. Sidpara, J. Paul, *J. Manuf. Processes* **2022**, *77*, 87.

[271] M. Saadat, M. Taylor, A. Hughes, A. M. Hajiyavand, *Adv. Mech. Eng.* **2020**, *12*, 168781402098271.

[272] A. Zhang, J. Xu, X. Li, Z. Lin, Y. Song, X. Li, Z. Wang, Y. Cheng, *Sensors* **2022**, *22*, 1124.

[273] U. Sarma, S. N. Joshi, *Opt. Laser Technol.* **2020**, *128*, 106257.

[274] J. Shin, J. Ko, S. Jeong, P. Won, Y. Lee, J. Kim, S. Hong, N. L. Jeon, S. H. Ko, *Nat. Mater.* **2021**, *20*, 100.

[275] X. Liu, Z. Dong, Q. Zhao, G. Li, *Microfluid. Nanofluid.* **2020**, *24*, 1.

[276] Y. Yan, Y. Sun, B. Li, P. Zhou, *Biomaterials and Polymers Horizon* **2022**, *1*, 15.

[277] G. Zhang, Y. Sun, X. Liu, H. Gao, D. Zuo, *Int J Adv Manuf Technol* **2022**, *118*, 2711.

[278] S. Razavi Bazaz, O. Rouhi, M. A. Raoufi, F. Ejeian, M. Asadnia, D. Jin, M. Ebrahimi Warkiani, *Sci. Rep.* **2020**, *10*, 1.

[279] R. Sivakumar, N. Y. Lee, *Analyst* **2020**, *145*, 4096.

[280] G. G. Slivinsky, W. C. Hymer, J. Bauer, D. R. Morrison, *Electrophoresis* **1997**, *18*, 1109.

[281] V. Dolník, *Electrophoresis* **1997**, *18*, 2353.

[282] A. Stolz, Y. Hedeland, L. Salzer, J. Römer, R. Heiene, L. Leclercq, H. Cottet, J. Bergquist, C. Neus, *Anal. Chem.* **2020**, *92*, 10531.

[283] P. Legrand, R. Gahoual, R. Benattar, B. Toussaint, C. Roques, N. Mignet, S. Goulay-Dufaÿ, P. Houzé, *J. Sep. Sci.* **2020**, *43*, 2925.

[284] R. Kumar, R. L. Shah, A. S. Rathore, *J. Chromatogr. A* **2020**, *1620*, 460954.

[285] J. Zhao, S. M. Cramer, L. B. Mcgown, *Electrophoresis* **2020**, *41*, 705.

[286] S. N. Wright, B. J. Huge, N. J. Dovichi, *Electrophoresis* **2020**, *41*, 1344.

[287] C. Sänger-van de Griend, *Analytical QbD Method Development for a CZE Method for Quantifying Virus Particles*, **2018**.

[288] M. Jackowski, J. Szeliga, E. Klodzinska, B. Buszewski, *Anal. Bioanal. Chem.* **2008**, *391*, 2153.

[289] S. A. Shamsi, I. M. Warner, *Electrophoresis* **1997**, *18*, 853.

[290] R. B. Yu, J. P. Quirino, *Microchem. J.* **2021**, *161*, 105763.

[291] E. Peris-Garcia, N. Pankajkumar-Patel, M. J. Ruiz-Angel, S. Carda-Broch, M. C. Garcia-Alvarez-Coque, *Sep. Purif. Rev.* **2020**, *49*, 89.

[292] S. Ahuja, *Handbook of Bioseparations*, Elsevier, Calabash North Carolina, **2000**.

[293] M. Li, Y. Xiong, G. Qing, *Trends Analyt Chem* **2020**, *124*, 115585.

[294] I. C. Santos, J. S. Brodbelt, *J. Sep. Sci.* **2021**, *44*, 340.

[295] L. Kartsova, D. Moskvichev, E. Bessonova, M. Peshkova, *Chromatographia* **2020**, *83*, 1001.

[296] M. Sertic, A. Mornar, B. Nigovic, *Chromatographia* **2020**, *83*, 993.

[297] S. Salido-Fortuna, M. Castro-Puyana, M. L. Marina, *J. Chromatogr. A* **2020**, *1626*, 461383.

[298] S. Bernardo-Bermejo, E. Sánchez-López, M. Castro-Puyana, M. L. Marina, *Trends Analyt Chem* **2020**, *124*, 115807.

[299] H. Rilbe, *Ann. N. Y. Acad. Sci.* **1973**, *209*, 11.

[300] D. A. Lytle, C. H. Johnson, E. W. Rice, *Colloids Surf., B* **2002**, *24*, 91.

[301] O. Vesterberg, in *Methods in Enzymology*, Elsevier, USA, **1971**, pp. 389–412.

[302] S. J. Luner, A. Kolin, *Proc Natl Acad Sci U S A* **1970**, *66*, 898.

[303] R. A. Mosher, W. Thormann, A. Graham, M. Bier, *Electrophoresis* **1985**, *6*, 545.

[304] X. Zhang, L. Chemmalil, J. Ding, Z. Li, *Electrophoresis* **2020**, *41*, 735.

[305] B. Michov, in *Electrophoresis*, De Gruyter, Berlin, Boston, **2020**, pp. 829–832.

[306] K. Icoz, B. D. Iverson, C. Savran, *Appl. Phys. Lett.* **2008**, *93*, 103902.

[307] X. Li, J. Wei, K. E. Aifantis, Y. Fan, Q. Feng, F.-Z. Cui, F. Watari, *J. Biomed. Mater. Res., Part A* **2016**, *104*, 1285.

[308] K. Wu, D. Su, J. Liu, R. Saha, J.-P. Wang, *Nanotechnology* **2019**, *30*, 502003.

[309] J. M. Perez, L. Josephson, T. O'loughlin, D. Högemann, R. Weissleder, *Nat. Biotechnol.* **2002**, *20*, 816.

[310] A. Fu, W. Hu, L. Xu, R. J. Wilson, H. Yu, S. J. Osterfeld, S. S. Gambhir, S. X. Wang, *Angew. Chem., Int. Ed.* **2009**, *48*, 1620.

[311] B. Srinivasan, Y. Li, Y. Jing, Y. Xu, X. Yao, C. Xing, J.-P. Wang, *Angew. Chem., Int. Ed.* **2009**, *48*, 2764.

[312] S. G. Balakrishnan, M. R. Ahmad, S. S. R. Koloor, M. Petru, *J Adv Res* **2021**, *33*, 109,.

[313] A. Rabehi, B. Garlan, S. Achtsnicht, H.-J. Krause, A. Offenhäusser, K. Ngo, S. Neveu, S. Graff-Dubois, H. Kokabi, *Sensors* **2018**, *18*, 1747.

[314] K. Icoz, C. Savran, *Appl. Phys. Lett.* **2010**, *97*, 014001,.

[315] M. Afzal, J. Park, J. S. Jeon, M. Akmal, T.-S. Yoon, H. J. Sung, *Anal. Chem.* **2021**, *93*, 8309.

[316] D. Vigolo, R. Rusconi, H. A. Stone, R. Piazza, *Soft Matter* **2010**, *6*, 3489.

[317] C. D. Chin, T. Laksanasopin, Y. K. Cheung, D. Steinmiller, V. Linder, H. Parsa, J. Wang, H. Moore, R. Rouse, G. Umviligihozo, E. Karita, L. Mwambarangwe, S. L. Braunstein, R. Van De Wijgert, R. Sahabo, J. E. Justman, W. El-Sadr, S. K. Sia, *Nat. Med.* **2011**, *17*, 1015.

[318] T. H. Schulte, R. L. Bardell, B. H. Weigl, *Clin. Chim. Acta* **2002**, *321*, 1.

[319] P. S. Dittrich, A. Manz, *Nat Rev Drug Discov* **2006**, *5*, 210.

[320] K.-A. Hyun, H-I. Jung, *Lab Chip* **2014**, *14*, 45.

[321] J. Zhang, S. Yan, D. Yuan, G. Alici, N.-T. Nguyen, M. Ebrahimi Warkiani, W. Li, *Lab Chip* **2016**, *16*, 10.

[322] B. Çetin, D. Li, *Electrophoresis* **2011**, *32*, 2410.

[323] T. P. Forbes, S. P. Forry, *Lab Chip* **2012**, *12*, 1471.

[324] Z. Wang, J. Zhe, *Lab Chip* **2011**, *11*, 1280.

[325] D. G. Grier, *Nature* **2003**, *424*, 810.

[326] M. Yamada, M. Nakashima, M. Seki, *Anal. Chem.* **2004**, *76*, 5465.

[327] L. R. Huang, E. C. Cox, R. H. Austin, J. C. Sturm, *Science* **2004**, *304*, 987.

[328] S. Yan, J. Zhang, C. Pan, D. Yuan, G. Alici, H. Du, Y. Zhu, W. Li, *J. Micromech. Microeng.* **2015**, *25*, 084010.

[329] A. Y. Fu, C. Spence, A. Scherer, F. H. Arnold, S. R. Quake, *Nat. Biotechnol.* **1999**, *17*, 1109.

[330] F. Petersson, A. Nilsson, C. Holm, H. Jönsson, T. Laurell, *Analyst* **2004**, *129*, 938.

[331] E. Özkumur, J. W. Needham, D. A. Bergstein, R. Gonzalez, M. Cabodi, J. M. Gershoni, B. B. Goldberg, M. S. Ünlü, *Proc Natl Acad Sci U S A* **2008**, *105*, 7988.

[332] T. B. Jones, *Electromechanics of Particles*, Cambridge University Press, New York **1995**.

[333] D. Ibraheem, A. Elaissari, H. Fessi, *Int. J. Pharm.* **2014**, *459*, 70.

[334] A. Sonnenberg, J. Y. Marciniak, E. A. Skowronski, S. Manouchehri, L. Rassenti, E. M. Ghia, G. F. Widhopf, T. J. Kipps, M. J. Heller, *Electrophoresis* **2014**, *35*, 1828.

[335] S. Manouchehri, S. Ibsen, J. Wright, L. Rassenti, E. M. Ghia, G. F. Widhopf, T. J. Kipps, M. J. Heller, *Int. J. Hematol. Oncol.* **2016**, *5*, 27.

[336] S. A. Peyman, E. Y. Kwan, O. Margarson, A. Iles, N. Pamme, *J. Chromatogr. A* **2009**, *1216*, 9055.

[337] Y. Xu, Z. Zhang, Z. Su, X. Zhou, X. Han, Q. Liu, *Micromachines (Basel)* **2020**, *11*, 187,.

[338] X. Lou, J. Qian, Y. Xiao, L. Viel, A. E. Gerdon, E. T. Lagally, P. Atzberger, T. M. Tarasow, A. J. Heeger, H. T. Soh, *Proc. Natl. Acad. Sci. USA* **2009**, *106*, 2989.

[339] N. Pamme, C. Wilhelm, *Lab Chip* **2006**, *6*, 974.

[340] A. Winkleman, R. Perez-Castillejos, K. L. Gudiksen, S. T. Phillips, M. Prentiss, G. M. Whitesides, *Anal. Chem.* **2007**, *79*, 6542.

[341] R. Burger, D. Kirby, M. Glynn, C. Nwankire, M. O'sullivan, J. Siegrist, D. Kinahan, G. Aguirre, G. Kijanka, R. A. Gorkin, J. Ducrée, *Curr. Opin. Chem. Biol.* **2012**, *16*, 409.

[342] M. Mizuno, M. Yamada, R. Mitamura, K. Ike, K. Toyama, M. Seki, *Anal. Chem.* **2013**, *85*, 7666.

[343] F. Del Giudice, H. Madadi, M. M. Villone, G. D'avino, A. M. Cusano, R. Vecchione, M. Ventre, P. L. Maffettone, P. A. Netti, *Lab Chip* **2015**, *15*, 1912.

[344] S. Chang, Y-H. Cho, *Lab Chip* **2008**, *8*, 1930.

[345] D. J. Collins, T. Alan, A. Neild, *Lab Chip* **2014**, *14*, 1595.

[346] S.-C. S. Lin, X. Mao, T. J. Huang, *Lab Chip* **2012**, *12*, 2766.

[347] M. C. Zalis, J. F. Reyes, P. Augustsson, S. Holmqvist, L. Roybon, T. Laurell, T. Deierborg, *Integr. Biol. (Camb.)* **2016**, *8*, 332.

[348] Y. Chen, M. Wu, L. Ren, J. Liu, P. H. Whitley, L. Wang, T. J. Huang, *Lab Chip* **2016**, *16*, 3466.

[349] A. Lenshof, T. Laurell, *Chem. Soc. Rev.* **2010**, *39*, 1203.

[350] K. C. Neuman, A. Nagy, *Nat. Methods* **2008**, *5*, 491.

[351] A. Ashkin, *Proc. Natl. Acad. Sci. USA* **1997**, *94*, 4853.

Aliakbar Ebrahimi received his Ph.D. in nanotechnology and nanomedicine in 2017 from Hacettepe University (HU) in Turkey. After obtaining his Ph.D., he undertook post-doctoral research in Ankara Yildirim Beyazit University (2019–2021) by focusing on single channel electrophysiology and lab-on-a-chip systems. Currently, he is a post-doctoral researcher at the Eskişehir Osmangazi University where he is working in the field of organ-on-a-chip systems, microfluidic separation, and biosensors.

Kutay Icoz received the Ph.D. degree from Purdue University Biomedical Engr. Department in 2010. He worked at Harvard Medical School and Massachusetts General Hospital Department of Neurosurgery as a postdoctoral research fellow and at Intel Corporation Assembly & Test Technology Development Division as a senior engineer. He currently works as a faculty member of Electrical-Electronics Engineering at Abdullah Gül University. His research focuses on novel applications of micro/nanotechnology in biology and medicine, biosensors, point-of-care devices, and wearable biomedical devices.

Reza Didarian first graduated with a D.V.M. (Doctor of Veterinary Medicine) degree at Urmia University (IRAN) and later pursued a Ph.D. in nanotechnology and nanomedicine at Hacettepe University (Turkey). He is currently a researcher at the Department of Biomedical Engineering at Ankara Yildirim Beyazit University and his scientific interests are microfluidic chips, organ-on-a-chip systems, and cancer treatment, with a specific emphasis on nanotechnology and nanomedicine.

Behzad Nasseri received his Ph.D. degree of Hacettepe University in Bioengineering (Turkey, 2016). He investigated postdoctoral projects at Shahid Beheshti University and Tabriz University of Medical Sciences from 2018. His study fields are synthesis of hybrid nanomaterials and their applications in the biophotonics in the treatment of different types of cancer. Since 2019, he is active in the study of the physical, chemical, and photothermal processes for tumor treatment.

Ali Akpek recieved his B.Eng. degree from the Department of Biomedical Engineering of Baskent University. During his education, he mainly focused on biomedical electronics. After graduation, he expanded his research interest to biotechnology and obtained a Master of Science degree in biotechnology from Ege University. In 2010, he was awarded Monbukagakusho scholarship from Japan and obtained a doctoral degree from the Tokyo Institute of Technology, Department of Mechano-Micro Engineering. Later, he worked as a visiting assistant professor at Harvard–MIT Division of Health Science and Technology. He is currently working as an associate professor of biomedical engineering at Yildiz Technical University.

Berivan Cecen is currently working as an adjunct professor at the Department of Biomedical Engineering at Rowan University. She was a visiting scholar in the Department of Mechanical Engineering and School of Medical Engineering at Rowan University (2021–2023). She was an assistant professor at the Faculty of Engineering and Natural Sciences of Istinye University, Turkey, in 2021. She received her Ph.D. degree in bioengineering from Dokuz Eylul University and Izmir Institute of Technology, Turkey, in 2014. Afterward, she joined as a post-doctoral fellow at Harvard–MIT Division of Health Sciences and Technology and Brigham and Women's Hospital, Harvard Medical School in 2016.

**ADVANCED
SCIENCE NEWS**

www.advancedsciencenews.com

**ADVANCED
MATERIALS
INTERFACES**
Open Access

www.advmatinterfaces.de

Ayca Bal-Ozturk is an associate professor at Istinye University, Faculty of Pharmacy. She also holds a faculty appointment at Istinye University Research and Application Center for Stem Cell and Tissue Engineering (ISUKOK). She received his B.Sc., M.Sc., and Ph.D. degrees in chemical engineering from Istanbul University. Awarded with TUBITAK in 2016, she joined Harvard Medical School as a postdoctoral research fellow. She received the Young Scientist Award (BAGEP 2023) from Turkish Science Academy in 2023. She is an expert in the field of biomaterials, nanomaterials, tissue engineering, and 3D-bioprinting. She is the co-founder of AdBioInk Biosystem Technology Corp., established in TUBITAK Marmara Technopark.

Yi-Chen Ethan Li is a faculty member in the Department of Chemical Engineering at Feng Chia University. His scientific interests include the fundamental research of tissue engineering, developing artificial tissues/organs and organs-on-chips models via 3D bioprinting and microfluidic technologies. Through this research, he wants to further apply the theories from fundamental research and the developed models to the applications of drug testing/screening, developmental biology, biosensors, and regenerative medicine.

H. Cumhur Tekin holds B.Sc. and M.Sc. degrees in electrical and electronics engineering from Middle East Technical University and Ecole Polytechnique Federal de Lausanne (EPFL), respectively. He earned his Ph.D. in microsystems and microelectronics from EPFL in 2012. After postdoctoral research roles at EPFL, Harvard Medical School, and Stanford School of Medicine, he joined the Bioengineering Department at Izmir Institute of Technology in 2016 as a faculty member, establishing the Laboratory of Biomedical Micro and Nanosystems. Dr. Tekin focuses on developing micro and nanotechnologies, point-of-care instruments, and intelligent systems for biomedical applications, aiming to enhance healthcare through cost-effective solutions.

Emine Alarçin is an assistant professor of pharmacy at Marmara University, Turkey. She received her Ph.D. from Marmara University, Turkey from the Faculty of Pharmacy, and Department of Pharmaceutical Technology in 2011. Her Ph.D. research was mainly focused on fabricating polymeric microspheres for VEGF delivery in nerve graft prefabrication. She carried postdoctoral research fellow at Harvard Medical School in 2016–2017. Her current research focuses on developing multifunctional biomaterials, nanocarriers, and hydrogels for drug delivery applications and regenerative medicine.

Hamed Ghorbanpoor received his Ph.D. degree from Eskişehir Osmangazi University (2018), he worked as a research fellow in the Biomedical Engineering Department, Ankara Yildirim Beyazit University (2018–2021). In March 2021, he started as an assistant professor Biomedical Engineering Department, Eskişehir Osmangazi University. His research focuses on Lab and organ on a chip, tissue engineering, and biosensors.

Ceren Özel, received a Ph.D. in stem cell and tissue engineering (2022) from Eskisehir Osmangazi University. She is a molecular stem cell biologist specializing in cellular programming and 3D tissue modeling. Her research covers tissue scaffold engineering, biomaterials, microfluidics, biotextiles, 3D biopirinting, organoids, and various types of stem cells including embryonic, mesenchymal, and cancer stem cells. As a postdoctoral researcher at ESTEM, she works on high-tech projects, such as phase 1/2 stem cell-derived exosome treatments and liver-on-a-chip platforms for regenerative medicine and tissue engineering.

Ayla Eker Sarıboyacı recieved her Ph.D. in histology and embryology at the Eskisehir Osmangazi University. She is the Director of the Cellular Therapy and Stem Cell Production, Application and Research Centre, ESTEM, and the Head of the Stem Cell Department, Institute of Health Sciences at Eskisehir Osmangazi University since 2015. Dr. Sariboyaci's research interests include embryonic/mesenchymal/induced pluripotent stem cells, cancer stem cells, cellular therapies, primary/secondary cell culture, genome editing, reproductive health. She has also received stem cell and cellular therapy research projects from various national and international funding agencies and the Scientific and Technical Research Council of Turkey.

Huseyin Avci received his Master's and Ph.D. degree in 2010 and 2013, respectively, from Fiber and Polymer Science, College of Textiles, at NC State University. Later, he joined the Department of Metallurgical and Materials Engineering at Eskisehir Osmangazi University since September 2014. He is also a faculty member in Cellular Therapy and Stem Cell Research Center (ESTEM) and Translational Medicine Research and Clinical Center (TATUM). As a research scientist at Harvard Medical School, he had the chance to work on tissue engineering and organ-on-a-chip platforms. His group focuses on microfluidics, organ-on-a-chip, separation, biosensor, biomaterials, toxicity analysis, and filtration.